Université de Montréal

La géographie et la biogéochimie des mares de tourbières tempérées

Patrons et processus à l'interface eau-tourbe

par Julien Arsenault

Département de géographie
Faculté des Arts et Sciences

Thèse présentée
en vue de l'obtention du grade de *Philosophiæ Doctor* (Ph.D.)
en géographie

Avril 2023

Université de Montréal

Département de géographie

Cette thèse intitulée

La géographie et la biogéochimie des mares de tourbières tempérées :

Patrons et processus à l'interface eau-tourbe

Présentée par

Julien Arsenault

A été évaluée par un jury composé des personnes suivantes :

François Courchesne
Président-rapporteur

Julie Talbot
Directrice de recherche

Jean-François Lapierre
Codirecteur de recherche

Julie Loisel
Membre du jury

Oleg Pokrovsky
Examinateur externe

William Skene
Représentant du doyen

Résumé

Les écosystèmes aquatiques sont de plus en plus reconnus pour leur rôle dans les cycles biogéochimiques locaux et globaux en raison de leur grand potentiel réactif. Les tourbières sont quant à elles des environnements relativement stables, mais qui participent aussi largement aux cycles biogéochimiques car elles accumulent de grandes quantités de carbone (C) et d'autres éléments dans leurs sols. À l'intérieur de certaines tourbières tempérées, de petites étendues d'eau se développent par la décomposition de la matière organique qui compose leur matrice, mais de larges pans de leur fonctionnement biogéochimique sont ignorés. La structure et la géographie de ces mares de tourbières, particulièrement l'interface eau-tourbe qui les caractérise, pourraient d'ailleurs en faire des écosystèmes d'un dynamisme peu commun.

Le but de cette thèse est de déterminer en quoi la géographie particulière des mares de tourbières, à commencer par celle des régions tempérées, influence leurs patrons et processus biogéochimiques. Les résultats démontrent que les mares de tourbières sont des écosystèmes sans commune mesure parmi les milieux aquatiques. Les mares sont biogéochimiquement distinctes des autres milieux lentiques en raison de la structure du paysage qui les entoure, faisant d'elles des environnements où les concentrations en C organique dissous (DOC) sont plusieurs fois plus élevées et où le pH est 100 fois plus acide que dans les lacs. La biogéochimie des mares est par contre variable dans le temps et l'espace en fonction de paramètres morphologiques et climatiques. Par exemple, les concentrations en DOC sont plus élevées dans les mares les moins profondes et sous un climat moins humide, mais ces concentrations fluctuent rapidement au cours des saisons en fonction de variations météorologiques, faisant d'elles des sentinelles climatiques. Les patrons biogéochimiques observés dans les mares de tourbières semblent tirer leur origine de leur structure plutôt que d'une influence allochtone à plus grande échelle comme c'est le cas pour la plupart des lacs. Une expérience menée dans une tourbière ombrotrophe du sud du Québec montre ainsi que les processus de décomposition de la matière organique qui caractérisent les mares de tourbières varient spatialement en fonction de la profondeur des mares et de la composition chimique du matériel à décomposer. Au final, les résultats de la thèse démontrent que les patrons et processus biogéochimiques observés dans les mares de tourbières tempérées sont effectivement dirigés par leur géographie particulière, où les mécanismes fonctionnels sont en partie dictés par l'interface eau-tourbe.

Mots-clés : limnologie, tourbières, biogéochimie, carbone, azote, phosphore, climat, matière organique, décomposition

Abstract

Aquatic ecosystems are increasingly recognized for their contribution to local and global biogeochemical cycles because of their high reactivity potential. Peatlands are relatively stable ecosystems but that nonetheless play a large role in biogeochemical cycles because they sequester large amounts of carbon (C) and other elements. Within temperate peatlands, waterbodies may develop by the decomposition of the organic matter that forms the soil but their biogeochemical functioning remain largely ignored. Their structure and their geography, especially the water-peat interface, may thus make peatland pools ecosystems that are more dynamic than other aquatic environments.

The goal of this thesis is to determine how the geography of temperate peatland pools influences their biogeochemical patterns and processes. Results show that peatland pools are biogeochemically distinct from other aquatic environments because of the structure of the landscape in which they develop, with dissolved organic C (DOC) concentrations being several-fold higher and pH being 100-fold more acidic than lakes. The biogeochemistry of peatland pools is, however, variable in both space and time in relation to morphological and climatic parameters. For example, DOC concentrations are higher in shallower pools and in arid climates, but these concentrations rapidly vary within and across seasons in relation to changes in temperatures and precipitation, highlighting their potential to act as climate sentinel. The observed biogeochemical patterns in peatland pools originate from their internal structure rather than from a broader-scale allochthonous influence like lakes. The influence of pool internal structure was revealed in an experiment we conducted in an ombrotrophic peatland of southern Québec that showed that organic matter decomposition processes vary spatially in relation to pool depth and to the chemical composition of the organic matter. Overall, the results demonstrate that temperate peatland pool biogeochemical patterns and processes are indeed controlled by their unique geography, and where functional mechanisms are partly driven by the water-peat interface.

Keywords : limnology, peatlands, biogeochemistry, carbon, nitrogen, phosphorus, climate, organic matter, decomposition

Table des matières

Liste des tableaux

Liste des figures

Liste des sigles et abréviations

$\delta^{13}C$	Ratio isotopique du carbone-13
$\delta^{15}N$	Ratio isotopique de l'azote-15
ANOVA	Analyse de variance
A_{254}	Absorbance à 254nm
C	Carbone
Ca	Calcium
CH_4	Méthane
CO_2	Dioxyde de carbone ou gaz carbonique
DOC	Carbone organique dissous (de l'anglais *dissolved organic carbon*)
DOM	Matière organique dissoute (de l'anglais *dissolved organic matter*)
DOY	Jour Julien (de l'anglais *day of the year*)
e.g.	Par exemple (du latin *exempli gratia*)
FTIR	Spectroscopie infrarouge à transformée de Fourier (de l'anglais *Fourier-transformed infrared*)
g C m^{-2} an^{-1} **g C m^{-2} yr^{-1}**	Gramme de carbone par mètre carré par année
g m^{-2} an^{-1} **g m^{-2} yr^{-1}**	Gramme par mètre carré par année
GHG	Gaz à effets de serre (de l'anglais *greenhouse gas)*
GLM	Modèle linéaire généralisé (de l'anglais *generalized linear model)*
GLMM	Modèle linéaire mixte généralisé (de l'anglais *generalized linear mixed model)*
GPB	Tourbière Grande plée Bleue de Lévis (Québec, Canada)
HCl	Acide chlorhydrique
HI	Indice d'humification (de l'anglais *humification index*)
i.e.	C'est-à-dire (du latin *id est*)
k	Taux de décomposition
K	Potassium

k-means	Partitionnement en k-moyennes
MAAT	Température annuelle moyenne (de l'anglais *mean annual air temperature)*
MAP	Précipitations annuelles moyennes (de l'anglais *mean annual precipitation)*
MANOVA	Analyse de variance multiple
Mg	Magnésium
mg CO_2 g C^{-1}	Milligramme de dioxyde de carbone par gramme de carbone
mg L^{-1}	Milligramme par litre
MIRS	Spectre dans l'infrarouge moyen (de l'anglais *mid-infrared spectra*)
MO	Matière organique
N	Azote
n	Taille de l'échantillon
N_2O	Protoxyde d'azote ou oxyde nitreux
Na	Sodium
NH_4	Ammonium
NO_3	Nitrate
O_2	Oxygène
OM	Matière organique (de l'anglais *organic matter*)
ρ	Coefficient de corrélation de Spearman (rhô de Spearman)
P	Seuil de signification (p-value)
P	Phosphore
P:PET	Indice d'aridité (ratio entre les précipitations et l'évapotranspiration potentielle)
PCA	Analyse en composante principale (de l'anglais *principal component analysis*)
PET	Évapotranspiration potentielle (de l'anglais *potential evapotranspiration*)
Pg	Pétagramme (10^{15} grammes; 1 Pg = 1 000 000 000 tonnes)
PLSR	Régressions des moindre-carrés partiels (de l'anglais *partial least-square regressions*)
PP	Production primaire

PO_4	Phosphate
ppm	Parties par million
r	Coefficient de corrélation de Pearson (r de Pearson)
R	Respiration
RDA	Analyse de redondance
SUVA	Absorbance UV spécifique (de l'anglais *Specific UV Absorbance*)
τ	Coefficient de corrélation de Keandall (tau de Kendall)
T	Température
TDN	Azote total dissous (de l'anglais *total dissolved nitrogen*)
Tg	Téragramme (10^{12} grammes; 1 Tg = 1 000 000 tonnes)
TN	Azote total (de l'anglais *total nitrogen*)
TP	Phosphore total (de l'anglais *total phosphorus*)
µg g^{-1}	Microgramme par gramme
µg CH_4 g C^{-1}	Microgramme de méthane par gramme de carbone
µg CH_4 g C^{-1} day^{-1}	Microgramme de méthane par gramme de carbone par jour
µg CO_2 g C^{-1}	Microgramme de dioxyde de carbone par gramme de carbone
µg CO_2 g C^{-1} day^{-1}	Microgramme de dioxyde de carbone par gramme de carbone par jour
µg L^{-1}	Microgramme par litre
UK	Royaume-Uni (de l'anglais *United Kingdom)*
VIP	Importance de la variable dans la projection multivariée (de l'anglais *variable importance in projection*)

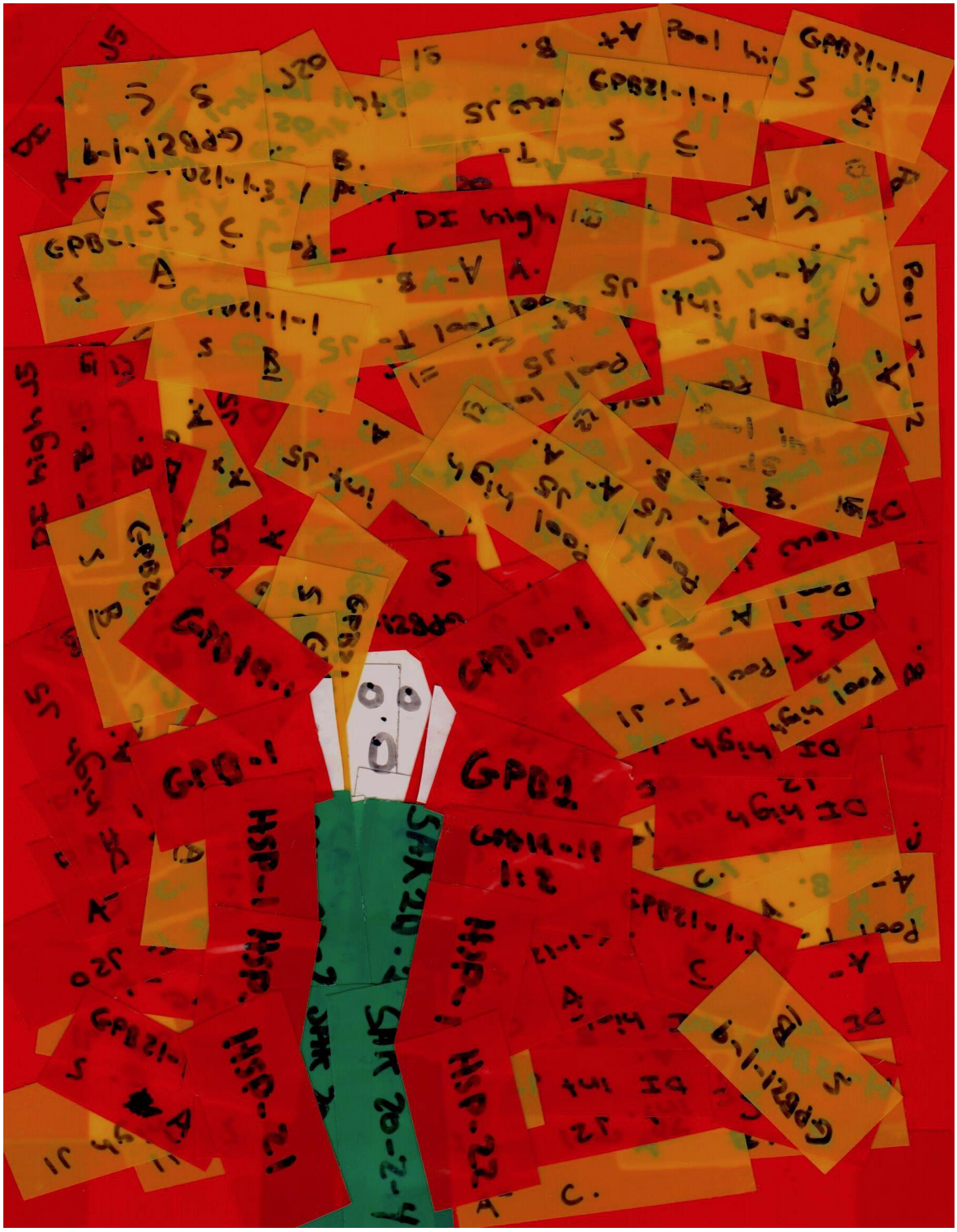

Le Cri du Doctorant

Collage d'étiquettes d'échantillons

Librement inspiré du chef d'œuvre d'Edvard Munch

Remerciements

Faisons les choses à l'envers.

À Marie. Cette thèse, c'est d'abord à toi que je la dois. Ta présence à mes côtés m'a permis d'entamer, de traverser et de terminer cette étape de ma, de notre vie. Sans ton support, tes encouragements, ton aide, jamais cette thèse n'aurait pu voir le jour. Le bac, la maîtrise, le doctorat, c'est toi qui m'as encouragé à les entreprendre. Aujourd'hui (ou hier ou demain, selon le moment où tu liras ces lignes), au bout de plusieurs années de travail au cours desquelles tu m'as accompagné dans toutes les facettes de ma vie professiono-personnelle de Montréal à Matane (en passant par Laval) et de la Minganie à la Patagonie, j'achève une étape de plus. Et tout ce que j'ai accompli en cours de route, c'est grâce à toi. Tu es ma colonne, mon cœur et mon âme. Je t'aime.

Aux miens. Maman, papa, beaux-parents, Nancy, Étienne, Vincent, Pitts, le Banquet. Vous m'avez supporté même si vous ne compreniez pas ce que je faisais. Vous m'avez serré dans vos bras aux moments où j'en avais besoin. Vous m'avez accueilli dans mes moments de bonheur comme dans mes moments de détresse, sans jugement. Vous définissez ce qu'est l'amour inconditionnel. Je vous aime aussi, inconditionnellement.

À Andy et Philou, Philou et Andy. J'ai trop peu de mots pour exprimer tout l'amour et le respect que j'ai pour vous, mes amis. Vous avez été à mes côtés depuis le début de ma maîtrise et vous ne m'avez jamais lâché. C'est rare de tomber sur des gens avec qui la connexion se fait naturellement, sans forcer, et je me considère extrêmement chanceux d'avoir pu vivre ce sentiment deux fois plutôt qu'une avec vous. Merci de m'avoir suivi dans mes niaiseries, d'avoir embarqué dans mes délires, de m'avoir supporté au cours des sept dernières années. Nous nous sommes géographiquement séparés il y a quelque temps, mais notre amitié est solide et le restera. Je n'en douterai jamais. Une tornade de bécots à vous!

À Émilie. Avec toi aussi, ç'a été si facile de connecter et si plaisant de travailler. En toi, j'ai trouvé une collègue hors pair et une amie merveilleuse. Je ne sais pas où je serais si tu n'avais pas été là pour prendre en charge le terrain en 2021, pour m'écouter dans mes moments d'angoisse, et pour partager avec moi mon amour pour les mares de tourbières depuis le début de ton propre cheminement à la maîtrise. Par ton aide, tu m'as sauvé le derrière à quelques reprises alors je t'en dois plusieurs ! Mais j'espère de tout mon cœur avoir été capable de te rendre la pareille. Je suis enchanté d'avoir croisé ton chemin et je souhaite ardemment que nos routes continueront de se rencontrer.

Au(x) labo(s). Beaucoup ont croisé mon chemin au cours des dernières années. Alejandra, Annie, Augustin, Evrard, Félix, Gaëlle, Jessie, Jules, Julie A., Jordan, Karine, Kim, Lara, Laurent, Léa, Manue, MP, Marion, Maxou, Nicholas, Olivier, Reyes, Roxane, Sophie, Thora, Xiaoyu, Willy et tant d'autres m'ont aidé et accompagné dans mon parcours. Que ce soit par votre assistance sur le terrain, en laboratoire, en chalet, ou encore par des tournois de Nintendo et des soirées-cinéma (le classique *Astérix : Mission Cléopâtre* aux Noëls prépandémiques), j'ai partagé avec vous plusieurs moments charnières de mon parcours universitaire. Je ne sais toujours pas ce que je ferai quand je serai grand, mais je sais que j'aurai toujours besoin d'être entouré de gens comme vous. Xxx.

Au département, étudiant.e.s et employé.e.s. Vous avez fait partie de ma vie pendant des années. Je vous ai côtoyé parfois en classe, parfois dans les 5@7, parfois en grève. Vous provenez d'horizons différents et vous m'avez permis d'élargir les miens. Vous côtoyer ou vous enseigner a été pour moi un privilège. Je serai toujours reconnaissant de ce que vous m'avez inculqué et j'espère être en mesure de faire honneur à mon passage à Géo UdeM tout au long de ma vie. La géographie est la plus belle science du monde, et c'est entre autres grâce à vous que j'en fais le constat.

Au Strath. T'étais sale, tu puais, tu coulais, t'étais plein d'amiante et de moisissures, mais je m'ennuie de toi quand même.

À Karla, Armando, Jorge, Nicola, Joe, Lee, Klaus, Henning et al. Pour chacun.e d'entre vous, il n'a suffi que d'un courriel pour vous convaincre d'embarquer dans mes projets de recherche. Il n'a suffi que d'une rencontre pour développer des collaborations qui, je l'espère, perdureront encore longtemps. Toute cette thèse repose sur l'aide que vous m'avez apportée. Mille mercis à chacun.e d'entre vous.

À McGill. Vous m'avez offert le *safe space* par excellence pour développer mes idées. Dans vos labos, que j'ai fréquentés régulièrement depuis 2016, je me suis toujours senti à ma place. Dans vos cours, dont le tout premier que j'ai suivi en tant qu'étudiant gradué, j'ai senti que j'étais à l'endroit où je devais être. Dans vos séminaires et symposiums, j'ai senti que j'étais un des vôtres. Je vous remercie d'avoir confirmé le futur que je me suis choisi. Sachez que je reviendrai.

À Tim, mentor ultime, éminence grise de mes projets, supporter de mes idées. La porte de ton bureau m'a toujours été ouverte; tu n'as jamais refusé de discuter avec moi, de répondre à mes questions, de m'aider. J'ai tant appris en te côtoyant que les mots me manquent pour

dire à quel point tu as formé le chercheur que je suis aujourd'hui. Je me compte très chanceux d'avoir eu la chance de t'avoir à mes côtés depuis le début de mes études supérieures, et choyé que nous ayons développé la relation que nous avons aujourd'hui. Merci pour tout.

À JF. Tu m'as dit il y a quelque temps que le rôle d'un co-superviseur peut parfois être assez ingrat. Sache que par toute l'énergie que tu as mise dans mon projet, à m'aider à diriger et exprimer correctement ma pensée, et à pousser ma réflexion toujours plus loin, tu mérites toute la reconnaissance du monde. Dès le départ, tu as embarqué dans mon projet avec un enthousiasme qui m'a nourri tout au long de mon parcours. Ç'a été un réel plaisir de t'avoir dans mon entourage au cours des dernières 5 années, et un honneur de travailler avec un grand prof d'université comme toi. D'ailleurs, je disais plus haut que je ne sais pas ce que je ferai quand je serai grand, mais je sais que je m'inspirerai du prof que tu es.

Enfin, à Julie. Tu portes les chapeaux de guide scientifique, de mère académique. Tu m'as permis d'intégrer ton laboratoire il y a sept ans (sans hésiter, j'ose croire), et, grâce à toi, je suis devenu le chercheur, l'enseignant et une bonne partie de la personne que je suis aujourd'hui. Je te dois tout ça. À l'automne 2015, quand tu m'as approché pour me recruter comme étudiant à la maîtrise, je n'étais qu'un ti-cul. Je le suis encore, et j'ai bien l'intention de le rester, mais malgré tout, peu importe ce que j'ai vécu au cours des dernières années, tu m'as accueilli, écouté, encouragé, challengé, et offert les plus belles opportunités du monde. On dit qu'on apprend par mimétisme. Par ton écoute, ta sensibilité, ta curiosité, ton amour pour la science et celui pour l'enseignement, je suis devenu le géographe, l'humain, que je suis. Je copie-colle donc ce que j'ai écrit dans mon mémoire de maîtrise : « merci de m'avoir permis de travailler avec toi, merci de m'avoir aidé à élaborer et à concrétiser un projet de recherche qui me ressemble et, surtout, merci pour la confiance que tu m'as accordée dès le départ. Je n'aurais jamais pu espérer une meilleure directrice. » Merci, mom.

Ayoye (bis).

Chapitre 1. Introduction

1.1 La lunette géographique

La géographie a marqué l'histoire des sciences naturelles par ses approches transdisciplinaires et grâce à sa vision holistique des processus qui ont forgé et qui forgent toujours notre monde. Elle permet non seulement de décrire le paysage et les mécanismes qui le forment, mais aussi de qualifier les interactions entre les composantes de la planète (la lithosphère, l'atmosphère, l'hydrosphère, la cryosphère, la biosphère et l'anthroposphère) et de quantifier leur magnitude. L'étude d'un système, naturel ou non, à travers une lunette géographique permet donc d'en saisir à la fois le fonctionnement et la structure de façon multiscalaire.

La géographie, comme ses objets d'analyse, est en constante évolution et s'est nourrit au cours des trois derniers millénaires de théories et d'hypothèses issues d'une multitude d'autres disciplines (Péaud, 2018). Ainsi, l'étude géographique des écosystèmes (aquatiques et autres milieux humides, sujets de cette thèse) pourrait d'abord tirer son origine dans les observations et réflexions des penseurs grecs de l'Antiquité, desquels nous retenons entre autres l'étude des dimensions physiques de la planète (e.g. Ératosthène qui estima, au III^{e} siècle avant J.-C., la circonférence de la Terre à 39 000 km) et de la répartition des espèces animales et végétales (par Hérodote et Théophraste). Les explorations européennes de la Renaissance et l'essor des sciences naturelles aux XVIII^{e} et XIX^{e} siècles (grâce entre autres aux travaux de Alexander von Humboldt, Alfred Wallace et Charles Darwin) ont ensuite permis à la géographie occidentale d'élargir ses champs de vision et aux géographes d'observer et d'expliquer des phénomènes à de nouvelles échelles spatiales et temporelles.

Les travaux d'Alexander von Humboldt, fondateur de la géographie moderne, et son apport au développement de nouvelles disciplines comme la climatologie, l'océanographie ou l'hydrologie, ont facilité la lecture et la compréhension des paysages tels qu'étudiés par la géographie contemporaine. Par exemple, les observations de von Humboldt au lac de Valencia (au Venezuela, en 1800) quant aux variations du niveau d'eau, aux taux d'évaporation et à la granulométrie des sols insulaires lui ont permis d'élaborer des théories liant la dynamique

hydrologique d'un plan d'eau à la composition et l'utilisation de son bassin versant (Wulf, 2016), des concepts aujourd'hui toujours centraux à l'étude des systèmes aquatiques. Ou encore, la description à la fois scientifique et poétique qu'il a fait des marais du delta de l'Orinoco et des communautés Warao qui les habitent[1] a offert à ses contemporains non seulement une meilleure compréhension de la structure des milieux humides mais aussi une réflexion sur leur importance socioculturelle et, ultimement, sur les effets des changements environnementaux d'origine anthropique sur les écosystèmes naturels (« Humboldt's Legacy », 2019). Les avancées scientifiques issues des travaux d'Alexander von Humboldt, et d'autres plus spécifiques en chimie, physique et biologie, ont ainsi mené à l'essor des sciences naturelles modernes. L'étude des écosystèmes d'eau douce (la limnologie), science développée par François-Alphonse Forel au tournant du XX^{e} siècle via ses recherches portant sur la structure et les fonctions du lac Léman (Vincent, 2014), l'étude des milieux humides et, plus largement, celle de la circulation des éléments chimiques entre les différents compartiments environnementaux (la biogéochimie) en sont de bons exemples.

> « La géographie est tenue de puiser aux mêmes sources de faits que la géologie, la physique, les sciences naturelles et, à certains égards, les sciences sociologiques. Elle se sert de notions dont quelques-unes sont l'objet d'études approfondies dans des sciences voisines [...] Dans la complexité des phénomènes qui s'entre-croisent dans la nature, il ne doit pas y avoir une seule manière d'aborder l'étude des faits; il est utile qu'ils soient envisagés sous des angles différents. Et si la géographie reprend à son compte certaines données qui portent une autre estampille, il n'y a rien dans cette appropriation qu'on puisse taxer d'anti-scientifique. » Paul Vidal de la Blache, 1913.

Nous savons donc aujourd'hui que la géographie d'un plan d'eau ou d'un milieu humide (sa position dans le continuum hydrologique, ses caractéristiques morphologiques ou encore la structure, la composition et l'utilisation de son bassin versant) détermine les patrons biogéochimiques et la magnitude des processus qui y sont à l'œuvre (Wetzel, 2001) et que l'échelle à laquelle un phénomène est étudié dicte la portée des conclusions que l'on peut en tirer. Par exemple, le métabolisme d'un écosystème aquatique (exprimé par le ratio entre la production primaire – PP – et la respiration – R) semble largement influencé par ses caractéristiques géographiques qui en contrôlent entre autres l'acidité (ou l'alcalinité) et les apports et concentrations en carbone organique dissous (DOC) (Prairie et al., 2002). Ainsi, les

[1] « The [Waraos] owe the preservation of their physical and perhaps even of their moral independence to the loose, semifluid bog soil across which they light-footedly move about [...] » Alexander von Humboldt (1849) *Views of Nature*. Traduction de l'allemand vers l'anglais par Mark W. Pearson, 2014.

lacs d'une région donnée peuvent être majoritairement autotrophes (PP > R; Carignan et al., 2000) tandis que ceux d'une région voisine, aux conditions climatiques semblables, peuvent être majoritairement hétérotrophes (R > PP; del Giorgio & Peters, 1994), en raison de différences structurelles et fonctionnelles dans leurs bassins versants. Cette situation soulève ainsi la question de l'échelle à laquelle un sujet est étudié (Seekell et al., 2018). Dans un cas comme dans l'autre, les conclusions sont robustes mais ne s'appliquent qu'à une zone géographique restreinte. N'eut été une compréhension approfondie de la géographie des systèmes étudiés, la simple extrapolation des résultats de l'une ou de l'autre des études à une échelle englobant les deux régions mènerait alors à une interprétation imprécise ou carrément erronée des patrons et processus biogéochimiques dans les écosystèmes d'intérêt. L'étude des milieux aquatiques et humides avec une lunette géographique permet cependant d'appréhender cette situation. On pourrait ainsi reconnaître la spécificité d'écosystèmes, ou simplement d'éléments particuliers du paysage, parmi d'autres qui pourraient leur ressembler mais dont la structure et les fonctions seraient invariablement distinctes. C'est dans cette optique que j'aborde l'étude des mares de tourbières.

1.2 La géographie des mares de tourbières

1.2.1 Structure et fonctions

Les tourbières sont des écosystèmes d'une importance capitale dans l'équilibre biogéochimique planétaire entre autres en raison de leur capacité à accumuler de la matière organique (MO) et séquestrer du carbone (C). Globalement, les tourbières auraient ainsi emmagasiné plus de 600 gigatonnes de C depuis le Dernier Maximum Glaciaire, il y a 20 000 ans (Yu et al., 2010). Bien que ne couvrant que 3% de la surface des terres émergées (Xu et al., 2018), elles stockeraient tout de même deux fois plus de C que les sols forestiers, tout biome confondu (Loisel et al., 2021; Pan et al., 2011).

Les mares qui se forment dans un grand nombre de tourbières de la planète pourraient être de ces écosystèmes dont l'existence et la répartition sont attestées, parfois depuis des siècles (Hamelin, 1957b), mais qui demeurent ignorés plus souvent qu'à leur tour car leur spécificité n'est pas totalement reconnue. Les études scientifiques sur les mares de tourbières, tant sur leur structure que sur leurs fonctions, sont en effet peu nombreuses comparativement à d'autres milieux aquatiques, humides ou terrestres. Il s'agirait néanmoins d'écosystèmes dont les particularités structurelles sont peu communes et qui les différencient à la fois des plans

d'eau ouverts communément étudiés en limnologie (les lacs, par exemple) et de leur environnement immédiat (la tourbière). La géographie des mares fait qu'elles se distinguent des lacs par leur très petite taille (< 2 m de profondeur et souvent moins de 2000 m^2) et par la nature presque uniquement organique, et non minérale, de la matrice dans laquelle elles se développent (voir chapitre 2). De même, parce qu'il s'agit de plans d'eau ouverts, elles sont aussi distinctes des sols qui les entourent parce que la lumière y pénètre en profondeur et que l'action du vent en favorise l'oxygénation, ce qui crée des conditions physicochimiques très différentes de celles retrouvées dans leur environnement immédiat.

D'un point de vue structurel, les mares de tourbières se situeraient donc à la jonction entre les systèmes aquatiques et terrestres, ce qui en définirait leurs fonctions écosystémiques. D'un point de vue fonctionnel, leur positionnement au croisement d'un milieu riche (l'eau des mares) et d'un milieu pauvre (la tourbe) en oxygène en ferait des environnements où les conditions sont idéales pour soutenir de forts taux de réactions biogéochimiques (Krause et al., 2017). Ainsi, les mares pourraient possiblement être qualifiées de 'points chauds biogéochimiques' (McClain et al., 2003) ou de 'points de contrôle écosystémiques' (Bernhardt et al., 2017) dans le paysage des tourbières, soit des portions du paysage situés à l'interface de différents compartiments écosystémiques (dans ce cas, la tourbe et l'eau) où les taux de réactions sont plus élevés que dans la matrice environnante et qui exercent une influence disproportionnée sur le comportement biogéochimique de l'écosystème dans lequel elles se trouvent. À l'échelle métrique, la quantité et la magnitude des processus biogéochimiques seraient alors particulièrement élevées à l'interface eau-tourbe qui caractérise le pourtour les mares. C'est entre autres dans ce dynamisme biogéochimique que réside l'intérêt d'étudier les mares de tourbières. En effet, il s'agit d'éléments du paysage des tourbières dont les fonctions diffèrent de celles de la matrice environnante puisqu'elles sont, contrairement aux sols, des sources nettes de C atmosphérique (e.g. McEnroe et al., 2009; Pelletier et al., 2014). Cette caractéristique est lourde de sens puisque des changements environnementaux, d'ordres physique, chimique, biologique ou anthropique, pourraient modifier la force ou la direction des interactions qui existent entre les mares et la tourbe (Holden et al., 2018; Tallis, 1994), et ultimement, même bouleverser la structure et les fonctions de puits de C des tourbières (Pelletier et al., 2015).

Les mares sont une composante aquatique de milieux terrestres et, à l'échelle du paysage, peuvent difficilement être séparées du milieu humide dans lequel elles s'insèrent, expliquant peut-être le peu d'intérêt scientifique qu'elles ont historiquement généré. Outre des

études sur les flux de dioxyde de carbone (CO_2) et de méthane (CH_4), la nature et la magnitude des processus biogéochimique ayant cours dans les mares de tourbières demeurent ainsi peu étudiées. On ignore donc de larges pans des cycles biogéochimiques d'autres éléments, comme l'azote (N) et le phosphore (P), et des mécanismes responsables de leur circulation dans ces systèmes. Cette thèse vise à combler en partie cette faille dans la littérature en explorant entre autres les possibles liens qui unissent la biogéochimie des mares de tourbières des zones tempérées et boréales à leurs géographies spécifiques.

1.2.2 Distribution et modes de formation

On trouve des mares autant en tourbières tropicales (e.g. Dommain et al., 2015) que tempérées (e.g. Glaser & Janssens, 1986) ou en zone de pergélisol (e.g. Laurion et al., 2010), à une élévation allant du niveau de la mer (e.g. Pelletier et al., 2014) jusqu'à plusieurs milliers de mètres d'altitude (e.g. Quenta et al., 2016), et autant en milieu ombrotrophe (e.g. Damman, 1986) que minérotrophe (e.g. Arlen-Pouliot & Payette, 2015) (Figure 1.1). Bien qu'elles se développent toutes dans une matrice similaire, composée en grande partie de matière organique, la géographie des mares de tourbières influence leurs modes de formation. En zone de pergélisol, les mares se forment principalement par l'inondation d'une dépression formée lors du dégel du sol (Vonk et al., 2015) (voir chapitre 2). En milieu tropical, les mares se forment quant à elles par le déracinement de grands arbres sous l'effet du vent, créant ainsi dans les sols des cavités qui s'emplissent de l'eau interstitielle (Dommain et al., 2015). Les études portant sur les mares de tourbières tropicales étant très parcellaires, il se peut cependant que d'autres processus mènent à leur formation.

En milieux tempérés ou en zones boréales exemptes de pergélisol, les mares de tourbières semblent se développer sous l'impulsion de différents mécanismes. En effet, diverses hypothèses ont été suggérées au cours des dernières décennies pour expliquer les processus d'initiation menant à la formation des mares. Dans les tourbières réticulées[2], Sjörs (1961) proposa que l'action du gel pouvait soulever des lanières du sol perpendiculairement à la pente

[2] « Une tourbière réticulée correspond au nid particulièrement mal drainé d'un marais ; ce centre est composé d'un faisceau (une centaine) de petites dépressions isolées par des lanières longitudinales et transversales de végétation. La réticulation est un phénomène superficiel enregistré par un tapis végétal (épais de 2 à 4 m) composé de sphaignes, de carex et d'éricacées. Les lanières ont souvent un relief de buttes (1 m de haut). Dans leur fantaisie et leur variété, les buttes et les mares montrent un certain agencement, voire même une certaine répétition dans l'espace de la même forme élémentaire, que celle-ci soit concentrique ou rectiligne. » (Hamelin, 1957a)

du sol, favorisant de fait la différenciation de la microtopographie de crêtes et de creux de la tourbière et mener à l'accumulation d'eau dans les dépressions ainsi formées (Figure 1.1). De leur côté, Swanson & Grigal (1988) ont attribué, à l'aide d'un très simple modèle incluant entre autres la hauteur de la nappe phréatique par rapport à la surface, la formation des mares à des variations aléatoires dans la microtopographie d'une tourbière. Ce modèle a été repris et complexifié par Rietkerk et al. (2004) qui ont expliqué l'initiation des mares par un effet de rétroaction de la végétation et des concentrations en nutriments dans le sol. Une hétérogénéité dans les nutriments favoriserait ainsi la différenciation spatiale des assemblages d'espèces végétales et mènerait à la formation d'une microtopographie de crêtes, peuplées de plantes vasculaires, et de creux, peuplés de mousses. L'eau s'accumulerait par la suite dans ces creux et initierait la formation des mares.

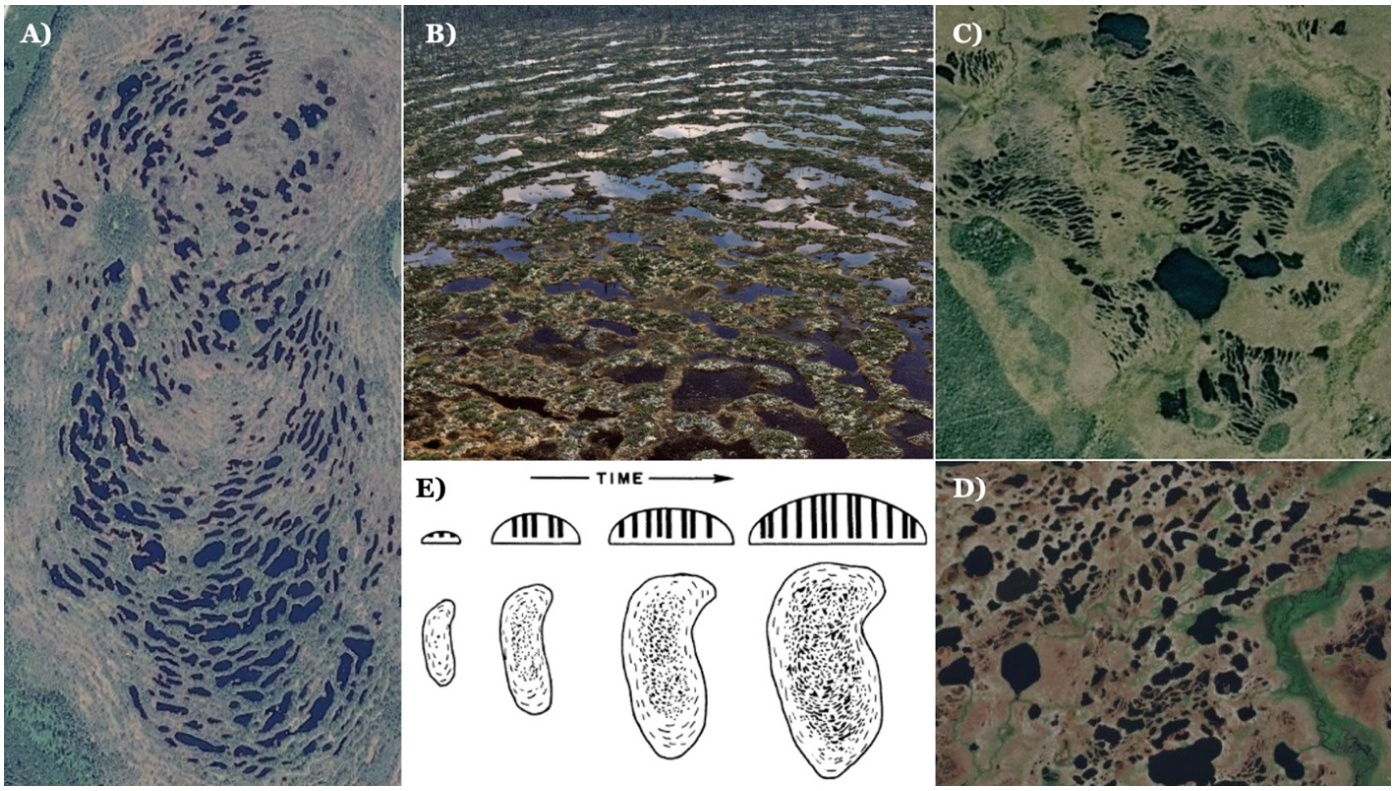

Figure 1.1. L'arrangement des mares varie dans l'espace et le temps, en fonction des caractéristiques géographiques des tourbières. La forme réticulée des tourbières A) Hammarmossen (Suède) et B) Duncan (Jamésie, Québec) contraste avec l'hétérogénéité des formes de tourbières moins surélevées de C) Russie occidentale et de D) Côte-Nord (Québec). E) La formation de la tourbière Hammarmossen a fait l'objet d'une reconstruction schématique qui retrace le dynamisme spatiotemporel de son patron de surface. Les images satellitaires (A,C et D) sont extraites de Google Earth, la photo de la tourbière Duncan (B) a été prise par Camille Laverdière et est tirée de la collection d'objets numériques de

l'Université de Montréal, et le schéma de la tourbière Hammarmossen (E) est extrait de Foster & Wright Jr, 1990.

Comas et al. (2005) ont fait état du possible contrôle de la géomorphologie sous-jacente aux tourbières pour expliquer la présence de mares sur une tourbière du nord-est des États-Unis. Les mares de cette tourbière se seraient en effet développées dans des dépressions de la surface elles-mêmes situées au-dessus d'eskers mis en place lors de la dernière glaciation. La présence des mares serait alors favorisée par une alimentation constante en eau souterraine, déviée vers la surface par les eskers, et qui s'accumulerait dans les creux de la microtopographie de la tourbière. Finalement, Belyea (2007) proposa quant à elle un modèle visant à déterminer les variables environnementales limitant l'abondance des mares qui est basé entre autres sur la situation géographique, les intrants et extrants en eau, la conductivité hydraulique des creux et crêtes de la tourbière et sa topographie. Selon ce modèle, l'inclinaison de la pente de la tourbière, autant en climat sec qu'humide, serait le principal contrôle de la présence de mares. Le nombre de mares serait ainsi plus élevé dans les tourbières ayant une pente forte (> 2%). La variable climatique influencerait indirectement l'abondance des mares en contrôlant l'assemblage végétal, la composition de la tourbe, son degré d'humification, sa conductivité hydraulique et les taux d'évapotranspiration.

Les hypothèses émises quant aux processus d'initiation des mares de tourbière font état de contrôles environnementaux différents sur les mécanismes originels de formation des mares. Il est donc difficile de déterminer avec précision ce qui en est réellement, puisque ces processus pourraient différer ou covarier dans le temps et l'espace. Le développement des mares semble en effet influencé par plusieurs variables d'ordre climatique, topographique, hydrologique, biologique et biogéochimique. Néanmoins, peu importe les mécanismes menant à la différenciation du patron de surface des tourbières, la formation des mares est initiée par l'accumulation d'eau dans les creux microtopographiques des sols qui prennent par la suite de l'expansion (Foster, Wright Jr, et al., 1988; Foster & Fritz, 1987).

1.2.3 Dynamique morphologique

Une fois initiées, les mares des tourbières tempérées et boréales se développent selon un processus de différenciation graduel du patron de surface, contrôlé par les taux d'accumulation de la MO plus faibles dans les mares que dans la tourbe sous l'impulsion de conditions physicochimiques (luminosité, température, oxygène) discordantes entre ces composantes. La plus grande pénétration de la lumière en profondeur (Hamilton et al., 1994)

et les températures et concentrations en oxygène (O_2) plus élevées (Foster & Glaser, 1986; Karofeld & Tõnisson, 2014) dans les mares que dans la tourbe y favorisent en effet des taux d'accumulation de la matière organique plus faible que dans le sol environnant. L'hydrologie des tourbières et le déplacement de l'eau et de la tourbe elle-même qui en découle influencent également le développement des mares (Belyea & Lancaster, 2002). Par exemple, l'examen d'images aériennes d'une tourbière de la Jamésie (Québec, Canada) montre des changements dans le nombre et l'arrangement spatial des mares au cours de la période 1950-2010 (Arlen-Pouliot & Payette, 2015). Toutes ces caractéristiques variant dans le temps et l'espace, elles font des mares des éléments dynamiques du paysage des tourbières et dont la morphologie et les dimensions varient à l'intérieur d'un même site (Figure 1.1) sur des échelles temporelles allant du mois (Karofeld & Tõnisson, 2014) jusqu'au siècle (Arlen-Pouliot & Payette, 2015).

En superficie, les mares peuvent atteindre plusieurs milliers de mètres carrés (e.g. Hamilton et al., 1994; Mataloni et al., 2015). Ces grandes mares sont probablement le résultat de la coalescence de plusieurs mares ayant chacune pris de l'expansion latéralement (Foster et al., 1983; Foster & Glaser, 1986), expansion exacerbée par l'érosion des berges des mares sous l'action des vagues (observation personnelle). Bien qu'il soit difficile de confirmer la coalescence de mares autrefois contigües à partir de la surface, un examen de la bathymétrie des mares permettrait d'observer ce phénomène. En effet, Foster & Fritz (1987) ont observé la présence de plusieurs bassins, sous la surface d'une mare, séparés par des crêtes de tourbes surélevées par rapport au fond, vestiges d'anciennes lanières de tourbe. Finalement, notons que la topographie des tourbières limite aussi l'étendue des mares. Dans les tourbières à forte pente (> 2%) comme les *blanket bogs*, des tourbières caractéristiques des milieux insulaires ou côtiers tempérés et qui épousent le relief du paysage sur lequel elles se forment (Rydin & Jeglum, 2013), les mares se développent perpendiculairement au gradient de surface ce qui restreint les possibilités d'expansion (Belyea, 2007; Foster & Glaser, 1986).

En profondeur, les mares seraient limitées dans leur expansion par les concentrations en O_2 et l'épaisseur de la tourbe. La plupart des mares de tourbière ne mesurent pas plus de 2 m de profondeur (e.g. Hamilton et al., 1994; Karofeld & Tõnisson, 2014; Pelletier et al., 2014) car, au-delà, les concentrations en O_2 seraient trop faibles pour soutenir une décomposition adéquate de la MO (McEnroe et al., 2009). À cette profondeur, les taux d'accumulation de la MO seraient donc égaux aux taux de décomposition. La profondeur maximale des mares est aussi limitée par des facteurs topographiques. Par exemple, les mares des tourbières ombrotrophes seraient en moyenne plus profondes que celles des *blanket bogs* (voir chapitre

3) en raison d'une plus grande épaisseur de tourbe dans laquelle les mares peuvent se développer et parce que la pente moins abrupte favorise l'accumulation de l'eau (Foster & Wright Jr, 1990).

Au cours du temps, les mares peuvent perdre en superficie et en profondeur. Les mares pourraient en effet être drainées via des canaux de surface ou souterrains (Foster, Wright Jr, et al., 1988), un phénomène particulièrement observé dans les tourbières à forte pente comme les *blanket bogs* (Holden et al., 2018). La stimulation de la croissance de la végétation arborée, sous l'effet d'un climat plus chaud, par exemple, pourrait aussi induire une hausse des taux d'évapotranspiration, une baisse dans le niveau de la nappe phréatique et mener à l'assèchement, à long terme, des mares (Arsenault et al., 2019). De plus, la présence de tapis de tourbe flottant à la surface de mares, conséquence de la formation et l'émission de bulles de méthane massives sous les sédiments de fond (Strack et al., 2005), pourrait quant à elle mener au comblement d'une mare. En effet, un tapis d'une superficie importante pourrait être colonisé rapidement par des espèces végétales avant qu'il ne soit décomposé dans la colonne d'eau (Figure 1.2). Ce tapis pourrait par la suite prendre de l'expansion jusqu'à couvrir toute la mare, réduisant de fait les concentrations en O_2 dans l'eau libre et diminuant les taux de décomposition. À terme, cette mare pourrait disparaître.

Figure 1.2. Le comblement d'une mare pourrait être le résultat de la colonisation par les plantes d'un tapis de tourbe flottant. Ce comblement semble ici être en cours et les deux flèches montrent deux mares résiduelles. En mortaise, une image extraite et modifiée de

Google Earth montrant l'extension possible maximale de cette mare. Photographie personnelle.

Les mares de tourbières sont des éléments du paysage qui présentent une dynamique morphologique caractéristique, intimement liée à sa dynamique biogéochimique. L'expansion des mares par la décomposition de la MO qui compose leur matrice résulterait en effet tout d'abord du fort gradient de température et des concentrations en O_2 qui existent entre les mares et la tourbe (Foster & Glaser, 1986). À ces gradients qui stimulent l'activité microbienne de décomposition à l'interface eau-tourbe, Hamilton et al. (1994) ont suggéré d'ajouter la présence de cyanobactéries comme facteur explicatif du dynamisme des mares. Les cyanobactéries qui tapissent le fond de certaines mares joueraient en effet le double rôle d'agent de production de O_2, via leur activité photosynthétique, et celui de producteur de N réactif via des processus de fixation. Les mares de tourbières se développant majoritairement dans des environnements pauvres en N, les cyanobactéries pourraient alors stimuler l'activité microbienne en augmentant la disponibilité de cet élément essentiel au métabolisme.

1.3 La biogéochimie des mares de tourbières

La géographie des mares de tourbières étant variable dans l'espace et le temps, il est possible et logique que leur biogéochimie le soit tout autant. Par exemple, le climat actuellement changeant (e.g. hausse des températures et modifications du régime des précipitations) pourrait modifier la structure physique des mares et bouleverser les conditions environnementales qui contrôlent leurs patrons et processus biogéochimiques.

1.3.1 Patrons biogéochimiques

Différentes études ont montré le lien entre la morphologie des mares de tourbières tempérées et boréales et leur potentiel réactif, autant en milieu ombrotrophe (e.g. McEnroe et al., 2009) que minérotrophe (e.g. Cliche Trudeau et al., 2014). À l'échelle locale, au sein d'une même tourbière tempérée, les mares de faible profondeur présentent des concentrations plus élevées en DOC, en N et en CO_2 et CH_4 dissous que les mares plus profondes (Arsenault et al., 2018; McEnroe et al., 2009). Ces différences dans la biogéochimie des mares s'expliquent d'abord et avant tout par des conditions physicochimiques (lumière, température et oxygène) plus optimales pour soutenir des taux de réactions biogéochimiques élevés dans les mares peu profondes que dans les mares plus profondes (Arsenault et al., 2018). À l'échelle régionale, une étude menée au Royaume-Uni montre des disparités dans la biogéochimie des mares de *blanket bogs* d'Écosse et d'Irlande du Nord (Turner et al., 2016). Ces variations s'expliqueraient

quant à elles par i) des mares moins profondes qu'ailleurs dans les sites du sud de l'Écosse; ii) un substrat (la tourbe) moins humifié en Irlande du Nord qui y augmenterait les concentrations en DOC; et iii) l'influence océanique que subissent certains sites où la conductivité électrique de l'eau est élevée, conséquence entre autres de fortes concentrations en anions chlorure et sulfate. Les contrôles à plus grandes échelles de la biogéochimie des mares demeurent par contre, pour le moment, peu étudiés (voir chapitre 3).

Dans les tourbières, la composition chimique des couches superficielles de la tourbe reflète l'assemblage de végétation qu'on retrouve en surface (Rydin & Jeglum, 2013). La biogéochimie des mares est aussi influencée par les assemblages de végétation qui les entourent. Ainsi, dans une tourbière ombrotrophe tempérée, les mares bordées par une végétation composée majoritairement de conifères ont des concentrations en DOC et en N plus élevées et les molécules organiques sont plus complexes que dans les mares qui se développent là où la végétation est plus clairsemée ou composée majoritairement de mousses et de petits arbustes (Arsenault et al., 2019). L'influence de la végétation sur la biogéochimie des mares pourrait alors se faire sentir à la fois par des échanges directs, via les exsudats des individus dont les racines sont dans ou près des mares, ou simplement par la décomposition de la tourbe et le lessivage de molécules organiques qu'elle contient. D'ailleurs, la majorité du DOC retrouvé dans les mares de tourbières ombrotrophes tempérées et boréales proviendrait de la végétation entourant les mares et non pas d'une production autochtone via des processus microbiens (Prijac et al., 2022).

Les tourbières ombrotrophes sont caractérisées par leur isolement du territoire environnant. Les échanges latéraux en eau et en éléments chimiques avec le reste du paysage sont en effet réduits au minimum en raison de la surélévation de ces tourbières (Rydin & Jeglum, 2013). Les apports allochtones ne s'effectuent alors que via les précipitations. Les patrons biogéochimiques des mares des tourbières ombrotrophes sont donc d'abord le reflet de facteurs internes aux tourbières et de la chimie des précipitations. Les mares de tourbières qui font l'objet de cette thèse proviennent de milieux ombrotrophes (voir chapitres 2, 3 et 4). Ceci permettrait alors d'isoler l'influence de ces facteurs environnementaux sur les processus biogéochimiques caractérisant les mares et possiblement de mettre l'emphase sur l'effet de la matrice tourbeuse sur les processus étudiés.

1.3.2 Processus biogéochimiques

La littérature susmentionnée pointe d'abord vers l'influence de l'interface eau-tourbe pour expliquer en partie les patrons biogéochimiques observés dans les mares de tourbières. Par exemple, l'activité microbienne qui y a lieu mènerait à la production de MO dissoute, via la dégradation de la tourbe, et à sa transformation, via humification ou minéralisation. Néanmoins, dans les mares de tourbières, la magnitude de ces processus de décomposition ou encore les facteurs environnementaux qui les contrôlent sont méconnus (voir chapitre 4).

Considérant la structure particulière des mares de tourbières, il se peut que les mécanismes de décomposition et leurs effets sur la circulation biogéochimique des éléments soient différents de ceux d'autres systèmes aquatiques ou terrestres. La géographie d'un environnement est en effet au cœur des processus de décomposition car elle contrôle à la fois la qualité et la quantité de substrat à décomposer, et les conditions environnementales dans lesquels ont lieu ces processus (Conant et al., 2011; Schmidt et al., 2011). Par exemple, le climat et les caractéristiques chimiques de la litière seraient les principaux facteurs de contrôle des taux de décompositions de la MO des sols forestiers (Joly et al., 2023). La variable climatique serait par contre moins importante pour expliquer les variations dans les taux de décomposition dans les sols des tourbières, où la décomposition serait contrôlée d'abord et avant tout par la qualité du substrat et hauteur de la nappe phréatique et la disponibilité en O_2 (Moore et al., 2007).

Les conditions environnementales locales seraient particulièrement importantes pour contrôler les taux de décomposition de la MO dans les écosystèmes terrestres et aquatiques (e.g. Aerts, 1997; DeGasparro et al., 2020). À large échelle, le climat serait le principal facteur déterminant la décomposition de la litière tandis qu'à l'échelle locale ou sous climat semblable, la qualité de la MO qui compose la litière serait le facteur dominant (Joly et al., 2023). Dans les milieux aquatiques comme les mares de tourbières, les concentrations en O_2 dissous influencent fortement les processus de décomposition de la litière fraîche. En effet, des concentrations élevées en O_2 dissous favorisent entre autres la remise en circulation du C et du N de la MO et augmentent la proportion d'organismes décomposeurs dans les communautés microbiennes (Liu et al., 2022). Dans les mares de tourbières, les concentrations en O_2 diminuent rapidement avec la profondeur, ce qui pourrait mener à des variations spatiales importantes dans les taux de décomposition entre des mares qui seraient contigües mais de tailles différentes (voir chapitre 4). La présence de tapis de cyanobactéries sur les sédiments des mares pourraient aussi augmenter les concentrations en O_2 à l'interface eau-tourbe,

faciliter la décomposition de la MO et la remise en circulation des nutriments qu'elle contient (Arsenault et al., 2018; Hamilton et al., 1994).

Les processus de décomposition dans les mares de tourbières sont peu étudiés, mais demeurent primordiaux à la compréhension de leur structure et de leurs fonctions. Les mares de tourbières sont des écosystèmes hétérotrophes, où les taux de respiration surpassent largement les taux de production primaire (Wetzel, 2001), qui se développent à l'intérieur d'écosystèmes autotrophes. La décomposition qui s'opère dans les mares de tourbières permet alors de les définir en tant qu'écosystèmes (des éléments du paysage où les flux de C sont contraires à ceux de la matrice environnante) et aussi en tant que possible points chauds biogéochimiques, tel qu'énoncé précédemment.

1.4 Objectifs et structure de la thèse

Loin d'être des acteurs passifs des cycles biogéochimiques du C, du N et du P (Maranger et al., 2018), les écosystèmes aquatiques forment un continuum, constitué d'une multitude de milieux différents, le long duquel l'eau et les éléments chimiques circulent, s'accumulent et se transforment (Ward et al, 2017). Par exemple, les lacs, rivières et réservoirs du monde accumuleraient dans leurs sédiments 150 Tg C, 16 Tg N et 5 Tg P par année et émettraient 1850 Tg C, sous forme de CO_2 et CH_4, et 39 Tg N sous forme de protoxyde d'azote (N_2O) (Maranger et al., 2018). D'ailleurs, les exercices d'estimations de la contribution des lacs, rivières et réservoirs aux cycles biogéochimiques globaux sont nombreux et facilités par le grand nombre de données disponibles sur ces systèmes (e.g. Bastviken et al., 2011; DelSontro et al., 2018; Raymond et al., 2013).

Malgré leur signalement dans les écrits scientifiques dès la fin du 18^{e} siècle (Hamelin, 1957), les mares de tourbières sont des systèmes aujourd'hui toujours peu étudiés. Outre des hypothèses sur les processus menant à leur développement et aux quelques études s'étant penchées sur des aspects spécifiques de leur biogéochimie (e.g. Pelletier et al., 2015; Turner et al., 2016) ou de leur biodiversité (e.g. Fontaine et al., 2007; Quiroga et al., 2013), leurs structures et leurs fonctions au sein des paysages demeurent méconnues. Le nombre de mares de tourbières et la superficie qu'elles occupent sur la planète sont d'ailleurs toujours ignorés, contrairement à d'autres systèmes aquatiques (e.g. Downing, 2012; Verpoorter et al., 2014). Ainsi, tout effort pour déterminer leur rôle dans les cycles biogéochimiques locaux et globaux est freiné par le manque de connaissances sur leur géographie et de son effet sur la biogéochimie de ces systèmes.

Dans ce contexte, l'objectif principal de cette thèse est de déterminer en quoi la géographie particulière des mares de tourbières tempérées influence leurs patrons et processus biogéochimiques. Plus précisément, les buts recherchés sont de i) définir la spécificité biogéochimique des mares de tourbières parmi les écosystèmes aquatiques; ii) déterminer les contrôles géographiques des patrons biogéochimiques des mares de tourbières tempérées; et iii) évaluer l'influence de l'interface eau-tourbe dans les processus biogéochimiques à l'œuvre dans les mares de tourbières (Figure 1.3). La thèse est séparée en quatre chapitres distincts (chapitres 2 à 5) permettant de rencontrer ces objectifs.

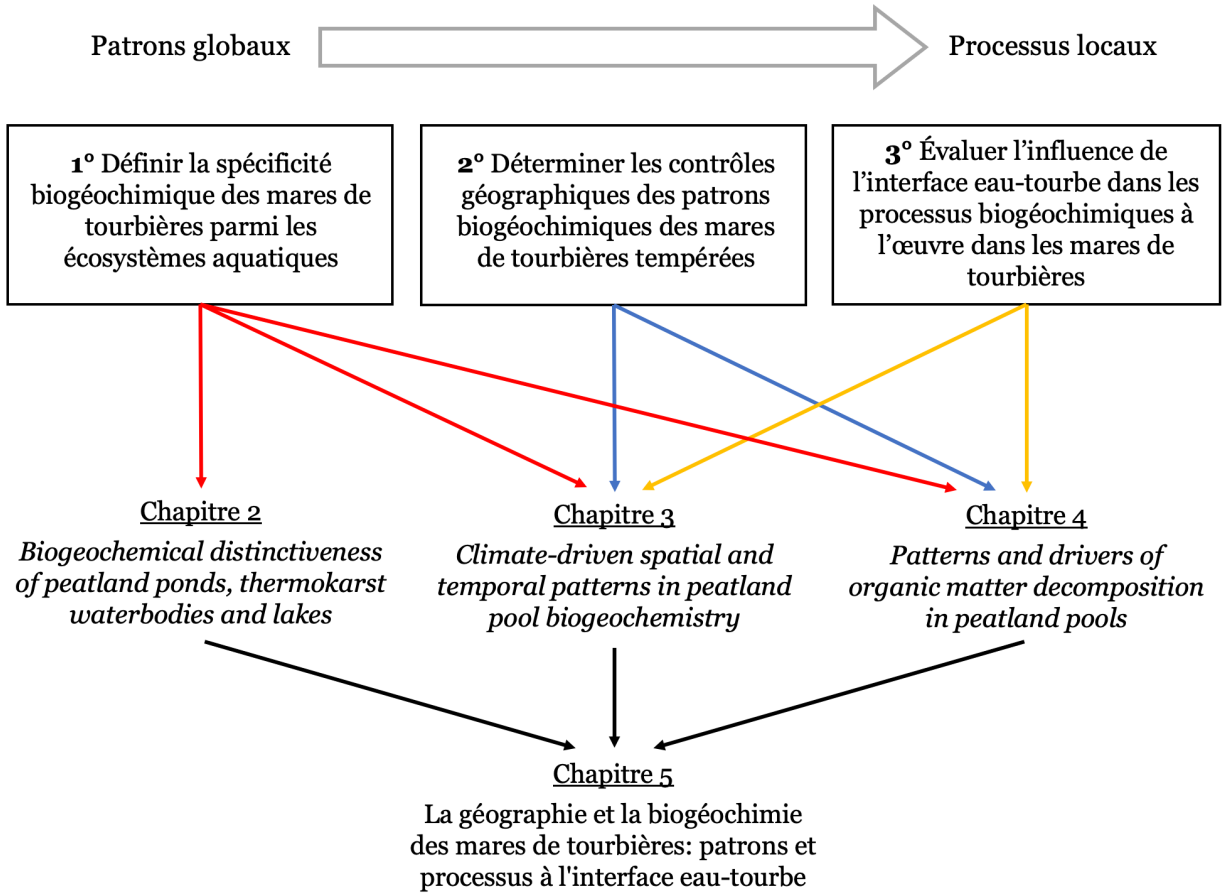

Figure 1.3. Design conceptuel de la thèse. Les chapitres 2 à 4 consistent en des articles scientifiques qui sont ou seront soumis pour publication dans des revues spécialisées et qui permettent de rencontrer les trois objectifs spécifiques de la thèse. Une combinaison de travail de terrain, en laboratoire et de recherche bibliographique forme le cœur des méthodologies utilisées. Le chapitre 5 permet de lier les résultats de chacune des études et d'atteindre l'objectif principal de la thèse, qui vise à la déterminer en quoi la géographie particulière des mares de tourbières des régions tempérées influence leurs patrons et processus biogéochimiques.

Le premier de ces chapitres consiste en une analyse comparative de la biogéochimie de plus de 12 000 plans d'eau répartis globalement. Le but de cette section est d'identifier les distinctions et similitudes biogéochimiques entre trois types d'écosystèmes aquatiques : les lacs, les plans d'eau thermokarstiques et les mares de tourbières. Le chapitre suivant est une étude des variations spatiotemporelles de la biogéochimie des mares. En comparant des données provenant de sites aux caractéristiques géographiques variées, dont un faisant l'objet d'un monitoring depuis 2016, cette section permet d'abord d'évaluer les différences spatiales et l'évolution temporelle de la biogéochimie des mares et d'identifier les facteurs géographiques responsables de telles variations. Le quatrième chapitre de la thèse rapporte les résultats d'une étude visant à déterminer les facteurs environnementaux qui contrôlent les processus biogéochimiques de décomposition de la MO dans les mares d'une tourbière du sud du Québec. Ces trois sections font finalement l'objet d'une discussion (chapitre 5) portant spécifiquement sur les liens entre la biogéochimie observée des mares de tourbières et leur géographie.

Chapitre 2. *Biogeochemical distinctiveness of peatland ponds, thermokarst waterbodies and lakes*

2.1 Avant-propos

Ce chapitre présente les résultats d'une étude comparative de la biogéochimie de plus de 12 000 plans d'eau répartis globalement. Le but de cet article est d'identifier les distinctions et similitudes biogéochimiques entre trois types d'écosystèmes aquatiques : les lacs, les plans d'eau thermokarstiques et les mares de tourbières. Cette étude a été conçue et imaginée par Julie Talbot, Jean-François Lapierre et moi-même. J'ai dirigé la collecte des données, effectué leur traitement et leur analyse, et rédigé l'article scientifique. Les co-auteurs ont toutes et tous aidé à la collecte des données et participé à l'enrichissement du propos. L'article a été publié dans la revue *Geophysical Research Letters* en juin 2022.

Référence complète :

Arsenault, J., Talbot, J., Brown, L., Holden, J., Martinez-Cruz, K., Sepulveda-Jauregui, A., Swindles, G. T., Wauthy, M., & Lapierre, J. F. (2022). Biogeochemical distinctiveness of peatland ponds, thermokarst waterbodies, and lakes. *Geophysical Research Letters, 49*: e2021GL097492

2.2 Abstract

Small lentic freshwater ecosystems play a disproportionate role in global biogeochemical cycles by processing large amounts of carbon (C), nitrogen (N) and phosphorus (P), but it is unlikely that they behave as one homogenous group for the purpose of extrapolation. Here, we synthesize biogeochemical data from > 12,000 geographically distinct freshwater systems: lakes, peatland ponds and thermokarst waterbodies. We show that peatland ponds are biogeochemically distinct from the more widely studied lake systems, while thermokarst waterbodies share characteristics with peatland ponds, lakes, or both. For any given size or depth, peatland ponds tend to have dissolved organic carbon concentrations several-fold higher and are 100-fold more acidic than lakes because of the organic matter-rich settings in which they develop. The biogeochemical distinctiveness of freshwater ecosystems highlights the need to account for the fundamental differences in sources and processing of organic matter to understand and predict their role in global biogeochemical cycles.

2.3 Introduction

Small waterbodies are major components of global biogeochemical cycles, despite their limited areal extent, as they display high biogeochemical processing rates compared to larger lakes, terrestrial or marine ecosystems (Downing, 2010; Kortelainen et al., 2006). Very small waterbodies (< 0.001 km^2) have been estimated to account for 15% of the carbon dioxide (CO_2) and ~37% of the diffusive methane (CH_4) emissions from lentic systems, despite only representing 8.6% of the global area of static surface freshwater bodies (Holgerson & Raymond, 2016; Rosentreter et al., 2021). An unquantified portion of small waterbodies consists of ponds commonly found in peatlands (Belyea & Lancaster, 2002), and thermokarst waterbodies (lakes and ponds) that form following water accumulation in soil depressions after the subsidence of thawing permafrost (Vonk et al., 2015). Thermokarst waterbodies account for approximately 25% of the total area covered by open freshwaters in the Arctic (Wauthy et al., 2018) and are estimated to cover a total of ~1,300,000 km^2 of the northern circumpolar permafrost region (Olefeldt et al., 2016). Estimates of the extent of peatland ponds are currently limited to the boreal-arctic domain where peatland waterbodies cover ~260,000 km^2. Thermokarst waterbodies and peatland ponds are highly reactive, with CO_2 and CH_4 fluxes estimated to be up to 10- and 2-fold higher, respectively, than lakes and impoundments, but these estimates are based on scarce data when compared to lakes (DelSontro et al., 2018; Hamilton et al., 1994; Kuhn, Varner, et al., 2021; Laurion et al., 2010; Pelletier et al., 2014; Serikova et al., 2019).

Lakes and ponds have no clear-cut definition, and their distinction is usually based on size, mostly surface area. Beyond size, the interaction of peatland ponds and thermokarst waterbodies with the surrounding landscape is different to non-thermokarst and non-peatland lakes and impoundments developing in geological depressions (hereafter simply referred to as lakes) because of the absence of extended watersheds (Arsenault et al., 2019; Holden et al., 2018; Kokelj & Jorgenson, 2013). Peatland ponds, especially, differ from lakes because they develop in organic-rich peat deposits. Thermokarst waterbodies are included in a vast group of systems formed by periglacial processes and comprise lakes and ponds that develop either in mineral or organic-rich permafrost and yedoma (carbon-rich, fine-textured, frozen aeolian sediments) (Elder et al., 2018; Kokelj & Jorgenson, 2013; Laurion et al., 2010). This results in a wide variety of transparencies and trophic conditions (Vonk et al., 2015; Wauthy et al., 2018) that often occupy extreme ends of lake gradients, but few studies have differentiated the effect of the surrounding matrix (organic or mineral) of thermokarst waterbodies on their biogeochemistry (Heslop et al., 2015). Hence, we postulate that while waterbodies form a continuum along environmental gradients, systems generally identified as peatland ponds and thermokarst waterbodies differ from lakes because of the large influence that climate and surficial material have on their development (Foster, King, et al., 1988; Kokelj & Jorgenson, 2013) and biogeochemistry (Kuhn, Thompson, et al., 2021; Wik et al., 2016).

Despite the growing interest in studying peatland ponds and thermokarst waterbodies given their responses to global change (Karofeld & Tõnisson, 2014; Serikova et al., 2019; Walter Anthony et al., 2018), knowledge of these systems is lagging behind other freshwater ecosystems. Because of the unique settings in which they develop, peatland ponds and thermokarst waterbodies are likely to show atypical combinations of morphometric and chemical properties among lentic systems. Recent studies have described the distribution and characteristics of peatland ponds and thermokarst waterbodies in specific regions of the world (e.g. Kuhn, Varner, et al., 2021; Stolpmann et al., 2021; Wik et al., 2016) or characterized the biogeochemistry of globally distributed freshwater systems without differentiating the matrix in which they develop (e.g. Abell et al., 2012; Sobek et al., 2010). However, currently, most freshwater models do not consider the heterogeneity in the biogeochemical processes among different types of lentic systems (Jones et al., 2018), limiting the robustness of regional estimates of C fluxes (Zwart et al., 2018) and their integration in earth system models. In this context, our aim was to identify the common and distinguishing features of lakes, peatland ponds and thermokarst waterbodies, in order to determine if these different ecosystems should

warrant system-specific scaling relationships and aid our understanding of such waterbodies. We focus on biogeochemical indicators that are central to ecosystem functioning and that are widely reported: pH, and dissolved organic carbon (DOC), total nitrogen (TN) and total phosphorus (TP) concentrations.

2.4 Methods

2.4.1 Data compilation

We initially classified lentic freshwater ecosystems in three broad categories, based on the nomenclature used in the articles from which data were extracted: (1) lakes, which develop in geological depressions not created by periglacial processes and in non-peatland settings; (2) thermokarst waterbodies, created by periglacial processes regardless of the matrix (organic or mineral) in which they develop; and (3) peatland ponds, defined as water filled depressions in organic soils not influenced by permafrost. All waterbodies found in peatlands of the continuous and discontinuous permafrost regions were considered as the result of thawing processes and thus categorized as thermokarst waterbodies.

We gathered morphometrical (area, depth) and chemical (pH, DOC, TN, TP) data for 11,357 lakes worldwide, 827 thermokarst waterbodies from the Arctic circumpolar and the Himalaya regions and 291 peatland ponds from North America, Europe and Patagonia, from published and unpublished sources (Figure 2.1; Annexe I, Text S2.1). We excluded systems that were clearly another type of aquatic ecosystem than lake, thermokarst waterbody or peatland pond (e.g. hydroelectric reservoirs, retention basins, vernal ponds). To avoid pseudoreplication and double-counting issues, we excluded duplicates from our dataset based on matching coordinates. Where repeated datasets were available for a variable in a single waterbody, means were calculated and used to average sampling effects of covariates such as seasonality and/or sample collector effects.

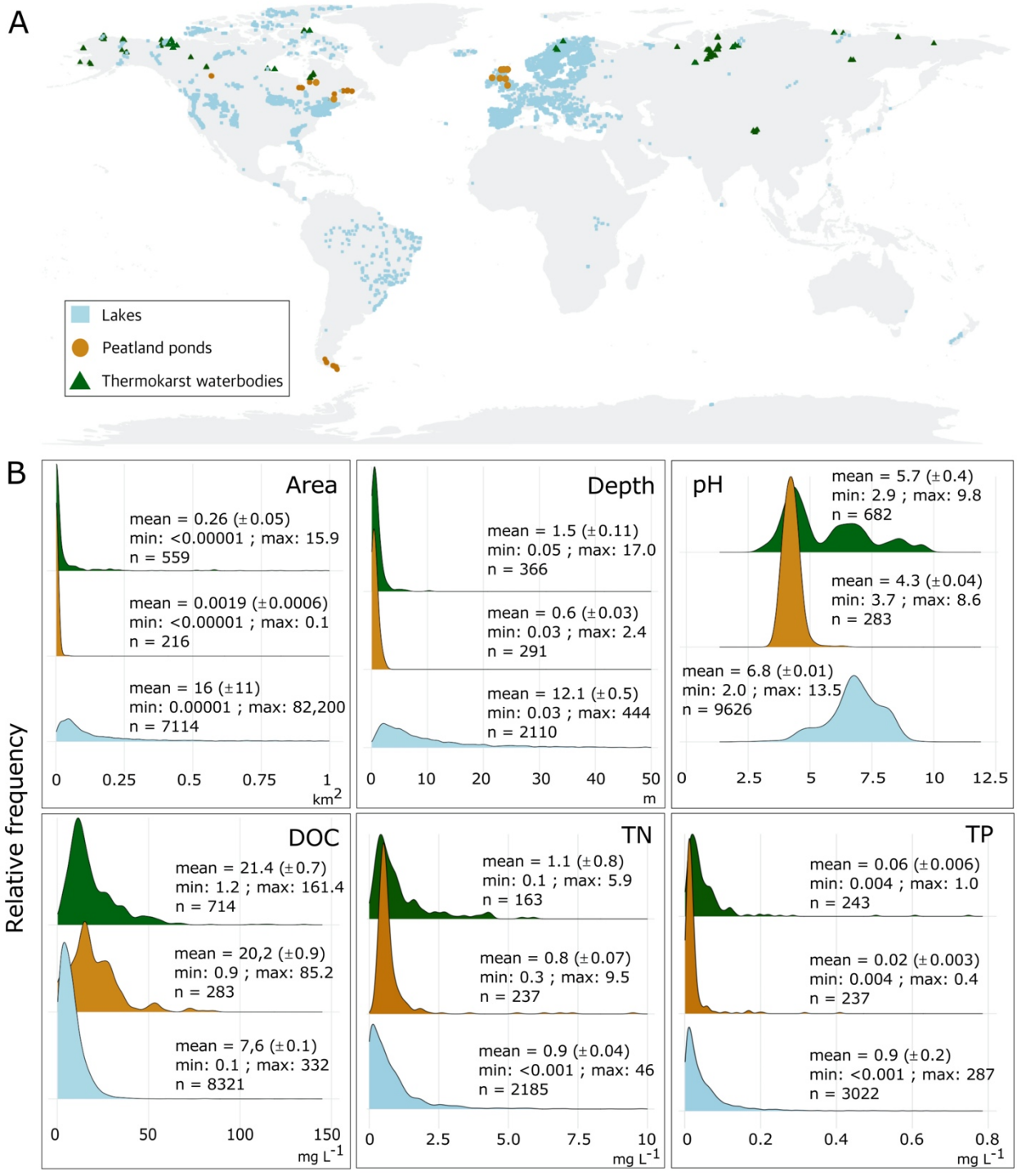

Figure 2.1. Biogeochemical properties of globally distributed peatland ponds, thermokarst waterbodies and lakes A) Global distribution of freshwater ecosystems for which we gathered morphometrical and chemical data. B) Relative frequency distributions, and mean (± standard error), minimum and maximum values for area, depth, pH and dissolved organic carbon (DOC), total nitrogen (TN) and total phosphorus (TP) concentrations.

2.4.2 Statistical analysis

The categories (lakes, thermokarst waterbodies and peatland ponds) we compared were broad representations and include systems found in relatively distinct environmental conditions. To compare the properties of freshwater ecosystems according to these groupings, we first ran general linear models (GLM) with biogeochemical variables as response variables and categories as predictors. However, to uncover in greater detail the environmental gradients associated with waterbody biogeochemistry and test the *a priori* classification, we used data-driven k-means analyses followed by principal component analyses (PCA), and a discriminant analysis. We also created a classification tree to determine the variables linked to each ecosystem's distinctiveness (Annexe I, Text S2.1 for detailed methodology).

2.5 Results and discussion

2.5.1 The biogeochemistry of globally distributed peatland ponds, thermokarst waterbodies and lakes

The dataset we assembled encompasses a total of 12,475 observations, ranging from small and shallow freshwater ecosystems located in agricultural settings, permafrost regions and peatlands, to very large and deep lakes with watersheds spanning thousands of square kilometers (Figure 2.1). This mosaic of landscapes includes a highly diverse range of aquatic ecosystems, with large variations in dissolved C and nutrient concentrations. The small amount of available data from peatland ponds and thermokarst waterbodies compared to lakes results in imbalanced sample sizes but our results nonetheless highlight major differences among the systems in both morphometrical (area and depth) and chemical variables (DOC, pH, TN and TP), especially when comparing lakes to peatland ponds (Figure 2.2).

The *a priori* classification of our dataset shows that area and depth, which are often used to define lakes and ponds, are typically lower in peatland ponds and thermokarst waterbodies than in lakes (general linear models, GLM: n = 7678; $P < 0.001$, and n = 2563; $P < 0.001$, respectively, Figure 2.1B; Annexe I, Table S2.1). There may be a bias for data availability toward large versus small lakes (Stanley et al., 2019), as we report that 50% of lakes are > 0.32 km^2 (Figure 2.1B). This differs from remote-sensing studies that estimated that 96% of the world's lakes are < 0.1 km^2 (Cael et al., 2017; Verpoorter et al., 2014), but it is unclear whether or not small peatland ponds and thermokarst waterbodies are included as lakes in these analyses. Regardless, peatland ponds in our dataset never exceeded 0.1 km^2 and 66% of

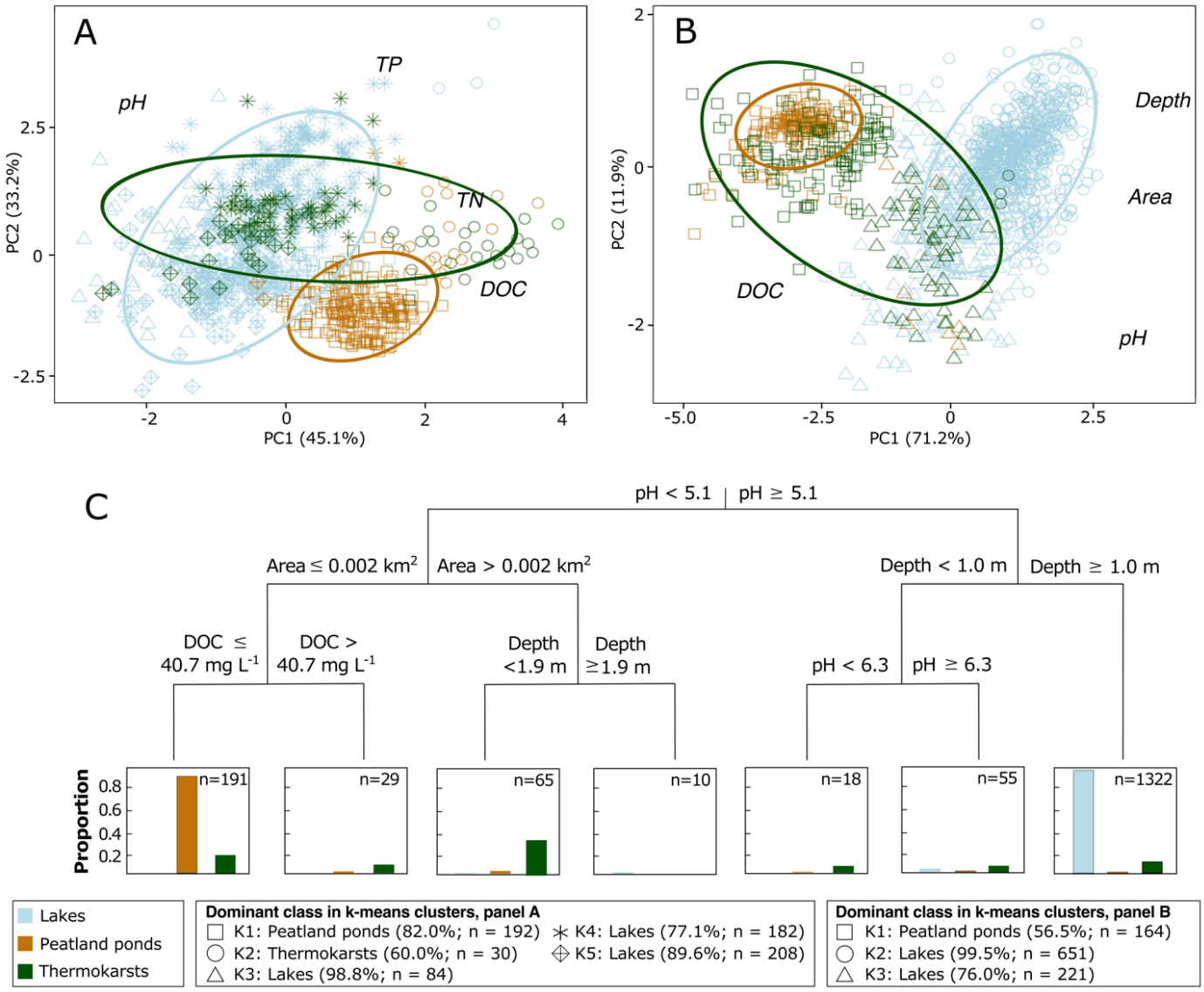

Figure 2.2. The distinctiveness of peatland ponds, thermokarst waterbodies and lakes is highlighted when comparing their different morphometric and biogeochemical properties. Principal component analysis of A) water chemistry focusing on sites for which pH, and dissolved organic carbon (DOC), total phosphorus (TP) and total nitrogen (TN) concentrations were available (n = 837), and B) small waterbodies of less than 0.1 km² for which data for morphometric properties and DOC and pH were available (n = 1235). Color code represents *a priori* classification mentioned in previous studies, whereas shape of the signs corresponds to k-means clusters (see Table S2 and S3 for details). C) Classification tree showing the distinction between lake and peatland pond biogeochemistry, and the ambivalent behaviour of thermokarst waterbodies (n = 1690, including 1347 lakes, 166 peatland ponds and 177 thermokarst waterbodies). Leaves of terminal nodes show the number of categorized waterbodies (n=) and the proportion of the systems predicted.

thermokarst waterbodies were < 0.01 km², suggesting that there is a true difference in the mean and upper limit for area and depth for peatland ponds compared to lakes, and that thermokarst waterbodies cover a range that encompasses both lakes and peatland ponds, while being skewed toward smaller values. Lake depth and area are limited by the geomorphology of the landscape and the mass water balance of the system. Peatland ponds and thermokarst waterbodies are dynamic systems that expand and contract over time, sometimes on a daily basis (Karofeld & Tõnisson, 2014), in relation to climatic, biological and physicochemical factors. In contrast, most lake depths and areas are rather stable in time when the landscape is undisturbed by human activities (Downing, 2010; Wetzel, 2001). Peatland ponds and thermokarst waterbodies can shrink and disappear following drainage (Bouchard et al., 2020; Foster, Wright Jr, et al., 1988), terrestrialization through vegetation growth, peat accumulation (Payette et al., 2004), or increased evapotranspiration (Riordan et al., 2006). These systems can, albeit rarely, reach thousands of square meters in extent for peatland ponds and several square kilometers for thermokarst systems as adjacent waterbodies may coalesce after bank erosion or soil organic matter (OM) decomposition (Bouchard et al., 2020; Foster & Fritz, 1987; Kokelj & Jorgenson, 2013), releasing millennial-old C in the process (Walter Anthony et al., 2018). With permafrost regions and temperate wetlands being highly sensitive to global change, future trends in peatland pond and thermokarst waterbody coverage and their influence on global biogeochemistry are particularly uncertain.

There are very few data on the biogeochemistry of peatland ponds, and those that exist originate primarily from temperate peatlands characterized by an organic and acidic matrix. This results in higher DOC concentrations (GLM; $P < 0.001$) and lower water pH ($P < 0.001$) when compared to lakes (Figure 2.1B; Figure 2.2; Annexe I, Table S2.1). In colder climates, many thermokarst waterbodies similarly develop in OM-rich soils, coherent with the higher DOC concentrations ($P < 0.001$) and lower pH ($P < 0.001$) than lakes (Figure 2.1B; Figure 2.2). In these peatland ponds and thermokarst waterbodies, the extensive interface between the oxygenated and DOC-concentrated water, and the anoxic character of the surrounding organic soil, creates ideal conditions for high biogeochemical activity. This sustains both elevated C emissions (peatland ponds, range = 20-103 g C m^{-2} yr^{-1}; thermokarst waterbodies, range = 219-1934 g C m^{-2} yr^{-1}), and nutrient release from decomposition processes as previously documented (McEnroe et al., 2009; Pelletier et al., 2014; Sepulveda-Jauregui et al., 2015; Serikova et al., 2019).

A large quantity of nutrients is processed within lakes where light penetration and water temperature influence their biogeochemical cycling (Cory & Kling, 2018; Maranger et al., 2018). However, generally lakes receive most of their nutrients from their watershed and nutrient concentrations are therefore not only linked to within-lake biogeochemical cycling but also to patterns and processes occurring upstream and in the surrounding landscape. Large variations in lake-landscape contexts in our dataset could thus explain the high range of observed nutrient data in lakes (Figure 2.1B) (Soranno et al., 2009). Indeed, lakes drain much larger catchments, sometimes perturbed by human activity, from which they receive OM and nutrients (Walter et al., 2020). On the other hand, nutrient concentrations vary less in peatland ponds and in thermokarst waterbodies presumably because of their development in smaller, and likely more homogeneous landscapes, and with much lower freshwater volumes (Arsenault et al., 2019; Holden et al., 2018; Kokelj & Jorgenson, 2013) compared to lakes.

2.5.2 Distinguishing freshwater ecosystem types

Peatland ponds and thermokarst waterbodies for which data were available had relatively narrower geographical contexts (Figure 2.1A) compared to lakes. It is unclear how the available data represent the true distribution of peatland ponds as we were unable to find datasets from tropical areas and large portions of temperate regions. By definition, thermokarst waterbodies will naturally be found in cold climates with little human land use. Nonetheless, despite these major differences in geographic coverage, there were no clear differences between the biogeochemical properties of thermokarst waterbodies and lakes and peatland ponds, but appreciable distinction emerged between lakes and peatland ponds (Figure 2.2).

By aggregating the systems solely according to their biogeochemistry, the k-means clustering highlights the contrasting characteristics of peatland ponds, thermokarst waterbodies and lakes (Annexe I, Table S2.2). It emphasizes how ecosystems *a priori* identified as lakes are scattered among four of the five clusters, with a wide range of biogeochemical properties, whereas ecosystems *a priori* identified as peatland ponds are mostly clustered in a fifth cluster (squares in Figure 2.2A). Ecosystems *a priori* classified as thermokarst were mostly found among lake-like clusters, with 69% of the thermokarst waterbodies (n = 74) found in two clusters dominated largely by lakes (n = 390, 76% of lakes) rather than by peatland ponds (n = 4, 2% of peatland ponds). This shows the similarity of thermokarst waterbodies to lake biogeochemistry, meaning that they tend to have similar concentrations, but also combinations of DOC, TN, TP and pH. The ordination of the k-means in a reduced space further supports the

differences and similarities between the freshwater ecosystems (Figure 2.2A). The observed pattern also holds when comparing freshwater ecosystems of all area and depth: peatland ponds and lakes form distinct types of ecosystems, clearly differentiated by their pH, while thermokarst waterbodies have multiple combinations of physical and chemical characteristics (Figure 2.2C).

Overall, lakes and peatland ponds thus behave as two divergent freshwater ecosystems with very little overlap in terms of the combination of their morphometric and chemical properties (Figure 2.2). This apparent pattern is supported by a discriminant analysis model that correctly predicts 94.2% (n = 340) of lakes and 95.3% (n = 142) of peatland ponds but fails to correctly identify 66.6% (n = 50) of the thermokarst waterbodies (Annexe I, Table S2.4). In fact, most of the thermokarst waterbodies (65.3%; n = 49) were predicted as lakes. This suggests that systems that have been identified as thermokarst waterbodies may not represent a homogenous group with a distinct combination of biogeochemical properties, but rather behave either as a peatland pond, a lake, or as a combination of both (Figure 2.2). Although many lakes and ponds of the permafrost regions are considered thermokarst waterbodies because of the mechanisms leading to their formation, it is well known that these systems develop in a wide variety of matrices that influence their biogeochemistry (Elder et al., 2018; Sepulveda-Jauregui et al., 2015). This is supported by their bimodal distribution for pH, as well as the multiple shoulders in nutrients and DOC concentrations that align well with either lake or peatland pond distributions (Figure 2.1).

We suggest that the OM-rich setting in which peatland ponds develop represents the fundamental difference that positions typical lakes and peatland ponds at opposite ends of the biogeochemical gradients, and that the underlying matrix for thermokarst waterbodies determine whether they behave as a lake or a peatland pond. For example, many thermokarst waterbodies primarily form in OM-rich permafrost, showing increasing pH with developmental stages (Peura et al., 2020), but decreasing pH with latitude because of the reduced peat thickness in higher latitudes from which to receive acidic OM (Pokrovsky et al., 2014). Thermokarst waterbodies may also form in mineral-rich soils and yedoma and have neutral to alkaline pH (Calmels et al., 2008; Rautio et al., 2011; Sepulveda-Jauregui et al., 2015) (Figure 2.1B), leading to large spatial variations in chemical and biological characteristics of these freshwater ecosystems (Rautio et al., 2011; Vonk et al., 2015). Like thermokarst waterbodies, previous studies have reported waterbodies in peatlands with different levels of transparency and pH close to neutral (Quenta et al., 2016). These were however typically found over very

shallow peat deposits (< 40 cm) of mountainous regions and had inorganic bed material, contrary to most other peatland ponds, supporting the idea that within the broad categories defined here, there is an array of possible conditions controlling pond biogeochemistry that are ultimately linked to the surrounding matrix and developmental mechanisms.

2.5.3 The distinct biogeochemistry of peatland ponds: more than small lakes

Both *a priori* and data-driven classifications showed that peatland ponds and thermokarst waterbodies were typically smaller and shallower than lakes (Figure 2.1B; Figure 2.2). It is well known that larger lakes tend to have lower concentrations of elements because of higher retention times and smaller interfaces with C- and nutrient-rich sediments and soils (Downing, 2010; Holgerson & Raymond, 2016). If peatland ponds and thermokarst waterbodies behaved as small lakes, it could be possible to make global predictions for these systems based on widely available lake data. If, on the other hand, they display a distinct biogeochemistry, then knowledge and scaling relationships derived from lakes cannot be transposed to predict the role of peatland ponds and thermokarst waterbodies in global biogeochemical cycles.

Even when comparing only freshwater ecosystems of small extent (< 0.1 km^2), our results suggest that peatland ponds do not function simply as small lakes (Figure 2.2B; Annexe I, Table S2.3). The intermediate and more variable patterns for the population of thermokarst waterbodies (Figure 2.1; Figure 2.2) also hold even when considering size- or depth-specific patterns (Figure 2.3), likely because this category of aquatic ecosystems includes systems developing in both mineral- and OM-rich matrices. In particular, our results demonstrate that peatland ponds and thermokarst waterbodies are ecosystems that are more connected to their surroundings than lakes, with the DOC available for biological and photochemical reactions being on average more than twice higher than for lakes, as well as a pH that can be as much as four orders of magnitude more acid, especially for the smaller peatland ponds and thermokarst waterbodies (Figure 2.3). Moreover, TN and TP concentrations in peatland ponds (GLM; TN: $P = 0.381$, and TP: $P = 0.135$; Annexe I, Table S2.1) and thermokarst waterbodies (GLM; TN: $P = 0.206$, and TP: $P = 0.145$; Annexe I, Table S2.1) are comparable to those observed in lakes, although lakes drain much larger watersheds from which to receive nutrients (Arsenault et al., 2019; Kokelj & Jorgenson, 2013; Walter et al., 2020). Then, if TN and TP concentrations in freshwater ecosystems were to be compared in terms of units of drained area, nutrient

concentrations would be much higher in peatland ponds and thermokarst waterbodies than in lakes, highlighting the distinctiveness of such systems.

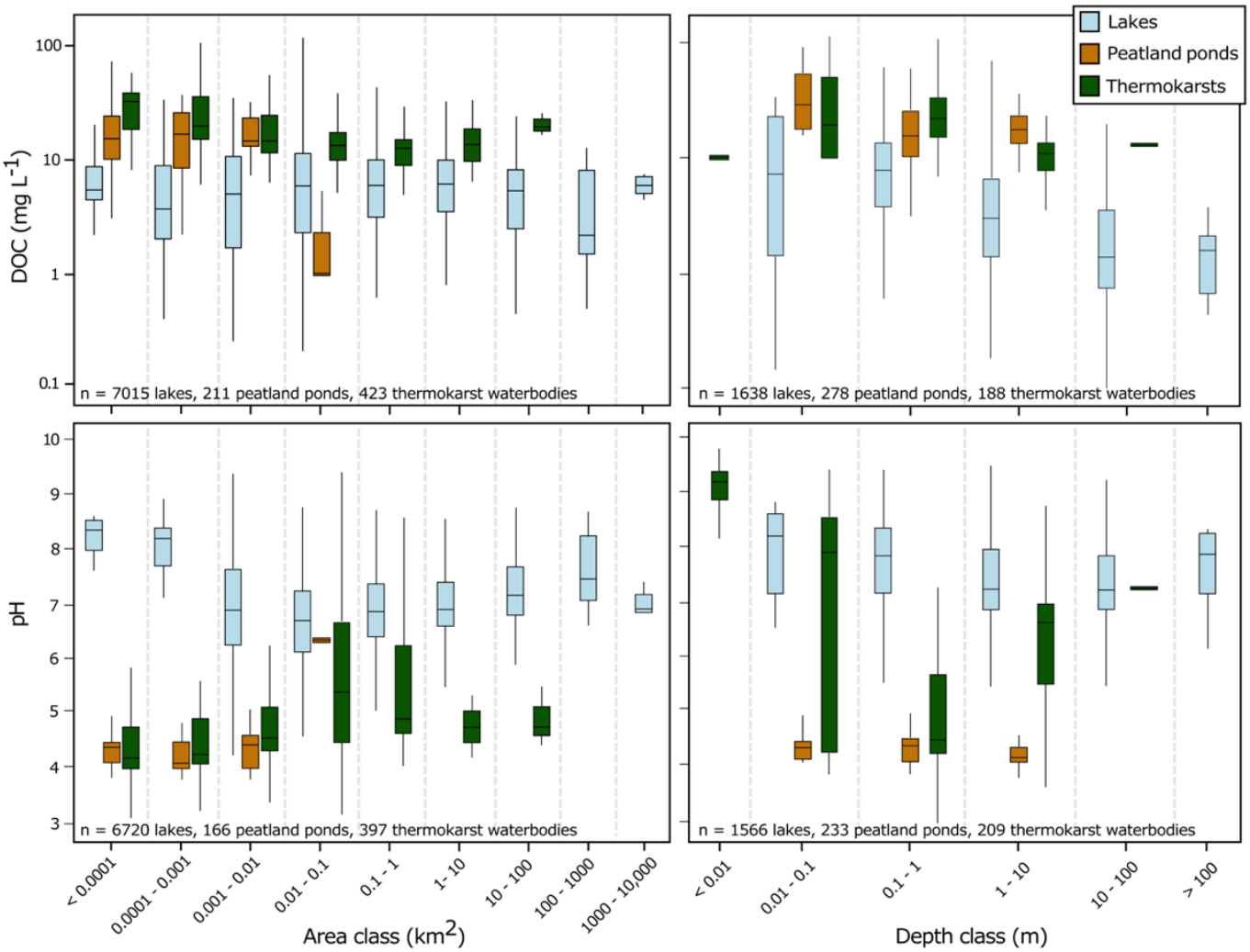

Figure 2.3. Distribution of dissolved organic carbon (DOC) concentration and pH in relation to area and depth for peatland ponds, thermokarst waterbodies and lakes. Generalized linear models show that variations in DOC concentrations are only related to freshwater system type, and not to area or depth (GLM, $P > 0.1$; Annexe I, Table S2.4). Interactions between the type of system and area may, however, explain variations in pH between lakes, peatland ponds and thermokarst waterbodies (GLM, $P < 0.05$; Supplementary Table 4). Boxes show the median and the 25th and 75th percentiles of the distributions, whiskers show the 10th and 90th percentiles.

Globally, lentic ecosystems emit 1.25-2.3 Pg C yr^{-1}, most of which likely originates from small freshwater systems (DelSontro et al., 2018). Most estimates of greenhouse gas emissions from limnological systems are based on the size of the systems and their C content (Bastviken et al., 2011; DelSontro et al., 2018; Raymond et al., 2013), and little attention has been given to

the distinctive nature of a large portion of the world's small freshwater systems apart from those located in the boreal-arctic region (Kuhn, Varner, et al., 2021; Matthews et al., 2020; Wik et al., 2016). Here, we have shown that peatland ponds and, to a lesser extent, thermokarst waterbodies, that account for a substantial proportion of small waterbodies worldwide, have distinct combinations of morphometric and chemical properties that are not observed in lakes. While lakes receive most of their OM and nutrients from their watersheds, peatland pond biogeochemistry is mostly influenced by internal cycling and exchanges with the surrounding peat (Figure 2.4) (Arsenault et al., 2018, 2019). For thermokarst waterbodies developing in OM- or mineral-rich permafrost, the surrounding matrix influences their biogeochemistry but lateral exchanges are not as important as in peatland ponds because of the frozen soil that reduces permeability (Figure 2.4) (Vonk et al., 2019). However, with permafrost regions experiencing warming temperatures, the relative contribution of the surrounding thawing soils to thermokarst waterbody OM and nutrient loading is expected to increase in the future (Pokrovsky et al., 2013), perhaps making peatland ponds better models than lakes for predicting future evolution of these waterbodies.

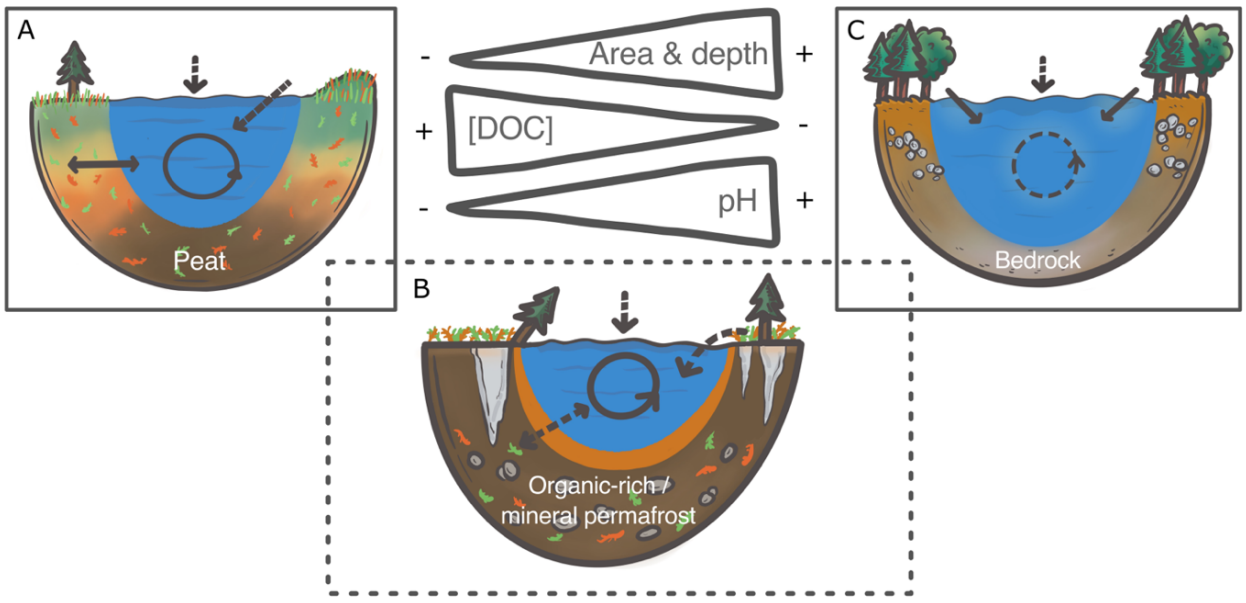

Figure 2.4. Relative contribution of landscape, internal cycling and atmospheric inputs to organic matter (OM) and nutrient sources to A) peatland pond, B) thermokarst waterbody and C) lake biogeochemistry. Area, depth and pH are lower and dissolved organic carbon (DOC) is higher in peatland ponds than in lakes, but thermokarst waterbodies show mixed biogeochemical patterns combining morphological and chemical characters of both lakes and peatland ponds, depending on the surrounding soil characteristics. We explain the distinct biogeochemistry of these freshwater systems by the different settings in which they develop, influencing the relative contribution of OM and nutrient sources.

Deepening our knowledge of the biogeochemistry of peatland ponds, especially in lower latitudes where data are particularly scarce, and of thermokarst waterbodies will improve prediction of the fate of climate-sensitive wetland and permafrost regions dominated by unique freshwater systems. Because of their distinct functional relationships with their surroundings, it is likely that peatland ponds and lakes will respond differently to climate forcing. Our results suggest that predictive relationships developed for lakes would not translate well to peatland ponds and most thermokarst waterbodies. This warrants the development of distinct scaling relationships for the integration of freshwater ecosystems in the next generation of land-surface components of earth system models. It also highlights the critical need for more data on peatland ponds and thermokarst waterbodies to feed such models.

Chapitre 3. *Climate-driven spatial and temporal patterns in peatland pool biogeochemistry*

3.1 Avant-propos

Ce chapitre présente les résultats d'une étude portant sur les variations spatiotemporelles de la biogéochimie des mares de tourbières. En comparant des données provenant de sites aux caractéristiques géographiques variées, dont un faisant l'objet d'un monitoring depuis 2016, l'étude vise à évaluer les différences spatiales et l'évolution temporelle de la biogéochimie des mares et à identifier les facteurs géographiques responsables de telles variations. Cette étude a été conçue et imaginée par Julie Talbot, Jean-François Lapierre et moi-même. J'ai dirigé la collecte des échantillons pour les tourbières de l'est du Canada et de la Patagonie, effectué les analyses en laboratoire, mené le traitement et l'analyse des données, et rédigé l'article scientifique. Les co-auteurs ont toutes et tous aidé à la collecte des données et participé à la rédaction de l'article. L'article est accepté pour publication et est, en date du 27 avril 2023, sous presse dans la revue *Global Change Biology*.

Référence complète :

Arsenault, J., Talbot, J., Brown, L.E., Helbig, M., Holden, J., Hoyos-Santillan, J., Jolin, E., Mackenzie, R., Martinez-Cruz, K., Sepulveda-Jauregui, A. & Lapierre, J.-F. (2023). Climate-driven spatial and temporal patterns in peatland pool biogeochemistry. *Global Change Biology, 29*, 4056-4068.

3.2 Abstract

Peatland pools are freshwater bodies that are highly dynamic aquatic ecosystems because of their small size and their development in organic-rich sediments. However, our ability to understand and predict their contribution to both local and global biogeochemical cycles under rapidly occurring environmental change is limited because the spatiotemporal drivers of their biogeochemical patterns and processes are poorly understood. We used (1) pool biogeochemical data from 20 peatlands in eastern Canada, the United Kingdom and southern Patagonia, and (2) multi-year data from an undisturbed peatland of eastern Canada, to determine how climate and terrain features drive the production, delivering and processing of carbon (C), nitrogen (N) and phosphorus (P) in peatland pools. Across sites, climate (24 %) and terrain (13 %) explained distinct portions of the variation in pool biogeochemistry, with climate driving spatial differences in pool dissolved organic C (DOC) concentration and aromaticity. Within the multi-year dataset, DOC, carbon dioxide (CO_2), total N concentrations and DOC aromaticity were highest in the shallowest pools and at the end of the growing seasons, and increased gradually from 2016 to 2021 in relation to a combination of increases in summer precipitation, mean air temperature for the previous fall, and number of extreme summer heat days. Given the contrasting effects of terrain and climate, broad-scale terrain characteristics may offer a baseline for the prediction of small-scale pool biogeochemistry, while broad-scale climate gradients and relatively small year-to-year variations in local climate induce a noticeable response in pool biogeochemistry. These findings emphasize the reactivity of peatland pools to both local and global environmental change and highlight their potential to act as widely-distributed climate sentinels within historically relatively stable peatland ecosystems.

3.3 Introduction

Biogeochemical cycles in freshwater bodies are increasingly altered by both large- and small-scale changes in climate and land use that lead to increased loading and processing of carbon (C), nitrogen (N) and phosphorus (P) (Maranger et al., 2018; Pilla et al., 2022). Small lakes or ponds (<0.01 km^2) are recognized for having disproportionate influence on local and global C, N and P cycles and GHG emissions (Holgerson & Raymond, 2016) because of their high surface-to-watershed area ratio that increases rates and quantities of biogeochemical processes (Downing, 2010). A large number of small water bodies (often < 0.001 km^2) consist of pools developing in peatlands, especially in the mid- and high latitudes. Peatlands are

globally important ecosystems, covering nearly 5 million km² (UNEP, 2022) and storing >600 Pg C (Yu et al., 2010) and 5-25 Pg N (Yin et al., 2022). However, while they are historically relatively stable ecosystems (Morris et al., 2015), they face challenges related to climate and land-use changes that could modify their current structural and functional state (Juutinen et al., 2018) and that of their components, such as streams and pools. Peatland pools form a relatively homogeneous group of water bodies that develop in similar landscapes of organic matter-rich matrix and that are potentially more biogeochemically dynamic than other aquatic ecosystems (Arsenault et al., 2022). For example, in permafrost-affected peatlands, the relative contribution of small pools to the landscape C budget is proportional to their area, regardless of their size, and peatland water bodies are large contributors to this budget (Polishchuk et al., 2018; Serikova et al., 2019). Despite this potential, the response of peatland pool biogeochemical patterns and processes to major drivers such as climate change and land-use modification, and their role in global biogeochemical cycles remain poorly understood.

Temperature and precipitation are broad scale (> 10 km) climate drivers of spatial and temporal variability in the biogeochemistry of freshwater bodies (Collins et al., 2019), but such factors often vary in response to small scale (< 1 km) land use and terrain differences (Cao et al., 2020). In permafrost-free temperate and boreal peatland pools, C and nutrient processing have been shown to be partly driven by local temperature and summer precipitation variations due to their effect on microbial activity dynamics, and on mass concentration, dilution, and transfer from the surrounding soil (Arsenault et al., 2018; Prijac et al., 2022). At larger scales, for a given set of terrain characteristics, spatial and possibly temporal patterns in biogeochemistry that follow climatic gradients may emerge in lakes (Soranno et al., 2019), but to our knowledge this has not yet been studied in more structurally homogeneous systems like peatland pools. Hence, it is difficult to predict how climate change affects peatland pool structure and functioning as the influence of climate on spatial and temporal patterns in peatland pool biogeochemistry, compared to that of other potentially important drivers, remains unclear.

Water balance and biogeochemical patterns and processes in most aquatic ecosystems are largely influenced by their connectivity to the watershed and other water bodies, and by surrounding land use and terrain structure (e.g. morphometry, elevation, geology) (Covino, 2017). Peatland pools are, however, biogeochemically distinct from typical lentic freshwater bodies because of the very small area of their watershed that limits external nutrient inputs, and because of the nature of the soil in which they develop that may influence lateral flow of

water and mass (C, N and P) (Arsenault et al., 2022) especially when peat hydraulic conductivity is elevated (Holden et al., 2018). In ombrotrophic settings, pools from both raised (i.e. dome-shaped) or blanket (i.e. peatlands that follow the landscape morphology) peatlands have little to no hydrological and biogeochemical connectivity with the surrounding landscape and groundwater (Fraser, Roulet, & Lafleur, 2001; Holden & Burt, 2003). Locally, pool biogeochemistry therefore relies almost entirely on intrinsic controls, related to their morphology, the composition of the surrounding vegetation, and soil chemistry (Arsenault et al., 2018, 2019; Prijac et al., 2022). These factors are constrained at a larger scale by altitudinal, topographical and hydrological influences (Belyea, 2007; Rydin & Jeglum, 2013). Regional dissimilarities in pool biogeochemistry emerging in Scotland and Northern Ireland have been related to peatland continentality, peat structure and composition, and pool morphology (Turner et al., 2016), highlighting the influence of broad-scale terrain factors on pool biogeochemistry. Landscape position, hydrological connectivity and morphometry also mediate the response of freshwater bodies to climate variability by regulating ecosystem metabolism, but these factors often co-occur with climate gradients (Lapierre et al., 2015; Oleksy et al., 2022). It is therefore challenging to disentangle broad scale controls of terrain on freshwater body biogeochemistry from climate influences.

Spatiotemporal variations in aquatic ecosystem biogeochemistry result from a combination of small and broad scale terrain and climatic drivers, that respectively control the origin of mass and the rates at which it is received, produced and processed by the systems (Dodds et al., 2019; Oleksy et al., 2022). The development of peatland pools is driven by both terrain- and climate-related mechanisms (Belyea, 2007), but it is unclear to what extent these geographic factors dictate peatland pool biogeochemistry hence limiting our ability to understand and predict their function in both local and global biogeochemical cycles under rapidly occurring environmental change. In this context, the goal of this research was to assess how climate and terrain (peatland elevation and pool depth and area) drive the broad-scale spatial and local-scale interannual patterns in peatland pool C, N and P biogeochemistry. More specifically, we first determined the main drivers of spatial variations in pool biogeochemistry, by comparing peatland pools from different geographic settings (in eastern Canada, the United Kingdom and southern Patagonia). We then assessed the interannual variation in pool C, N and P biogeochemistry from an undisturbed peatland of eastern Canada, based on five ice-free season surveys over the 2016-2021 period.

3.4 Materials and methods

3.4.1 Sites description

A total of 240 pools were sampled between 2011 and 2021 in 20 undisturbed peatlands of eastern Canada, the United Kingdom (UK) and southern Patagonia (Table 3.1). The peatlands were in different geographic settings, from maritime to more continental locations, and from sea level to > 550 m in altitude to ensure a broad array of climatic variability was captured. Mean annual precipitation ranged from ~ 400 mm to > 2000 mm per year and mean annual air temperature ranged from -0.7 °C to 9.2 °C over the 1991-2020 period (Harris et al., 2020). All peatlands were classified as raised or blanket bogs and had numerous pools at their surface.

3.4.2 Pool sampling and chemical analyses

Pools from eastern Canada and southern Patagonia were sampled between 2016 and 2021 during the growing season (May to October in Canada, January-February in Chile; Table 3.1). They were selected to cover a wide range of depth, area and surrounding vegetation composition, but also for accessibility and water availability. The pools we sampled were not in contact with the mineral substrate of the peatlands and their bottom was composed of peat and limnic material. There was therefore little to no connectivity to groundwater and lithology. Sampling and water analyses are further described in Arsenault et al. (2018). Pools from the UK were sampled between 2011 and 2014, and pool measurements, and water sample collection and analyses were performed as reported by Brown et al. (2016) and Turner et al. (2016).

To assess interannual variation in pool biogeochemistry, nine pools from one peatland in eastern Canada (Grande plée Bleue – GPB, a raised bog) were sampled repeatedly during the 2016, 2017, 2019, 2020 and 2021 growing seasons (from May to October). These pools were selected to represent three pool archetypes found at the study sites: three large (>1200 m2) and moderately deep (~1m) pools, three small (< 400 m^2) and shallow (<0.8 m) pools, and three small (< 400 m^2) and deep (> 1.8 m) pools (Arsenault et al., 2018). All pools were sampled on the same day, between 4 and 10 times per growing season. Water samples were analyzed for pH, DOC, total nitrogen (TN), total phosphorus (TP), water color at 254 nm (A_{254}), specific UV absorbance at 254 nm (SUVA), and dissolved CO_2 and CH_4 concentrations.

Table 3.1. Description of the sites where pools were sampled. Peatland elevation estimates were taken from Google Earth. Climate variables for the 1991-2020 period were taken from the Climate Research Unit gridded Time Series (Harris et al., 2020). MAAT - Mean annual air temperature; MAP - Mean annual precipitation; PET - Potential evapotranspiration.

Region	Site	Latitude	Longitude	Peatland type	n pools sampled	n sampling events (year range)	Elevation (m)	MAAT (°C)	MAP (mm)	PET (mm)
Eastern Canada	Grande plée Bleue	46.781	-71.052	Raised bog	53	1 (2016)	87	3.9	1329	641
	Grande plée Bleue	46.781	-71.052	Raised bog	9	28 (2016-21)	87	3.9	1329	641
	Rivière-au-Tonnerre	50.315	-64.927	Raised bog	10	1 (2019)	80	1.5	962	506
	Kegaska	50.194	-61.556	Raised bog	10	1 (2019)	35	1.4	1022	446
	Havre-Saint-Pierre	50.256	-63.445	Raised bog	10	1 (2019)	32	1.7	901	487
	La Romaine	50.523	-63.206	Raised bog	10	1 (2019)	109	-0.7	962	445
	Saint-Alexandre-Kamouraska	47.740	-69.610	Raised bog	11	8 (2020-21)	126	3.2	1055	530
	Miscou	47.940	-64.526	Raised bog	9	1 (2021)	7	4.7	1198	655
United Kingdom	Cross Lochs	58.373	-3.959	Blanket bog	6	5 (2013-14)	211	7.6	1109	472
	Loch Lier	58.388	-3.783	Blanket bog	6	5 (2013-14)	185	7.6	1109	472
	Munsary	58.396	-3.343	Blanket bog	6	5 (2013-14)	105	8.3	1247	436
	Silver Flowe	55.128	-4.400	Blanket bog	22	1 (2013)	280	7.6	2046	449
	Slieveanorra	55.085	-6.193	Raised bog	15	1 (2013)	307	9.2	1164	488
	Garron Plateau	55.004	-6.073	Blanket bog	11	1 (2013)	337	9.2	1164	504
	Upper Midhope	53.475	-1.722	Blanket bog	10	3 (2011-12)	515	8.9	1177	530
	Moor House	54.690	-2.388	Blanket bog	5	3 (2011-12)	571	7.4	1199	460
	Cold Fell	54.892	-2.604	Blanket bog	5	3 (2011-12)	546	8.5	1216	513
Southern Patagonia	Navarino	-54.937	-67.888	Blanket bog	11	1 (2019)	300	4.4	501	620
	Punta Arenas	-53.396	-71.25	Blanket bog	9	1 (2019)	256	5.9	419	691
	Karukinka	-54.532	-68.795	Raised bog	6	1 (2019)	36	3.9	537	665
	Cape Horn	-55.963	-67.229	Blanket bog	6	1 (2019)	45	4.9	763	467

3.4.3 Data handling

For the spatial component of the study, most pools were sampled only once and during the growing season (Table 3.1). When pools were sampled repeatedly, means were calculated for all variables to average sampling effects of covariates. Given the influence of pool morphology (Arsenault et al., 2018) and regional variations in pool biogeochemistry (Turner et al., 2016), analyses considered the effects of variables describing climate (mean annual air temperature - MAAT, mean annual precipitation - MAP, potential evapotranspiration - PET, annual number of days with precipitation - Wet days, annual number of frost days - Frost days, and precipitation to potential evapotranspiration ratio -P:PET) and terrain (elevation, and pool area and depth). We used global gridded climate data (Harris et al., 2020) to ensure consistency in our analyses because most peatlands did not have nearby meteorological stations and those that did, did not report all the variables of interest.

For the temporal component, to deal with uneven sample sizes and irregular sampling dates between years at our study site, we averaged data for each pool for 50-day windows between day of year 150 to 300 to encompass all sampling dates while reducing data repetition to a minimum (Legendre & Legendre, 2012). Averages of all biogeochemical parameters (pH, A_{254}, SUVA, and DOC, TN, TP, and dissolved CH_4 and CO_2 concentrations) were calculated for each window (days of the year 150-200, 175-225, 200-250, 225-275 and 250-300). For example, day of the year (DOY) 175 and 200 were used to compare pool biogeochemistry for windows 150-200 and 175-225, respectively. We used the windows to assess changes in pool biogeochemistry patterns among and within years, and between groups of pools. To assess the effect of climate on temporal changes in pool biogeochemistry, we collated meteorological data from the nearest station with complete data (Saint-Michel station, 13 km east from the study site; Environment Canada, 2022) for each year: mean summer temperature, number of summer days where maximum temperature exceeded 30°C, mean previous spring, winter and fall temperature, total summer and previous spring, winter and fall precipitation, and number of summer precipitation days.

3.4.4 Statistical analyses

3.4.4.1 Spatial variation

In the multivariate analyses of spatial variation in pool biogeochemistry, we only included pools for which pH, SUVA, and DOC, TN, TP, and dissolved CO_2 and CH_4

concentrations data were available (n = 150). We first performed a multiple analysis of variance (MANOVA) after transforming the non-normally distributed data to determine if biogeochemistry was different among the three studied regions. We then ran individual Tukey HSD post-hoc tests on individual biogeochemical variables when differences were found. We also performed a one-way analysis of variance to determine if terrain variables (elevation, pool area and depth) were related to peatland type (blanket or raised bog). We used Kruskall-Wallis followed by pairwise Wilcoxon rank sum tests on non-transformed data to determine if climate and terrain influenced pool biogeochemistry, and isolate dissimilar sites. To assess how each climate and terrain variable influenced the individual biogeochemical variables while dealing with the several tied ranks in the distributions, we ran Kendall rank correlations.

To determine the effect of climate and terrain predictors on pool biogeochemistry, we used partial least-square regressions (PLSR) because they are robust even if there is collinearity among variables (Lindgren et al., 1993), as was the case for climate predictors. Both dependent and independent matrices were standardized to a mean of 0 and a standard variation of 1. We then calculated the variable importance in projection (VIP) to determine which of the climate and terrain predictors mostly influenced the spatial variation in pool biogeochemistry, using a threshold of VIP > 1 (Farrés et al., 2015). We used variance partition to differentiate the effect of "climate" (i.e. combined effect of MAAT, MAP, PET, P:PET ratio, annual number of wet days, and annual number of frost days) from that of the terrain (i.e. combined effect of pool area and depth, and peatland elevation) on pool biogeochemistry. We finally used generalized linear mixed effects models to determine the response of the variables with the most variation explained by the PLSR (DOC and TN concentrations) to changes in climate and terrain. We used gamma distribution family for both DOC and TN. We rejected from the models the predictors that showed collinearities (P:PET ratio, annual number of wet days, and annual number of frost days) and kept MAAT, MAP, PET, peatland elevation and pool area and depth as fixed effects. These variables were scaled to a mean of 0 and a standard deviation of 1 to standardize units. Peatland type and regions were added as random intercepts to the models.

3.4.4.2 Temporal variation

We first ran a principal component analysis (PCA) based on biogeochemical variables from each group of pools at every DOY to assess the temporal changes and the effect of morphology on pool biogeochemistry. In the PCA, we also added climate data (MAAT and total annual precipitation) recorded at the nearest meteorological station to allow cross-comparison

with the spatial component of the research. We performed two-way MANOVAs with interactions and Tukey HSD post-hoc tests to determine how pool biogeochemistry varied among years, across growing seasons, and among groups of pools, and how pool morphology influenced pool biogeochemical response over time. We then used linear mixed effects models to assess the random effect of pool morphology on temporal changes in pool biogeochemistry and tested fixed effects using analyses of variance for likelihood ratio. We also ran Kendall rank correlations to assess the relationships between pool biogeochemistry, time, and meteorological variables regardless of pool morphology. To identify the main drivers of temporal variations of pool biogeochemistry at the GPB site, we conducted PLSR of biogeochemical vs meteorological variables based on three principal components, and calculated VIPs. While the experimental design at the study site was originally built to compare the effect of pool size, we here focused on meteorological drivers because within-pool controls on biogeochemistry had previously been established (Arsenault et al., 2018, 2019). For each biogeochemical variable and at every DOY, we then averaged the data of all pools regardless of their size.

For both spatial and temporal variation analyses, except for Kruskall-Wallis and Wilcoxon tests and Kendall correlations, variables that were not normally-distributed were $\log_{10}$-transformed to fulfill the normality condition prior to all analyses. All statistical analyses were undertaken using R, version 4.2.0 (R Core Team, 2022), and packages 'pls' and 'plsdepot' for PLSR, 'vegan' for variance partition and 'lme4' for generalized linear mixed effects models.

3.5 Results

3.5.1 Spatial variation in pool biogeochemistry

There were large variations in peatland pool morphological and biogeochemical properties among the three studied regions. Peatland type (raised or blanket bog) was related to peatland elevation, pool area and depth, with blanket bogs in our dataset developing at higher altitude and having shallower and smaller pools than raised bogs (ANOVA, $P < 0.001$). Overall, pools from Canada were deeper, more acidic and had higher concentrations in dissolved CH_4, pools from the UK were smaller and had lower concentrations in DOC, and pools from southern Patagonia had higher concentrations in TN and TP than other regions (Table 3.2). There was no difference in dissolved CO_2 between regions, and pool SUVA was similar between Canada and the UK, but higher in Patagonia. On average, pools from all regions were

supersaturated in CH_4, especially in eastern Canada where the lowest concentration was around three times that of the atmosphere but went up to 250-fold, while CO_2 concentrations were on average slightly below atmospheric values (Table 3.2). There were also large within-site variations in biogeochemistry, especially in terms of DOC, TP and dissolved CH_4 concentrations (Annexe II, Table S3.1).

Table 3.2. Morphological and biogeochemical parameter means ± standard error (minimum-maximum) for peatland pools of Canada, United Kingdom and southern Patagonia. Letters in indices show differences and similarities between regions as determined by Tukey HSD tests (log_{10}-transformed variables for the analyses are indicated by an asterisk).

	Eastern Canada	United Kingdom	Southern Patagonia
Area (m^2)*	$_a$1067 ± 249 (23-24,542); n = 122	$_b$130 ± 39 (4-1757); n = 59	$_a$1419 ± 675 (2-21,328); n = 32
Depth (cm)*	$_a$73 ± 4 (13-219); n = 122	$_b$29 ± 2 (3-60); n = 86)	$_b$34 ± 7 (4-142); n = 32
pH	$_a$4.07 ± 0.02 (3.72-4.80); n = 122	$_b$4.34 ± 0.02 (3.90-4.90); n = 86	$_b$4.47 ± 0.06 (4.04-5.48); n = 32
DOC (mg L^{-1})*	$_a$25.7 ± 0.8 (6.7-51.7); n = 122	$_b$17.9 ± 1.7 (3.1-85.2); n = 86	$_a$28.6 ± 3.0 (8.0-73.1); n = 32
TN (mg L^{-1})*	$_a$0.6 ± 0.0 (0.3-1.9); n = 122	$_a$0.7 ± 0.0 (0.3-1.8); n = 66	$_b$1.1 ± 0.1 (0.4-3.6); n = 32
TP (µg L^{-1})*	$_a$17 ± 1 (6-102); n = 122	$_a$19 ± 1 (6-76); n = 66	$_b$55 ± 15 (7-409); n = 32
SUVA (L mg C^{-1} m^{-1})	$_a$2.83 ± 0.10 (0.87-6.04); n = 120	$_a$2.99 ± 0.16 (0.76-7.21); n = 66	$_b$3.57 ± 0.10 (2.12-4.77); n = 32
Dissolved CH_4 (µg L^{-1})*	$_a$76.9 ± 11.8 (3.8-336.5); n = 67	$_b$16.2 ± 2.2 (0.2-93.0); n = 66	$_b$21.0 ± 6.9 (0.5-159.3); n = 26
Dissolved CO_2 (mg L^{-1})*	$_a$0.7 ± 0.06 (0.09-2.1); n = 67	$_a$0.7 ± 0.05 (0.2-2.0); n = 66	$_a$0.8 ± 0.2 (0.2-5.4); n = 26

Multivariate analyses showed how peatland pool biogeochemistry tended to be much more similar within than among regions, and how spatial variations in climate and terrain both drive clear geographic patterns in peatland pool biogeochemistry among the three regions (Figure 3.1). Overall, the six-components PLSR explained 34.9% of the variance in pool biogeochemistry, with the first axis being driven by climate predictors (MAP, PET and P:PET ratio) and mostly explaining variations in DOC concentration and aromaticity (SUVA). The second axis of the PLSR was driven by peatland elevation and pool area, and mostly explained variations in TN, TP and dissolved CH_4 concentrations. However, differences in pool biogeochemistry among regions and sites were not systematically attributed to variations in the same sets of climate and terrain predictors (Figure 3.1A; Annexe II, Figures S3.3-S3.11). For example, the different regions were mainly discriminated along the bottom-left (higher number of frost days and pool area) to top-right (higher MAAT and peatland elevation) axis, but pool biogeochemistry appeared mainly driven by wetness conditions (Figure 3.1A). In particular,

DOC, TN and TP concentrations seemed higher under the high PET typically found in Patagonia (except for Cape Horn) and continental eastern Canada (Grande plée Bleue site) (Table 3.1). At the terrain level, however, TN and TP were both correlated to peatland elevation, and pool area and depth ($P \leq 0.001$), but DOC was not correlated to any of these predictors ($P > 0.1$) (Annexe II, Figures S3.3-S3.5).

The independent effect of climate and terrain was supported by the partition of the variance in pool biogeochemistry explained by both sets of predictors (Figure 3.1B). Among the three regions, climate (24% of the variance) and terrain (13% of the variance) drove almost entirely distinct parts of the spatial variation in pool biogeochemistry, with only 1% of the variation explained by their joint effect. This means that while there was co-variation between terrain and climate properties, with pool morphology being correlated to climate and peatland elevation (Annexe II, Figure S3.1-S3.2), there was virtually no overlap in the effect these predictors have on pool biogeochemistry as they did not influence the same biogeochemical properties (Annexe II, Figure S3.3-S3.11).

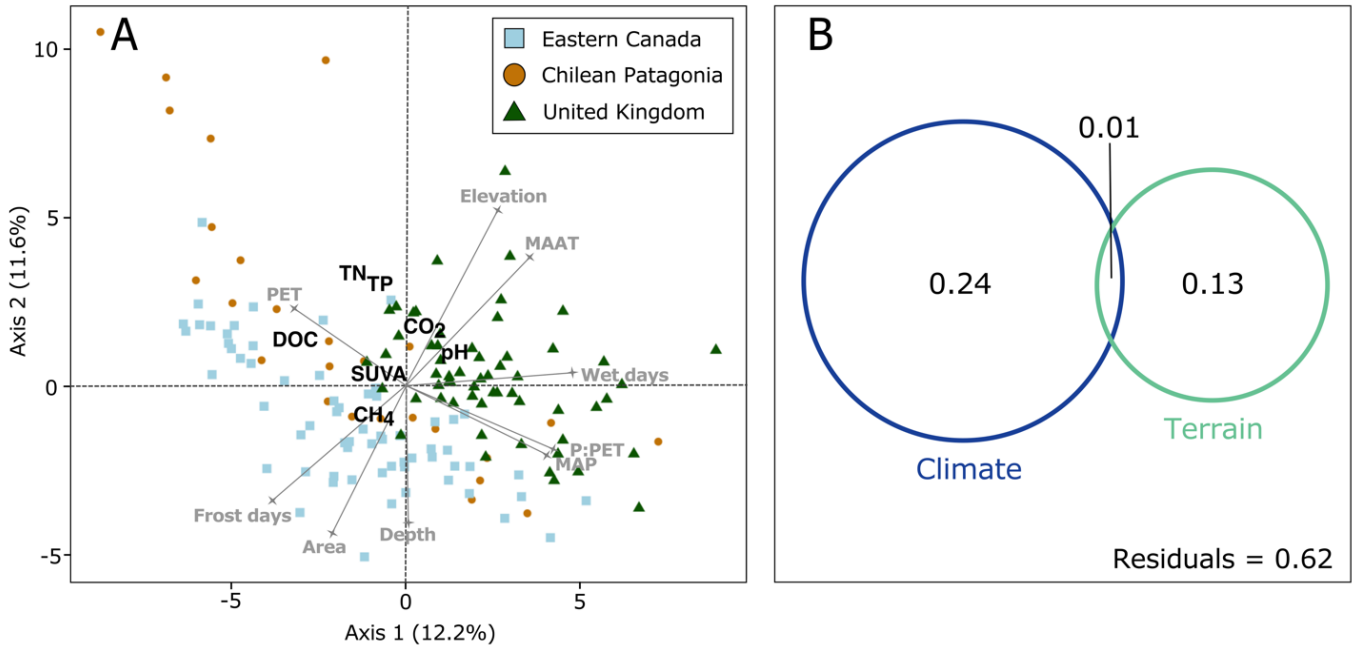

Figure 3.1. Peatland pool biogeochemistry varies across space. A) Partial least square regressions of biogeochemical (black) vs. climate and terrain (grey) variables for pools of eastern Canada, the United Kingdom and southern Patagonia. Only depth (0.90) was a predictor with a VIP score < 1. B) Partition of the variance in peatland pool biogeochemistry explained by climate (MAAT, MAP, PET, P:PET ratio, annual number of wet days, and annual number of frost days) and terrain (area, depth and elevation) predictors.

In particular, generalized linear mixed effects models showed a strong influence of climate and terrain predictors on DOC and TN concentrations which were the two variables with the most variation explained by the PLSR (Figure 3.1A, upper left quadrant). The random effects of peatland type and region showed clear patterns of increasing DOC with MAAT and elevation (Figure 3.2A, C) but decreasing with MAP and pool area and depth (Figure 3.2B, D, E). The relationships of TN to climate and terrain were not as clear as for DOC, with the strongest relationships being with elevation (positive, Figure 3.2H) and depth (negative, Figure 3.2J). For either DOC or TN, PET was not a driver of variation. In both models, the estimated among-type variance was much lower than among-region variance, meaning that peatland type only had a small influence on DOC and TN concentrations compared to peatland location. Overall, region and peatland type had little influence on TN variation compared to climate and terrain predictors (Annexe II, Table S3.3).

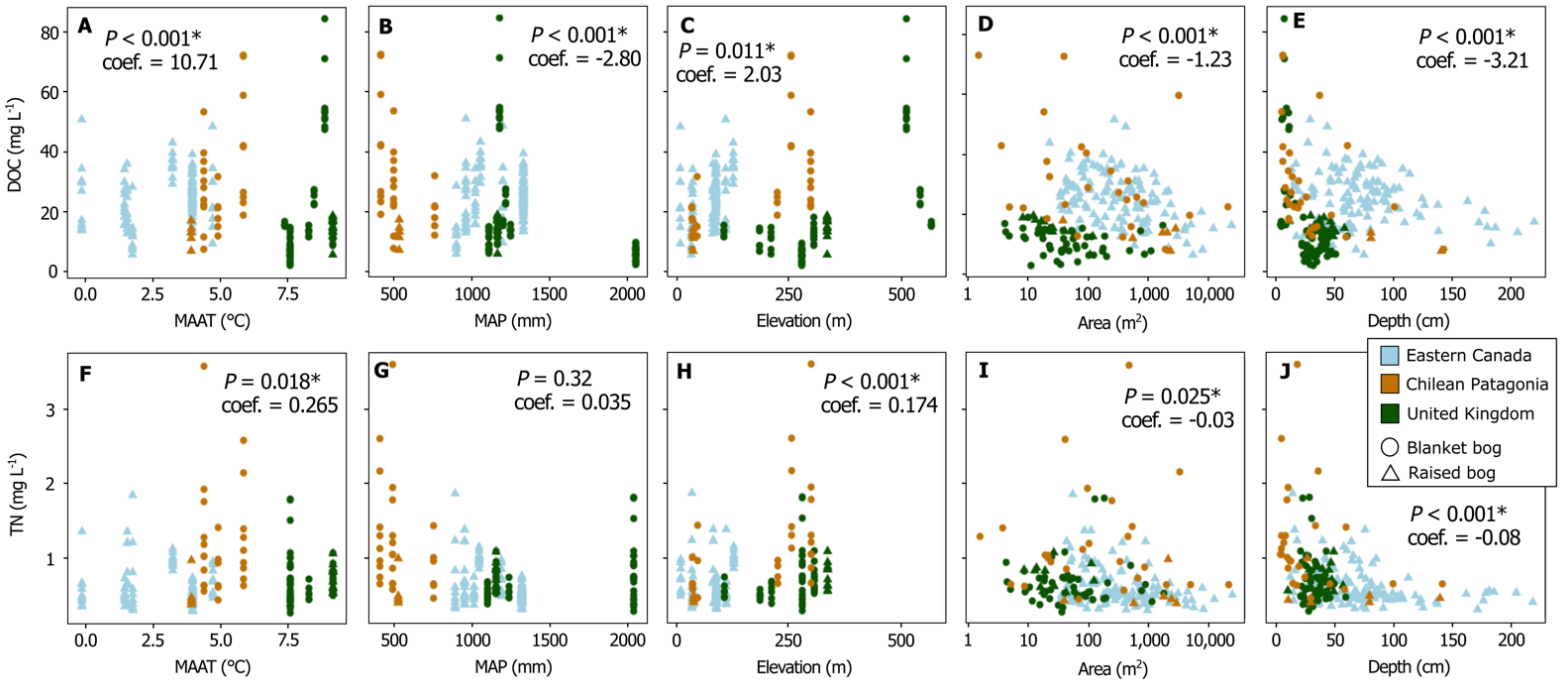

Figure 3.2. Spatial patterns among regions emerged when comparing dissolved organic carbon (DOC, boxes A-E) and total nitrogen (TN, boxes F-J) concentrations to climate and terrain predictors. Coefficient estimates (coef.) and p-values (*P*) of the generalized linear mixed effects models of DOC and TN concentrations to predictors, with peatland type and regions as random effects, are shown for each plot. Asterisks (*) indicate models with p-values (*P*) < 0.05.

3.5.2 Temporal variation in pool biogeochemistry

Meteorological conditions at the Grande plée Bleue site (eastern Canada) considerably varied between 2016 and 2021. For example, total summer rain ranged from 317 mm in 2017 to 472 mm in 2021 (~50% difference), and there were more than twice the number of days of high heat (> 30°C) in 2020 (14) and 2021 (13) than in 2017 (6) (Annexe II, Table S3.7). Pools at the GPB site also exhibited highly variable biogeochemistry during this period (MANOVA, $P < 0.001$, Annexe II, Table S3.4), both seasonally ($P = 0.01$) and among pools of different morphology ($P < 0.001$). For example, SUVA, DOC, TN and CO_2 concentrations increased gradually from 2016 to 2021, with the highest numbers systematically recorded in the shallowest pools (blue signs, Figure 3.3), and generally at the end of the growing seasons (Figure 3.3, 3.4; Annexe II, Table S3.8). There was usually no interaction between the effects of time and morphology ($P \geq 0.05$; Figure 3.3). When adding a random effect of pool morphology on biogeochemistry, only DOC and CO_2 concentrations changed over the growing seasons ($P < 0.05$), but all parameters varied over the 2016 to 2021 period ($P < 0.1$), highlighting the influence of climate variations on pool biogeochemistry (Table Annexe II, S3.5). For each pool, morphology and surrounding vegetation composition did not change over the study period.

The multi-dimensional representation of the different variables highlighted the effect of both pool morphology and time on pool biogeochemistry (Figure 3.4A). Shallower pools (circle signs in the upper right quadrant) tended to have higher concentrations in DOC, TP and dissolved CO_2 and CH_4 concentrations, and lower pH than deeper pools, and for all variables there was a general increasing trend from 2016 (orange) to 2021 (grey) in relation to higher MAAT and lower total annual precipitation. The PLSR further emphasized the seasonal and interannual variability in the biogeochemistry of pools regardless of their size (Figure 3.4B). The three components of the analysis together explained 62.8% of the variance in pool biogeochemistry, with the first axis (22.4% of the variance) highlighting the interannual pattern of increasing DOC, TN and CO_2 concentrations and higher A_{254}, SUVA and pH from 2016 to 2021. This pattern was driven by a combination of increasing summer precipitation, increasing mean air temperature the previous fall and the higher number of extreme heat days in 2020 and 2021 (Annexe II, Table S3.6). The second axis (20.3% of the variance) showed the seasonal pattern of increasing DOC and CO_2 concentrations from early summer (square signs in the lower quadrants) to early fall (star signs in the upper quadrants) (Annexe II, Table S3.7).

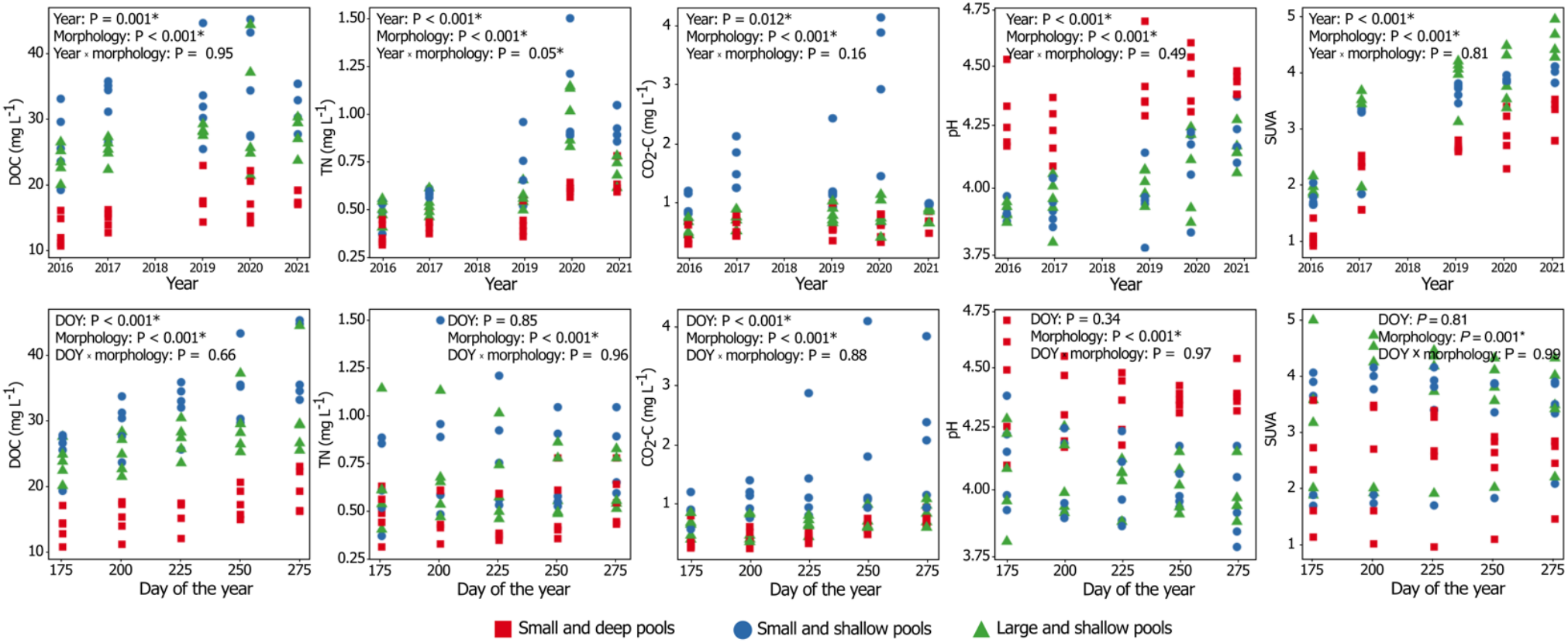

Figure 3.3. Interannual (upper boxes) and seasonal (lower boxes) variations in pool dissolved organic carbon (DOC), total nitrogen (TN) and dissolved carbon dioxide (CO_2) concentrations, pH and specific UV absorbance (SUVA) in pools of different sizes at the Grande plée Bleue site (eastern Canada). Each dot represents the mean for a specific day of the year (DOY), between 2016 and 2021. Results (p-values, *P*) of analyses of variance with interactions among time (year or DOY) and groups of pools (morphology) are shown, with asterisks (*) indicating p-values < 0.05.

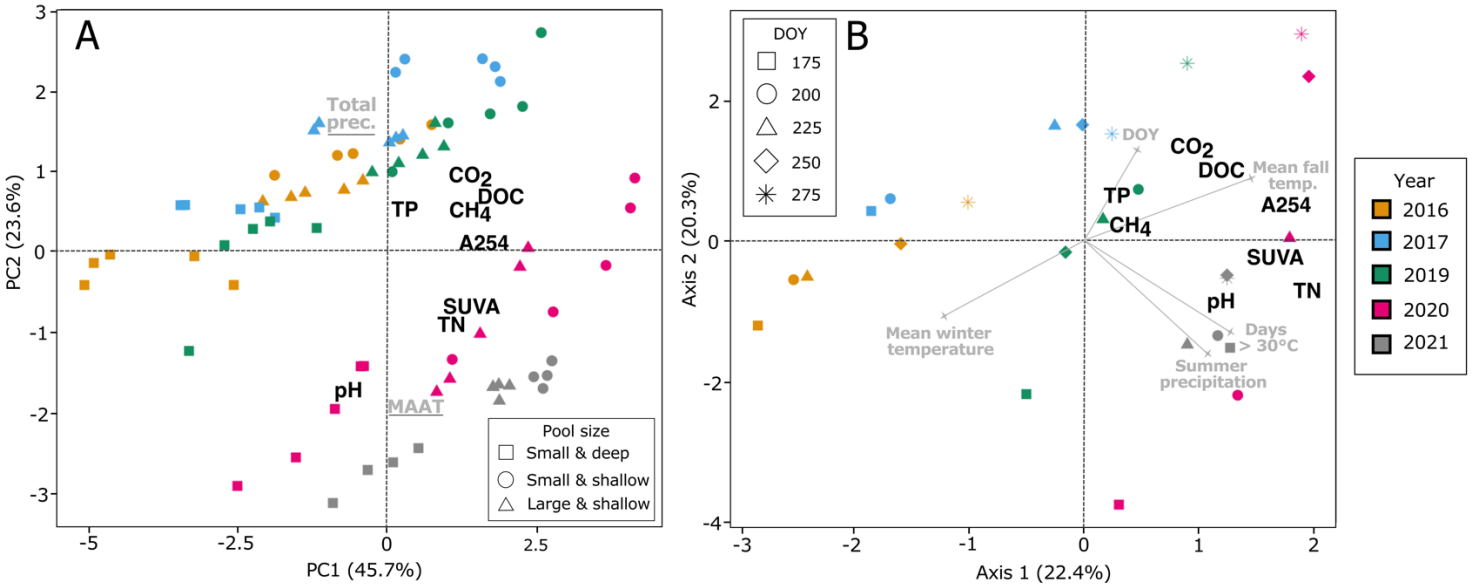

Figure 3.4. At the Grande plée Bleue site (eastern Canada), peatland pool biogeochemistry varies over time in response to local variations in climate. A) Principal component analysis of pool biogeochemistry (black) and climate (mean annual air temperature – MAAT – and total annual precipitation; grey) evolution from the GPB site over the 2016-2021 period. Dot shapes represent pools of different sizes, color represent year of sampling. B) Partial least square regressions (PLSR) showing annual (color) and seasonal (shape) variation in pool biogeochemistry (black) vs. meteorological (grey) variables. Each dot is the average of all nine pools sampled at different days of the year (DOY). Only predictors with a VIP score > 1 are shown on the PLSR graph.

3.6 Discussion

Our results show that both spatial and temporal variations in the biogeochemistry of peatland pools are controlled by sets of distinctive processes related to climate and terrain. At a broad scale, climate has the largest influence, explaining 24% of the variation in pool biogeochemistry, and mostly drives pool organic C concentrations and aromaticity (Figure 3.1). Similarly, local temporal patterns of C, N and P biogeochemistry are driven by small scale differences in pool morphology in addition to seasonal and interannual fluctuations in temperature and precipitation (Figure 3.4). The fact that climate and terrain predictors did not influence the same biogeochemical predictors suggest there may be factors driving pool biogeochemistry that were not considered in our analysis, such as peatland hydrology or peat thickness under the pools (Fraser, Roulet, & Moore, 2001; Holden et al., 2018; Pokrovsky et al., 2014). Nevertheless, due to the strong independent effects of terrain and climate (Figure 3.1B), this means that any given change in climate conditions may impact pool biogeochemistry

regardless of terrain properties, and likewise, that any alteration in peatland terrain characteristics (e.g. water table drawdown) may similarly impact pool biogeochemistry in any given climate. It is thus crucial to distinguish the effects of terrain and climate because both may independently dictate future directions of pool biogeochemistry but at different time scales. In undisturbed conditions, variations in climate indeed occur faster than peatland terrain changes (Morris et al., 2015). Climate variations are however accelerating (IPCC, 2022) and atmospheric deposition chemistry is changing (Monteith et al., 2007) which will drive structural and functional changes in peatland ecosystems (Bridgham et al., 2008), further limiting our understanding of current and future peatland pool function in both local and global biogeochemical cycles.

3.6.1 Terrain characteristics as a baseline for the prediction of pool biogeochemistry

Morphology is a fundamental driver of peatland pool biogeochemistry (Figure 3.3; Arsenault et al., 2018; McEnroe et al., 2009; Pelletier et al., 2014), and is constrained by altitudinal and topographical factors (Belyea, 2007). Our results show that differences in pool morphology, and indirectly in pool biogeochemistry, among regions may first be attributed to peatland types, with pools from blanket bogs being smaller and shallower than pools from raised bogs, where thicker peat deposits allow pool deepening (Foster & Wright Jr, 1990). In blanket bogs, pools develop perpendicularly to the surface gradient which limits their maximum areal extent in comparison to less sloping raised bogs (Belyea, 2007; Foster & Glaser, 1986). The raised and blanket bogs contrast then partially drives the biogeochemical differences among eastern Canada (raised bogs) and the UK and southern Patagonia (mostly blanket bogs) (Table 3.1, Figure 3.1), with shallower and smaller pools having higher concentrations in DOC and TN in every region (Figure 3.2).

Pools from southern Patagonia had higher TN and TP concentrations than elsewhere. Given its remoteness, this region receives little atmospheric pollution (Kleinebecker et al., 2008); pool TN and TP concentrations in southern Patagonia are therefore associated to local controls, possibly related to maritime influence that increases nutrient inputs from oceanic sources to the pools (Vizza et al., 2017) or to the distinctive vegetation of Patagonian peatlands (Kleinebecker et al., 2008; Mathijssen et al., 2019). It is also possible that higher TN and TP concentrations were related to dry and wet deposition of dust in more continental parts of southern Patagonia (Kleinebecker et al., 2008) or to the positive effect volcanic ash has on OM

decomposition and nutrient cycling and loading (Broder et al., 2012; Modenutti et al., 2013). Similarly, spatial trends in pH and SUVA may reflect differences in plant diversity among regions, as pool acidity and the aromaticity of DOC have been related to the composition of vegetation surrounding the pools (Arsenault et al., 2019; Prijac et al., 2022). Pools in our dataset represented a wide range of depth, area, and vegetation, and the 20 peatlands that were compared cover large gradients of altitudinal and topographic parameters. Under a rapidly changing climate, given the strong relationships that emerge between terrain and pool biogeochemistry and the distinct effect climate and terrain have (Figure 3.1B), broad-scale and more stable terrain characteristics may therefore offer a baseline for the estimation of small-scale pool biogeochemistry from temperate and boreal settings. Predictive relationships between pool terrain and their biogeochemistry could thus be incorporated into upscaling efforts and for better integration of peatland pools in global biogeochemical models.

3.6.2 The broad- and small-scale influence of climate

Broad-scale climate patterns drove spatial variations in pool biogeochemistry, with increasing DOC, TN and TP concentrations in regions with higher PET and lower MAP, and increasing pH and dissolved CO_2 in warmer climates (Figure 3.1A). These patterns in pool biogeochemistry followed gradients in peatland structure that also correlate with increases or decreases in climate properties. For example, warmer MAT favors greater DOC export from peatlands (Rosset et al., 2022) because of changes in vegetation composition and increased decomposition rates (Dieleman et al., 2015, 2016). A lowered water table under warmer and drier climates also stimulates the production of DOC (Strack et al., 2008) and CO_2 (Huang et al., 2021) in the upper layer of the peat profile by exposing labile C to newly-created aerobic conditions. The produced DOC and CO_2 can then be transported to and processed in the pools. Dry summers have also previously been associated with high DOC and dissolved CO_2 and CH_4 concentrations in peatland pools (Chapman et al., 2022). Our findings support the importance of these climate-driven mechanisms in controlling peatland pool biogeochemistry, and further suggest that climate may be the overarching driver of broad patterns at the cross-regional scale, where other sources of variation may not be as strongly expressed.

The broad scale climate effect is coherent with the relatively higher concentrations (up to 250-fold supersaturation), variation, and climate response of CH_4 than CO_2 across the studied sites. Part of this effect could be directly linked to climate, considering that CH_4 production is more sensitive than CO_2 to temperature (Yvon-Durocher et al., 2014). This

pattern could further be explained by indirect climate effects linked with carbon turnover. The lower DOC and dissolved CO_2 and CH_4 concentrations in larger and deeper pools further suggest that slower water turnover time in large pools enables the processing of C over a longer period of time leaving more recalcitrant, high-SUVA C in the pools (Holden et al., 2018). C emissions from pools have previously been positively correlated to DOC concentrations and SUVA (Pelletier et al., 2014). If pool DOC concentrations and SUVA were to increase in drier conditions, as proposed by our results, then the C balance of pools, and incidentally of peatlands, from regions expected to experience smaller P:PET ratio in the future may therefore be affected, potentially increasing C emissions from pools, especially CH_4, and decreasing overall C sequestration in peatlands.

At a small scale, the magnitude of temporal variations in pool biogeochemistry at the GPB site in eastern Canada was in the range of what was reported in the spatial component of the study (Table 3.1, Annexe II, Table S3.5), even if there was high within-site variability from one year to another (Annexe II, Table S3.4). This means that the climate effect on pool biogeochemistry at GPB may be transposable and used to foresee changes in peatland pool biogeochemistry in other temperate and boreal regions. In particular, increased TN concentrations and pH may be broadly expected in eastern Canada in response to projected higher summer precipitation and number of extreme heat days (Figure 3.3B, Prairie Climate Centre, 2019). Increases in TN concentrations could be related to higher N cycling and fixation in and around the pools under warmer summer temperatures and increased soil wetness (Weedon et al., 2012; Živković et al., 2022). Mechanisms leading to higher pH are however less clear but could be explained by lower phenolics coming from the surrounding peat because of more intense water table fluctuations during wet summers (Kim et al., 2021). Similarly, the sustained increases in SUVA, A_{254} and DOC, TN, TP and dissolved CO_2 and concentrations measured at GPB between 2016 and 2021 were driven by warmer temperature in the falls preceding the growing seasons we sampled (Figure 3.4B). These trends may be related to differences in decomposition and production rates in the pools during the warmer falls. Warmer temperatures may sustain elevated decomposition processes late after the end of the growing season and release nutrients that can not be taken up efficiently because of slower production rates under low photointensity and photoperiod, and a decrease in temperature right after. It is also possible that changes in DOC concentration and composition in peatland pools reflect the worldwide trend of inland water browning under warmer climate and higher soil pH (Evans et al., 2006; Freeman et al., 2001). While our results do not provide a definitive

explanation for the underlying mechanisms behind these climate-driven trends, they suggest that the biogeochemical dynamism of pools could increase under a warming climate, altering small-scale biogeochemical cycles and possibly overall peatland functions.

Capturing a climate signal in freshwater ecosystems within only six years is difficult as climate parameters rarely follow monotonic relationships (Soranno et al., 2019). Our results nonetheless show that relatively small year-to-year variations in climate induce a noticeable response in pool biogeochemistry, possibly due to the fast reaction of these small waterbodies to changes. Fast reaction times can be caused by their small water content and high surface to volume ratio, and by the relative stability of their terrain characteristics compared to other freshwater ecosystems (Oleksy et al., 2022). Here, we demonstrate that even short-term variation in climate can induce ecologically meaningful increases in pool reactivity, which may inform future predictions of peatland pool function under an increasingly warmer climate.

3.7 Conclusion

Our results show that freshwater bodies in peatlands are highly susceptible to terrain and climate variations that influence biogeochemical patterns at both local (e.g. Arsenault et al., 2018) and regional (e.g. Turner et al., 2016) scales. Given the relatively large influence that intrinsic controls exert on their biogeochemistry and their distinctiveness among aquatic ecosystems, peatland pools would therefore be at the forefront of freshwater body response to local and global environmental change. It is indeed likely that peatland pools act as climate sentinels (i.e. Williamson et al., 2009), where small variations in temperature or precipitation induce large structural and functional changes. In fact, peatland pools appear to be even more responsive than previously-defined freshwater climate sentinels (i.e. lakes and reservoirs; Williamson et al., 2009) as we showed that relatively small and short-term climate variations within a six-years period had considerable impact on C and nutrient cycles. Considering the relatively stable influence terrain exerts on pool biogeochemistry, the role climate plays in controlling variability at both small and broad scales may then increase if it keeps changing rapidly, bringing a considerable level of uncertainties to future predictions of peatland pool biogeochemistry and its effects on the local and global environment. Further survey and monitoring efforts conducted in understudied terrain and climate settings should thus be pursued to reduce this uncertainty.

Chapitre 4. *Patterns and drivers of organic matter decomposition in peatland pools*

4.1 Avant-propos

Ce chapitre présente les résultats d'une étude visant à déterminer les facteurs environnementaux qui contrôlent les processus biogéochimiques de décomposition de la MO dans les mares d'une tourbière du sud du Québec. Cette étude a été conçue et imaginée par Julie Talbot, Jean-François Lapierre, Tim R. Moore et moi-même. J'ai créé le dispositif expérimental, dirigé la collecte des échantillons, mené les incubations en laboratoire, effectué le traitement et l'analyse des données, et rédigé l'article scientifique. Les co-auteurs ont toutes et tous participé à l'enrichissement de l'étude et du manuscrit. L'article est en préparation pour une soumission prochaine à la revue *Biogeosciences*.

Référence complète :

Arsenault, J., Talbot, J., Moore, T. R., Knorr, K. H., Teickner, H. & Lapierre, J. F. (en préparation). Patterns and drivers of organic matter decomposition in peatland pools.

4.2 Abstract

Peatland pools are net carbon (C) sources that develop within C-accumulating ecosystems. The emission of carbon dioxide (CO_2) and methane (CH_4) from peatland pools comes from the degradation of organic matter (OM) that comprise the surrounding matrix because of higher oxygen (O_2) concentrations, warmer temperature, and deeper light penetration in the pool than in the peat. These properties vary spatially within and among pools, but the relationships between the structure and the functions of peatland pools and, more generally, the role they play in the C budget of a peatland, remain unclear. This study aimed at providing a mechanistic understanding of OM decomposition in peatland pools. We quantified rates of OM decomposition from fresh litter at different depths in six pools of distinct morphological characteristics in a temperate ombrotrophic peatland using litterbags of *Sphagnum capillifolium* and *Typha latifolia* over a 27-month period and measured potential CO_2 and CH_4 production of pool sediments in laboratory incubations. Rates of decomposition were higher for *T. latifolia* than *S. capillifolium*. Overall, decomposition rates were higher at the pool surface and decreased with increasing depth. Pool sediment chemistry was variable among pools and influenced the production of CH_4 and CO_2 from sediments, with decreasing CO_2 production with increasing OM humification and decreasing CH_4 production with increasing nitrogen-to-phosphorus ratio. Both CH_4 and CO_2 production from pool sediments were higher in the ~1 m deep pools, but similar in the < 1 m and > 1.5 m deep pools. Our results show that OM decomposition in peatland pools is highly variable, but the chemistry of OM alone can not explain spatial variations in decomposition rates. Rather, decomposition depends primarily on the environmental conditions in which it occurs, with spatial patterns emerging in both fresh litter and pool sediment decomposability as a function of pool depth.

4.3 Introduction

Peatlands are among the largest carbon (C) reservoirs on the planet, storing twice the C of forest soils (Loisel et al., 2021; Pan et al., 2011) but covering only 3% of the Earth's surface (Xu et al., 2018). The positive C balance of peatlands is the result of slower organic matter (OM) decomposition rates than net primary production in response to anoxic conditions in the cool and water-saturated soils, to functionally limited decomposer communities, and to plant species that are slow to decompose (Rydin & Jeglum, 2013). Open-water pools that develop in many temperate and boreal peatlands are small (often < 2000 m^2 and < 2 m deep; Arsenault et al., 2022) and generally have a negative C balance because of distinct environmental

conditions (e.g. higher oxygen – O_2 – availability and warmer temperature) than in the surrounding soils (Foster & Glaser, 1986) that lead to higher OM decomposition than production (Pelletier et al., 2015). Because pools form through the decomposition of the surrounding peat matrix, peatlands that have pool covers greater than 37% may be net sources of C to the atmosphere (Pelletier et al., 2014). Within a single peatland, pool morphology (i.e. depth, area, shape) and OM quality may be heterogeneous (Arsenault et al., 2019), which influences the biogeochemical patterns of pools and the magnitude of the processes that control them as shallow pools (< 1 m) show higher concentrations in dissolved organic C (DOC), total nitrogen (TN), CO_2 and CH_4, and lower pH than deep pools (> 1.5 m) (Arsenault et al., 2018). For example, in a spatiotemporal study of peatland pool biogeochemistry, Hassan et al. (2023) found positive relationships between dissolved carbon dioxide (CO_2) and methane (CH_4) supersaturation and dissolved OM (DOM) concentration and composition. Assuming most of the DOM processed in temperate and boreal peatland pools originate from the surrounding peat and vegetation (Prijac et al., 2022), and with regards to the role pool morphology exerts on biogeochemical patterns and processes, OM degradation rates may vary spatially in response to different environmental conditions. It is however unclear how environmental heterogeneity affects decomposition processes in peatland pools and, more broadly, the general capacity of peatlands to sequester C.

Spatial variations in decomposition and C emission rates from pools may emerge as a function of pool depth and hydrological connectivity with the surrounding peat soil. Pools are more oxygenated, warmer and light penetrates deeper in their profile than in the surrounding peat, but O_2 concentrations, temperature and light intensity at the sediments decrease with increasing pool depth (Arsenault et al., 2018). Degree of anoxia, temperature and luminosity are major drivers of OM decay in aquatic ecosystems as they control microbial activity of production and decomposition (Pace & Prairie, 2005). Then, OM decomposition rates may be higher in shallow than in deeper pools because of increased microbial activity at the water-peat interface.

Decomposition rates in aquatic and terrestrial ecosystems are also related to the chemical and physical composition of the substrate. For example, in a northern peatland, decay rates (*k* values) of litter ranged, over up to six years, from 0.05 yr^{-1} for some *Sphagnum* species to 0.25 yr^{-1} for vascular plants and > 0.9 yr^{-1} in soft-tissued plants such as *Maianthemum* (Moore et al., 2007). Spatial variations in peat-forming vegetation composition affect the chemistry of the peat and potentially that of the litter that falls in the pools (e.g. Kaštovská et

al., 2018). Peat chemistry also varies in depth, with deeper layers of peatland soils being generally depleted in phosphorus (P) and enriched in nitrogen (N) and aromatic organic C molecules that are more recalcitrant to decomposition compared to the surface layers (Cocozza et al., 2003; Wang et al., 2015). It is thus possible that OM decomposition rates in pools also vary within a peatland because of vegetation heterogeneity and changing substrate quality with increasing pool depth. However, the relationships between the physical conditions of temperate peatland pools and the chemical properties of decaying OM, and the control they exert on decomposition rates in peatland pools, have seldom been studied.

Decomposition is a function of both the reactivity of the environment in which it occurs and the quality of the OM to be degraded. The litterbag technique is a commonly used method to measure monthly to multi-year decomposition rates in aquatic (Tonin et al., 2018) and terrestrial (Karberg et al., 2008) ecosystems. In peatlands, litterbags have been used to compare rates of decomposition of peat-forming plants in different environmental conditions, ranging from anoxic peat layers to oxygenated pond water (Moore et al., 2007). While litterbags provide insights on environmental controls of OM decomposition, they can hardly account for variations in material molecular composition such as observed along peat profiles as both environmental conditions and peat quality change with depth. Laboratory incubations of peat and pool sediments, where decomposition of different materials can be measured under controlled conditions (Schädel et al., 2020), can provide this extra information on the degradability of OM of different molecular composition. Hence, a combination of *in situ* and laboratory experiment approaches are needed to isolate the mechanisms controlling OM decomposition in peatland pools.

Pools are often overlooked in peatland studies (Loisel et al., 2017). While several studies have quantified the negative C budget of peatland pools and related it to high levels of decomposition (e.g. Pelletier et al., 2014), little focus has been put on the mechanisms controlling the rates at which these decomposition processes occur. Hence, the relationships between the structure and the functions of peatland pools and, more generally, the role they play in the C budget of a peatland, remain unclear. In this context, this study aimed at providing a mechanistic understanding of OM decomposition in peatland pools. Specifically, the objectives were to i) quantify rates of similar fresh OM litter decomposition in pools of different morphological and chemical properties; ii) measure the degradability of individual pool sediments under controlled conditions; and iii) assess the role both litter and sediment OM chemistry plays on decomposition rates. Using the litterbag technique for a 27 month *in situ*

experiment and laboratory incubations of pool sediments, we measured rates of decomposition of OM in and from peatland pools and characterized spatiotemporal changes in OM composition.

4.4 Methodology

4.4.1 Site description

In situ experiments and organic matter (OM) samples for degradation experiments were collected in Grande plée Bleue (GPB) (Figure 4.1), a 15 km² mostly undisturbed ombrotrophic peatland located 12 km southeast of Québec City, Canada (46°47'N, 71°03W, altitude ~88 m). Its climate is cool continental, with a mean annual air temperature of 4.8 °C and a mean annual precipitation of 1066 mm (206 of which fell as snow) for the 1991-2020 interval at the nearest meteorological station (4.2 km from the study site) (Environment Canada, 2022). The peatland was initiated over marine sediments of the Goldthwait sea 9500 years ago and expanded laterally through the paludification of surrounding forests (Lavoie et al., 2012). Ombrotrophic conditions prevailed for the last 8300 years, and peat depth reaches 5 m in the centre of the peatland (Lavoie et al., 2012). Vegetation composition varies in the peatland, with some areas dominated by *Sphagnum* mosses, small ericaceous shrubs (e.g. *Kalmia angustifolia, Chamaedaphne calyculata*) or graminoids (e.g. *Carex* spp., *Eriophorum virginicum* and *Rhyncospora* spp.), some by continuous shrub covers (e.g. *K. angustifolia, Rhododendron* spp. and *Gaylussacia baccata*) underlain by *Sphagnum* mosses, and others by dense and tall coniferous trees (e.g. *Picea mariana* and *Larix laricina*).

The southern and central parts of the peatland are characterized by the presence of > 600 pools of different shape, area (10-2350 m², mean 381 m²; n = 152) and depth (15-219 cm, mean 93 cm; n = 158) (Figure 4.1). For this study, we selected six pools: three pools located in an open area with vegetation mainly composed of extensive *Sphagnum* moss mats and small, sparse *C. calyculata* and *K. angustifolia* shrubs, and three pools in a treed area with *P. mariana* (height > 2 m) dominating the canopy. In each area, the three pools that we selected were of different depths (shallow, < 1 m; average, ~ 1 m; deep, > 1.5 m). In each pool, we installed litterbags, took samples of the sediment and underlying peat, and collected water and gas samples.

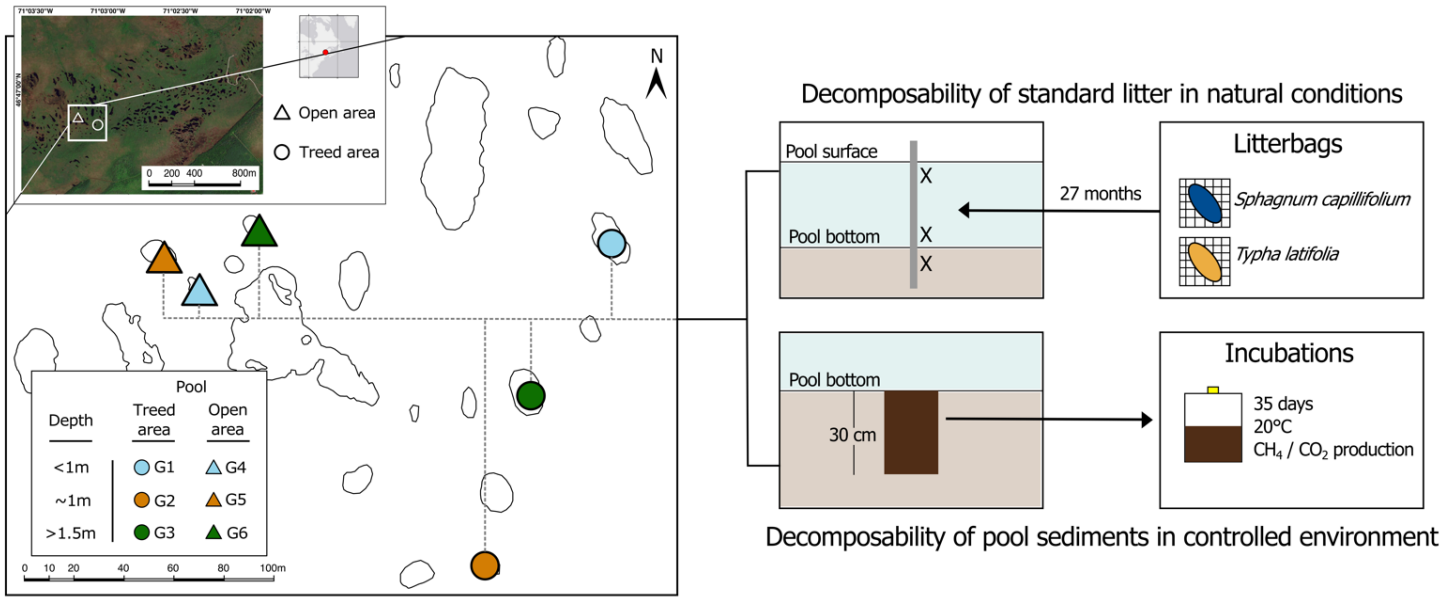

Figure 4.1. Conceptual framework of the experiment. Six pools of different depth categories were selected in two areas of the peatland characterized by distinct vegetation assemblages. We installed litterbags of *Sphagnum capillifolium* and *Typha latifolia* over a period of 27 months at the surface, near the bottom and in the sediments of each pool to measure the decomposability of standard fresh litter under natural conditions, conducted incubations on sediment samples collected at the centre of each pool to measure the decomposability of pool bottom material under controlled settings, and assessed pool sediment chemistry and changes in litter chemical composition after 27 months.

4.4.2 Litterbags

To assess for the effect of pool chemical and physical characteristics on decomposition rates, we installed litterbags of *Typha latifolia* leaf and stem tissues (collected at Mer Bleue peatland, Ontario, and cut in 10 cm lengths) and *Sphagnum capillifolium* (capitulum and first 5 cm of the stem, harvested *in situ*) in each of the 6 pools and in the surrounding peat. Upon collection, litter was oven-dried (40 °C). Litterbags were made of fibreglass mosquito netting with a 1 x 1 mm mesh size. Bags were numbered, weighed, filled with approximately 2 g of dry material, then weighed again to obtain the initial mass of litter.

In June 2019, we installed triplicates of both types of litter at three depths (at the surface, 15 cm above the pool bottom, and 15 cm below the peat-water interface) in each pool. Surface litterbags were attached to a buoy. To reach deep locations, bags were fixed on wood stakes that were inserted in the pool sediments. In the two areas, we also installed triplicates of litterbags of the two litter types in the unsaturated, surficial layer of the peat surrounding the pools (5 cm under the peatland surface) to compare decomposition rates between the acrotelm and the pools.

Litterbags were retrieved five times over the course of three growing seasons. A first set of bags was retrieved from each pool and from the peat in the two zones at the end of the 2019 growing season (4 months after installation). The other bags were retrieved in the spring and fall 2020 (respectively 11 and 16 months after installation) and again in the spring (23 months) and fall 2021 (27 months). Upon collection, litterbags were stored at -20 °C until analysis. After thawing at 4 °C, bags were carefully washed using deionized water and tweezers to remove any alien material. Remaining litter was oven-dried (40 °C) for 72 h, then weighed, and percent of original mass was calculated. We then milled the litter and analyzed for molecular composition of C compounds to assess changes between the original material and material that has been exposed to environmental conditions for 27 months in the pools.

4.4.3 Incubations

To test for differences in peat composition and degradability between pools, we collected samples of bottom material at the centre of the six studied pools. Using a Kajak-Brinkhurst corer, in spring 2021, we sampled the first 30 cm of pool sediments to reach both limnic sediments and the underlying peat. We transferred each core in clean low-density polyethylene bags and homogenized the material. Back in the lab, we drained the samples of excess water using a cheese cloth (24 h at 4 °C). We then brought the samples to room temperature for another 24 h before we started the incubations.

From each pool sediment sample, we took five subsamples for incubations. At the initial time, we half-filled 250 mL glass jars with the drained, homogenized pool bottom subsample, added 30 mL of deionized water to measure DOC production after incubations and sealed the jars with lids equipped with stopcock valves attached to rubber tubes for headspace sampling. Jars were kept at 20 °C with no direct sunlight for the entire incubation time. For each set of pool subsample, we also added a sealed, empty jar to measure ambient air gas concentrations.

Five-milliliter gas samples were taken from the headspace of each jar using a syringe at initial time (T = 0 day) and after T = 0.5, 1, 2, 3, 5, 7, 11, 14, 21, 29 and 35 days. Gas sampled in the headspace was replaced with ambient air. Gas samples were rapidly analyzed for CH_4 and CO_2 concentrations on a Shimadzu GC-14 gas chromatograph, equipped with a flame ionization detector for CH_4, and a methanizer with a 0.7 m column of Ni-reduced catalyst for CO_2. Concentrations were corrected to account for the addition of ambient air at every sampling time.

At the end of the incubations, material from each jar was drained to collect water, was oven-dried for 5 days at 40°C and weighed. We also dried the remaining original material at the same time. Because we were unable to retrieve more than 5 mL of water from any jar, we bulked the incubation water samples per pool and analyzed for DOC and TDN concentrations on a Shimadzu TOC-V total organic carbon analyzer after acidification with HCl (ASTM methods D7573-09 and D8083-16). All dried material was milled and analyzed for molecular composition to characterize differences in sediment material between pools.

We calculated CH_4 and CO_2 production rates in each jar from between each of the sampling as the linear change in gas concentration over time, allowing for changes from replacing headspace with ambient air (Kim et al., 2015). We measured ambient CO_2 and CH_4 concentrations and estimated the post-sampling concentration as the new concentration in the jars until the next sampling by taking into account the addition of 5 mL of ambient air in each jar. Production rates from the five replicates were averaged and reported relative to the dry mass of C. We estimated the 35-days total production of CH_4 and CO_2 by summing the rates of production in a sampling interval multiplied by the number of days between samplings. Rates were treated as production when >0 and as consumption when <0. Rates were expressed in μg CO_2 g C^{-1} day^{-1} and in μg CH_4 g C^{-1} day^{-1}.

4.4.4 Litter and peat chemistry

To account for temporal changes in fresh litter chemistry and spatial variations in pool sediment chemistry, we analyzed final and initial litter and sediment elemental contents (C, N, P, K, Ca, Na, K, Mg), isotope signatures $\delta^{13}C$ (‰ V-PDB), $\delta^{15}N$ (‰ air nitrogen), and absorbance of mid-infrared radiation in the range 650 to 4000 cm^{-1} providing information on the relative abundances of molecular structures.

Concentrations and isotopic composition of C and N were measured with an elemental analyzer (EA 3000, Eurovector, Pavia, Italy) coupled to an isotope ratio mass spectrometer (IRMS; Nu Horizon, NU Instruments, Wrexham, UK), using certified reference materials and working standards. All other elemental contents (P, K, Ca, Na, K, Mg) were measured on a wavelength dispersive X-ray fluorescence spectroscope calibrated with certified and own reference standards (WD-XRF; ZSX Primus II, Rigaku, Tokyo, Japan). To this end, 500 mg of ground, powdered samples were pressed to a pellet with 13 mm diameter (without pelleting aids) at a load of approximately 7t.

Mid-infrared spectra (MIRS) were measured on 13 mm diameter pellets pressed from a mixture of 2 mg of milled sample material and 200 mg of KBr (FTIR grade, Sigma Aldrich) on a transmission Fourier transformed infrared spectrometer (Cary 660 FTIR spectrometer, Agilent) in the range 600 to 4000 cm^{-1} at a resolution of 2 cm^{-1} and by averaging 32 scans per spectra. Prior to each measurement, the optical path was purged for 180 s with synthetic dry air. Spectra were background corrected by subtracting a KBr background and converted to absorbance.

In a next step, the spectra were exported to R version 4.2.0 (R Core Team, 2022) and the following preprocessing steps were applied using the 'ir' package version 0.3.0 (Teickner, 2023): (1) Baseline correction using a convex hull-based algorithm in the 'hyperSpec' package version 0.100.0 (Beleites & Sergo, 2021), (2) clipping of the first and last 5 cm^{-1} and a second baseline correction step to remove artifacts from the first baseline correction step, (3) normalization (so that all intensity values of a spectrum sum to one). These preprocessing steps are commonly applied heuristic procedures to reduce effects such as internal reflectance not directly related to the relative abundance of molecular structures in the sample.

The preprocessed MIRS were analyzed with the 'irpeat' package version 0.2.0 (Teickner & Hodgkins, 2022) by computing the four humification indices defined in Broder et al. (2012); ratios of the intensities at 1420 (OH and CO of phenols, CH_2 and CH_3 groups, C–O–H in-plane bending), 1510 (C=C stretching of aromatics, N–H bending and C–N stretching in proteins), 1630 (NH_2 bending and C=O stretching in proteins, aromatic C=C and COO^- stretching), and 1720 cm^{-1} (C=O stretching in carbonyls, carboxyls, esters) to the intensity at 1090 cm^{-1} (attributed mainly to C–O stretching of cellulose in absence of silicates) (Broder et al., 2012; Parikh et al., 2014; Stuart, 2004).

4.4.5 Pool water chemistry

At each litterbag retrieval, we collected water samples from each pool. Samples were taken 20 cm below the surface at the centre of the pools and analyzed for DOC, total N and P (TN and TP), nitrate (NO_3), ammonium (NH_4), phosphate (PO_4), pH, and absorbance (A_{254}) to calculate Specific UV absorbance at 254 nm (SUVA) and estimate DOC aromaticity (Weishaar et al., 2003). During summer 2021, we measured methane (CH_4) and carbon dioxide (CO_2) fluxes in each of the six pools using a Li-Cor 8200-01S Smart Chamber coupled to a Li-Cor LI-7810 analyzer. At the same time, we measured pool dissolved CH_4, CO_2 and N_2O concentrations using the headspace technique. Dissolved gas samples were analyzed in the lab on a Shimadzu

GC-14 gas chromatograph and concentrations in the pools were obtained using Henry's law for the headspace concentrations. Barometric pressure, wind speed and air temperature were measured *in situ* using a Kestrel 4000 weather meter. Pool water temperature was measured with a DO200A YSI probe. Laboratory analyses were performed as described in Arsenault et al. (2018).

4.4.6 Statistical analyses

We first determined the differences and similarities in pool morphometry and water chemistry between the six studied pools using Kruskall-Wallis rank and Dunn post-hoc tests for non-normally distributed variables. We measured pool depth and water chemistry at all retrievals, and we used the average to compare the pools. We did not compare pools for which we only had one sampling time (e.g. area, dissolved CH_4, CO_2 and N_2O concentrations, and CH_4 and CO_2 fluxes).

To determine litterbag decomposition over time, we calculated decay rates (k value) by computing a single-exponential linear regression model ($ln[y] = a - kt$) based on the average percentage of mass remaining (y) of triplicates of litter at each retrieving time, with a = intercept, k = decay constant, and t = time in years (Trofymow et al., 2002). After testing for normality and homogeneity of variances, we used two-way analyses of variance (ANOVA) to compare decay k values among pool, depth and litter types, and account for the possible interacting effects of pool water chemistry and depth on decomposition. To determine the effect of water chemistry on decomposition rates, we used generalized linear models (GLM) with gamma distribution families of the percentage of mass remaining in the bags at the surface and at the bottom of the pools with water chemistry measured at each retrieving. We also used GLMs (gamma distribution) and Spearman's rank correlations for non-normally distributed variables to quantify the relationship of decay k values and depth of incubation and to assess the influence of decay k values on final litter material chemistry.

We used Kruskall-Wallis rank and Dunn post-hoc tests for non-normally distributed variables to compare differences in CO_2 and CH_4 production and sediment chemical properties among pools and between the treed and open areas of the peatland. We also used Spearman's rank correlations and a principal component analysis (PCA) to explore the relationships of CO_2 and CH_4 total production and sediment chemistry.

All statistical analyses were performed on R, version 4.1.2 (R Core Team, 2022).

4.5 Results

4.5.1 Decomposability of standard litter in natural conditions

4.5.1.1 Effects of incubation position on litter decomposition rates

After 27 months in the pools, *T. latifolia* was more degraded than *S. capillifolium*, and decay rates were higher at the surface of the pools than at depth (Figure 4.2; Table 4.1). In particular, decay *k* values derived from single-exponential linear regression models for *T. latifolia* ranged 0.101-0.193 yr^{-1} at the surface of the pools and 0.030-0.084 yr^{-1} in depth (Table 4.1). For *S. capillifolium*, *k* values ranged 0.052-0.110 yr^{-1} at the surface of the pools and 0.038-0.091 yr^{-1} at depth (Table 4.1). In the surficial layer of the soil surrounding the pools (10 cm under the surface), *T. latifolia* had *k* values of 0.562 yr^{-1} in the treed and 0.389 yr^{-1} in the open area while *S. capillifolium* had *k* values of 0.090 yr^{-1} and 0.070 yr^{-1} respectively (Table 4.1).

Two-way ANOVAs showed no difference in decay rates among pools ($P = 0.524$) and no interacting effect of pool and depth on decomposition ($P = 0.965$) (Annexe III, Table S4.1). In all pools, decay rates for *T. latifolia* were higher at the surface than at the bottom of the pools and in the sediments (Figure 4.2; Table 4.1, $P < 0.011$) but were similar at the bottom of the pools and under the sediments ($P = 0.978$) (Annexe III, Table S4.2). There was little difference in *k* values for *S. capillifolium* between the different depths ($P = 0.1$) (Annexe III, Table S4.3). Overall, *T. latifolia* had higher decay rates than *S. capillifolium* at the surface ($P < 0.001$), but not at depth ($P = 0.248$) (Annexe III, Table S4.4). Decay rates were also higher in the peat than at any depth in the pools for *T. latifolia* (Table 4.1; $P < 0.001$) but were similar in all locations for *S. capillifolium* (Table 4.1; $P > 0.1$). These results suggest that both environmental reactivity and litter chemistry are important drivers of OM decomposition in peatland pools.

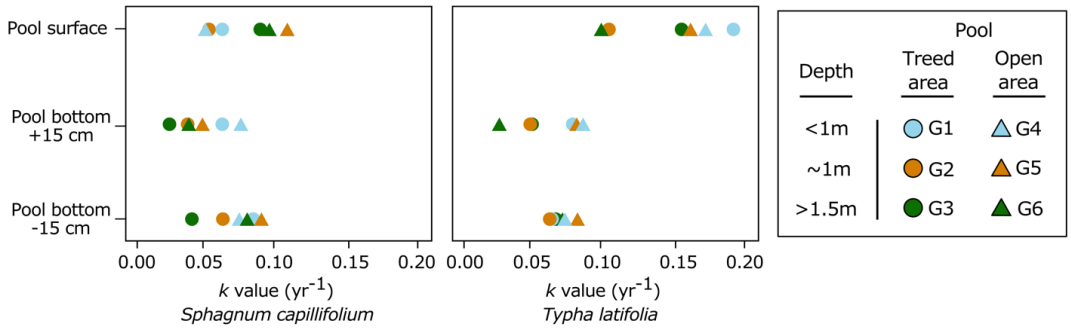

Figure 4.2. Decay *k* values (yr^{-1}) of *Sphagnum capillifolium* and *Typha latifolia* decomposition along the pool depth profiles in both treed and open areas of the peatland after 27 months of incubation.

Table 4.1. Single-exponential linear regression models and percentage of remaining mass (± standard deviation) of *Typha latifolia* and *Sphagnum capillifolium* litterbags after 27 months of incubation in 6 pools of different morphometry (depth at the centre and surface area are shown) and in the unsaturated, surficial layer of the surrounding peat. Material was incubated at the surface of the pools (depth = 0), 15 cm over the pool bottoms in the centre of the pools (depth = +15), and 15 cm below the pools, in the sediments (depth = -15). In the peat (acrotelm), litterbags were installed ~5 cm under the peatland surface. The single-exponential linear regression model ($ln[y] = a - kt$) was based on the percentage of mass remaining (y), with a = intercept, k = decay constant, and t = time in years. *P* = p-value of the regression model; % MR = percentage of original mass remaining in the litterbags after 27 months.

Pool	Depth	*Typha latifolia*					*Sphagnum capillifolium*				
		a	k (yr^{-1})	r^2	*P*	% MR	a	k (yr^{-1})	r^2	*P*	% MR
G1 (91 cm; 190 m^2)	0	4.57	0.193	0.83	<0.001	67.7 ± 1.4	4.59	0.065	0.53	<0.001	89.3 ± 4.1
	+15	4.59	0.079	0.83	<0.001	84.5 ± 3.0	4.61	0.066	0.54	<0.001	87.4 ± 0.8
	-15	4.60	0.067	0.54	<0.001	89.4 ± 2.6	4.66	0.087	0.54	<0.001	90.7 ± 4.0
G2 (106 cm; 10 m^2)	0	4.58	0.106	0.66	<0.001	74.8 ± 5.5	4.57	0.053	0.53	<0.001	90.7 ± 1.1
	+15	4.57	0.051	0.22	0.029	89.3 ± 2.9	4.58	0.044	0.57	<0.001	90.1 ± 0.7
	-15	4.59	0.065	0.51	<0.001	88.3 ± 2.6	4.62	0.066	0.73	<0.001	90.2 ± 1.0
G3 (170 cm; 180 m^2)	0	4.56	0.161	0.85	<0.001	68.3 ± 4.4	4.58	0.091	0.85	<0.001	79.8 ± 0.3
	+15	4.59	0.052	0.68	<0.001	87.9 ± 1.9	4.59	0.038	0.51	<0.001	94.4 ± 0.6
	-15	4.59	0.068	0.65	<0.001	86.1 ± 2.4	4.63	0.044	0.29	0.014	96.3 ± 1.7
G4 (60 cm; 35 m^2)	0	4.61	0.166	0.92	<0.001	70.1 ± 4.2	4.56	0.052	0.42	0.002	87.5 ± 4.2
	+15	4.61	0.084	0.85	<0.001	81.6 ± 1.0	4.62	0.076	0.48	<0.001	85.7 ± 6.0
	-15	4.61	0.073	0.65	<0.001	84.4 ± 9.1	4.62	0.077	0.47	0.001	87.0 ± 4.0
G5 (107 cm; 129 m^2)	0	4.58	0.158	0.91	<0.001	69.7 ± 4.0	4.57	0.110	0.63	<0.001	77.1 ± 4.0
	+15	4.59	0.080	0.69	<0.001	83.7 ± 4.4	4.60	0.050	0.41	0.003	90.6 ± 0.8
	-15	4.59	0.081	0.46	0.001	85.2 ± 8.0	4.63	0.091	0.60	<0.001	81.2 ± 3.8
G6 (177 cm; 48 m^2)	0	4.57	0.101	0.78	<0.001	80.5 ± 0.6	4.60	0.093	0.66	<0.001	81.6 ± 6.1
	+15	4.58	0.030	0.18	0.046	94.5 ± 6.4	4.59	0.041	0.59	<0.001	89.3 ± 1.5
	-15	4.60	0.070	0.92	<0.001	85.8 ± 1.2	4.64	0.079	0.52	<0.001	88.7 ± 2.7
Acrotelm, treed area		4.74	0.562	0.82	<0.001	28.1 ± 6.9	4.56	0.090	0.52	<0.001	79.5 ± 5.0
Acrotelm, open area		4.68	0.389	0.82	<0.001	38.5 ± 6.0	4.58	0.070	0.31	0.018	87.3 ± 5.4

4.5.1.2 Effects of incubation depth on litter chemistry

Distinctive patterns in litter chemistry appeared after 27 months of incubation. At the end of the experiment and compared to the initial material, there was no change in C

concentration at any position of incubation for both *T. latifolia* and *S. capillifolium*. For *T. latifolia*, there was generally a net gain of P, ranging from 3 to 157 µg P g^{-1} on average over time and with the highest gain at the bottom of the pools from the treed area, indicative of retention of initial P, but little change in N concentration (gain < 5 µg N g^{-1}). There was little change in N and P concentrations for *S. capillifolium* at all positions. Spearman correlations showed that C/N (ρ = 0.50, P = 0.002) and N/P (ρ = -0.59, P < 0.001) ratios in both *T. latifolia* and *S. capillifolium* respectively increased and decreased with depth of incubation, regardless of the pool (Figure 4.3).

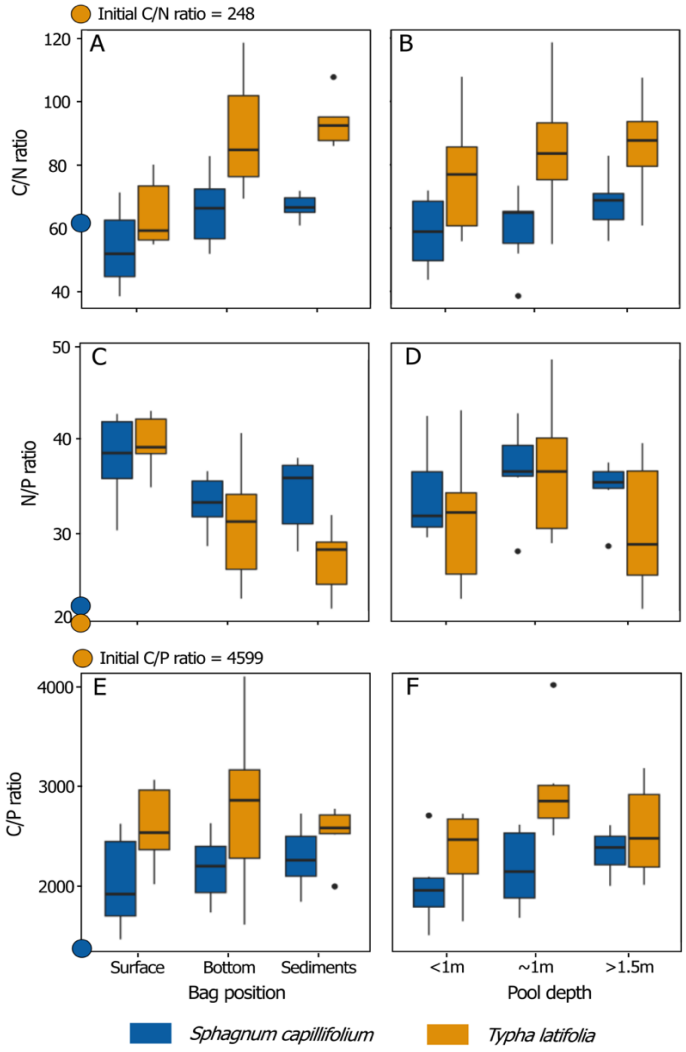

Figure 4.3. Changes in *Sphagnum capillifolium* (blue) and *Typha latifolia* (orange) C/N/P ratios after 27 months in relation to position of incubation in the pools (surface, at the bottom, and in the sediments, all pools together) and pool depth category (<1 m, ~ 1 m, and > 1.5 m, regardless of depth of incubation). Boxes show the median and the 25th and 75th percentiles of the distributions, and whiskers show the 10th and 90th percentiles. Colored dots on the Y-axes of the graphs show the initial chemistry of the litter.

Changes in isotopic signatures emerged spatially, with $\delta^{13}C$ ratio for *S. capillifolium* slightly increasing in depth, from -27.5 ‰ at the surface to -27.3 ‰ at the bottoms of the pools and in the sediments. For *T. latifolia*, $\delta^{13}C$ also slightly increased in depth from -27.0 ‰ at the surface to -26.6 ‰ at the bottoms of the pools and to -26.7 ‰ in the sediments. Changes in $\delta^{15}N$ followed the same trends for both litter types, with decreasing values from surface > bottom of the pools > sediments (0.45 ‰ > -1.10 ‰ > -2.59 ‰ and -5.97 ‰ > -7.72 ‰ > -7.90 ‰ for *T. latifolia* and *S. capillifolium*, respectively).

For both litter types, there was no variation in humification indices (HIs) among position of incubations and all HI increased over time, except for 1720/1090 ratio of *S. capillifolium* which decreased from 0.51 in the initial material to 0.47 on average at the end of the experiment. Compared to the initial material, HIs 1510/1090 and 1630/1090 were larger for both *S. capillifolium* and *T. latifolia* after 27 months in the pools. There was also an increase in HI 1720-1090 (carboxylic acids and aromatic relative to carbohydrates) over time for *S. capillifolium*, but a decrease for *T. latifolia*.

4.5.1.3 Relationships between litter chemistry and decomposition rates

There were strong relationships between decomposition and litter chemistry for *T. latifolia*, as shown by the GLMs of decay *k* values and $\delta^{13}C$, $\delta^{15}N$ and C/N and N/P ratios, (Figure 4.4B-E; Annexe III, Table S4.5). There were also strong interactions between *T. latifolia* decomposition rates and humification indices, as measured by the 1510/1090 and 1630/1090 FTIR peak ratios, showing increasing proportions of aromatic C and microbial proteins with increasing decay *k* values (Figure 4.4F-I). There was however no discernible relationship between decomposition rates and OM chemistry for *S. capillifolium*.

Regardless of litter type, there were correlations between decomposition rates and residual (i.e. 27 month) litter chemistry (Figure 4.4B-I). Decay *k* values were indeed negatively correlated to C/N ratio (ρ = -0.28, P = 0.1) and positively correlated to N/P ratio (ρ = 0.34, P = 0.05) and $\delta^{15}N$ (ρ = 0.40, P = 0.02). Similarly, litter humification indices were all positively correlated to decay *k* values: 1420/1090 (ρ = 0.30, P = 0.08), 1510/1090 (ρ = 0.42, P = 0.01), 1630/1090 (ρ = 0.43, P = 0.01), and 1720/1090 (ρ = 0.29, P = 0.08). Overall, these results suggest that decomposition rates in peatland pools respond to changes in litter chemistry regardless of environmental reactivity.

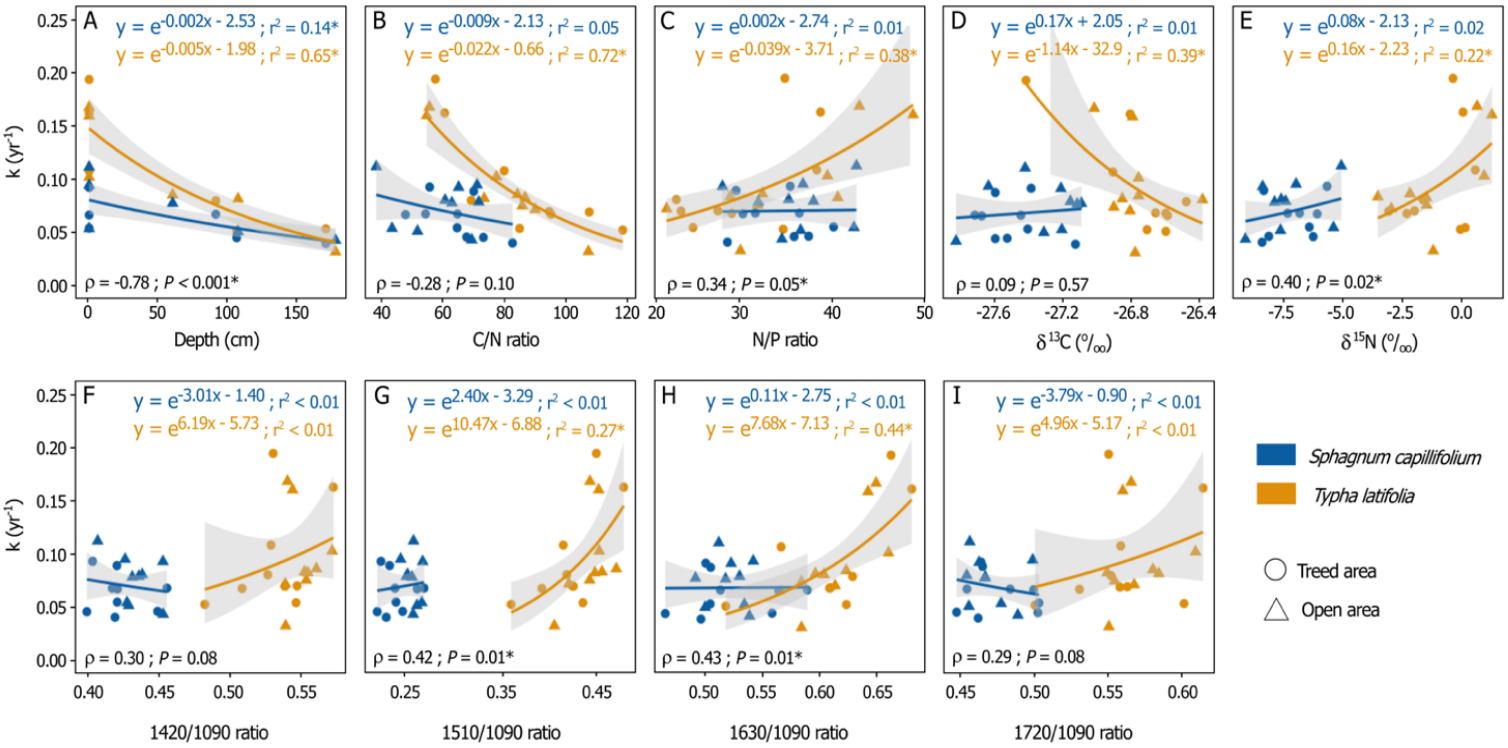

Figure 4.4. Decay *k* values for *Sphagnum capillifolium* and *Typha latifolia* in relation to A) depth of incubation in the pools, and final litter chemistry (after 27 months of incubation in the pools): B) C/N ratio, C) N/P ratio, D) $\delta^{13}C$ (‰), E) $\delta^{15}N$(‰), and humification indices (ratios of MIRS intensities) at F) 1420 cm^{-1}, G) 1510 cm^{-1}, H) 1630 cm^{-1}, and I) 1720 cm^{-1} to the intensity at 1090 cm^{-1} after 27 months of incubations in the pools. In A), bags that were incubated in the pool sediments are not shown. Colors (blue and orange) and shapes (circles and triangles) respectively represent litter type and the peatland area in which the litter was incubated (treed or open area). Generalized linear models for individual litter types using gamma distribution, model r^2, and Spearman correlation's rhô (ρ) and p-values (*P*) of the relationships of *k* values to the identified properties, regardless of litter type, are shown. Models and correlations with p-values < 0.05 are indicated with an asterisk (*).

4.5.1.4 Effects of pool morphology and chemistry on litter decomposition

The six pools we selected had different physical and chemical characteristics. Pools located in the treed area, though being similar in depth to pools of the open area (Kruskal-Wallis; $P = 0.967$), had higher DOC concentration ($P = 0.007$), higher SUVA ($P = 0.044$) and lower pH ($P = 0.002$) (Table 4.2). Regardless of the differences in vegetation assemblages surrounding the pools, deep pools (> 1.5 m) had lower TN ($P = 0.002$), TP ($P = 0.009$) and NO_3 ($P = 0.015$) concentrations than shallow (< 1 m) and average (~ 1 m) pools, which had similar chemistry (Table 4.2). Individually, pools also had different chemical characteristics. For example, pool G2 had higher DOC and TP concentrations than any other pool throughout the

study (Table 2.2). However, GLMs showed little relationships between water chemistry and litter decomposition (Annexe III, Table S4.6), indicating that degradation rates are mostly driven by litter type and the position in the pools (Figure 4.2).

Table 4.2. Mean values (± standard deviation) of pool water physical and chemical variables measured at the beginning and at the end of the 2019, 2020 and 2021 growing seasons. Letters in indices show levels of difference in water chemistry between individual pools for variables measured at every sampling time as determined by Kruskall-Wallis and Dunn post-hoc tests at $P < 0.05$.

	Treed area			**Open area**		
	G1	G2	G3	G4	G5	G6
Depth (cm)	91 (± 4)^{a}	106 (± 9)^{b}	170 (± 5)^{c}	60 (± 10)^{d}	107 (± 5)^{b}	177 (± 4)^{c}
*Area (m^2)	190	10	180	35	129	48
pH	4.12 (± 0.20)^{ab}	3.86 (± 0.19)^{a}	4.11 (± 0.15)^{ab}	4.36 (± 0.17)^{b}	4.41 (± 0.15)^{b}	4.13 (± 0.17)^{ab}
DOC (mg L^{-1})	27.6 (± 13.2)^{a}	39.6 (± 19.9)^{b}	22.0 (± 10.5)^{a}	21.6 (± 10.8)^{a}	22.1 (± 11.6)^{a}	22.6 (± 10.8)^{a}
TN (mg L^{-1})	1.0 (± 0.4)^{a}	1.0 (± 0.3)^{a}	0.6 (± 0.1)^{a}	1.0 (± 0.5)^{a}	1.0 (± 0.4)^{a}	0.6 (± 0.2)^{a}
TP (µg L^{-1})	18.4 (± 6.8)^{a}	51.8 (± 41.3)^{b}	11.7 (± 2.9)^{a}	19.6 (± 11.3)^{a}	14.9 (± 3.5)^{a}	10.0 (± 3.6)^{a}
NO_3 (µg L^{-1})	7.2 (± 4.0)^{ab}	7.3 (± 3.8)^{ab}	3.7 (± 2.5)^{a}	6.2 (± 5.0)^{ab}	10.9 (± 2.4)^{b}	3.8 (± 3.2)^{a}
NH_4 (µg L^{-1})	207.6 (± 287.8)^{a}	47.3 (± 23.1)^{a}	40.7 (± 17.7)^{a}	161.3 (± 185.5)^{a}	296.4 (± 216.0)^{a}	34.0 (± 15.3)^{a}
PO_4 (µg L^{-1})	4.2 (± 0.8)^{a}	5.3 (± 2.4)^{a}	6.0 (± 5.3)^{a}	4.3 (± 3.4)^{a}	3.4 (± 2.3)^{a}	3.6 (± 2.8)^{a}
A_{254}	1.15 (± 0.19)^{ab}	1.67 (± 0.41)^{b}	0.97 (± 0.19)^{a}	0.87 (± 0.43)^{a}	0.79 (± 0.36)^{a}	0.87 (± 0.13)^{a}
SUVA (L mg C^{-1} m^{-1})	4.17 (± 0.31)^{a}	4.28 (± 0.24)^{a}	4.31 (± 0.26)^{a}	4.02 (± 1.05)^{a}	3.80 (± 1.26)^{a}	3.93 (± 0.42)^{a}
†Dissolved CO_2 (mg L^{-1})	1.24	7.85	1.85	2.28	1.50	1.86
†Dissolved CH_4 (mg L^{-1})	0.061	1.44	0.036	0.40	0.17	0.011
†Dissolved N_2O (µg L^{-1})	0.9	0.6	0.9	0.8	0.9	0.9
†Flux CO_2 (mg CO_2 m^{-2} hr^{-1})	42.5	208.2	100.9	148.7	111.8	83.8
†Flux CH_4 (mg CH_4 m^{-2} hr^{-1})	0.76	13.32	0.54	9.61	4.68	0.15

*Pool area was measured once using a 2020 0.12m x 0.12m resolution satellite photo. †GHG dissolved concentrations and fluxes were only measured at the end of the 2021 growing season.

4.5.2 Decomposability of pool sediments under controlled conditions

4.5.2.1 Spatial variations in sediment chemistry and CO_2 and CH_4 production

There were large differences in sediment chemistry between pools and areas of the peatland. For example, P concentrations were higher in pools of the open area of the peatland while the both the lowest and highest N concentrations were respectively recorded in the ~1 m deep pools of the treed and of the open area (Table 4.3). There were also large variations in $\delta^{13}C$ and sediment humification indices among pools.

Table 4.3. Mean total production for CO_2 and CH_4 and chemical properties of pool sediments (± standard deviation, n = 5 replicates per pool) after 35-day incubations. For gas production, negative values are considered consumption. Letters in indices show levels of difference between individual pools as determined by Kruskall-Wallis and Dunn post-hoc tests at p-values < 0.05.

	Treed area			**Open area**		
	G1	G2	G3	G4	G5	G6
Depth (cm)	91 (± 4)^{a}	106 (± 9)^{b}	170 (± 5)^{c}	60 (± 10)^{d}	107 (± 5)^{b}	177 (± 4)^{c}
CO_2 production (µg CO_2 g C^{-1})	1393 (± 581)^{a}	2324 (± 940)^{a}	1415 (± 218)^{a}	1573 (± 579)^{a}	2449 (± 731)^{a}	1720 (± 598)^{a}
CH_4 production (µg CH_4 g C^{-1})	-0.03 (± 0.02)^{a}	123 (± 222)^{a}	0.2 (± 0.3)^{a}	-0.6 (± 1.6)^{a}	3.0 (± 6.3)^{a}	10.2 (± 11.5)^{a}
C (g g^{-1})	0.506 (± 0.012)^{ab}	0.517 (± 0.002)^{c}	0.508 (± 0.003)^{abc}	0.501 (± 0.003)^{b}	0.501 (± 0.003)^{b}	0.513 (± 0.003)^{ac}
N (g g^{-1})	0.033 (± 0.001)^{a}	0.029 (± 0.001)^{b}	0.035 (± 0.001)^{c}	0.034 (± 0.001)^{a}	0.041 (± 0.000)^{d}	0.035 (± 0.000)^{c}
P (µg g^{-1})	299 (± 4)^{a}	409 (± 15)^{b}	255 (± 8)^{c}	369 (± 11)^{d}	448 (± 17)^{e}	518 (± 13)^{f}
C/N ratio	15.4 (± 0.2)^{a}	17.7 (± 0.4)^{b}	14.4 (± 0.3)^{c}	14.9 (± 0.5)^{ac}	12.3 (± 0.1)^{d}	14.6 (± 0.3)^{c}
C/P ratio	1689 (± 55)^{ab}	1265(± 43)^{acd}	1990 (± 71)^{b}	1358 (± 43)^{abc}	1119 (± 35)^{cd}	992 (± 22)^{d}
N/P ratio	110 (± 3)^{a}	72 (± 2)^{b}	138 (± 3)^{c}	91 (± 1)^{d}	91 (± 3)^{d}	68 (± 2)^{b}
$\delta^{13}C$ (‰)	-27.26 (± 0.01)^{a}	-27.73 (± 0.05)^{b}	-27.43 (± 0.02)^{c}	-25.61 (± 0.10)^{d}	-26.03 (± 0.05)^{e}	-28.67 (± 0.06)^{f}
$\delta^{15}N$ (‰)	-1.75 (± 0.02)^{a}	-1.89 (± 0.05)^{ab}	-1.57 (± 0.04)^{c}	-1.98 (± 0.07)^{b}	-2.03 (± 0.07)^{b}	-1.91 (± 0.14)^{ab}
1420/1090 ratio	0.641 (± 0.010)^{ab}	0.668 (± 0.017)^{bc}	0.689 (± 0.018)^{c}	0.628 (± 0.012)^{a}	0.616 (± 0.009)^{a}	0.663 (± 0.021)^{bc}
1510/1090 ratio	0.687 (± 0.013)^{a}	0.697 (± 0.020)^{ab}	0.738 (± 0.017)^{c}	0.675 (± 0.019)^{a}	0.720 (± 0.014)^{bc}	0.756 (± 0.019)^{c}
1630/1090 ratio	1.188 (± 0.020)^{abc}	1.173 (± 0.033)^{ab}	1.246 (± 0.015)^{d}	1.155 (± 0.017)^{ab}	1.179 (± 0.018)^{ab}	1.218 (± 0.030)^{cd}
1720/1090 ratio	0.791 (± 0.014)^{ac}	0.818 (± 0.018)^{b}	0.822 (± 0.027)^{b}	0.763 (± 0.023)^{c}	0.718 (± 0.024)^{d}	0.777 (± 0.027)^{ac}

After 35 days of incubations, mean total production for CO_2 and CH_4 respectively ranged between 1393 and 2449 µg CO_2 g C^{-1}, and -0.03 and 123 µg CH_4 g C^{-1} (Table 4.3). The highest total CO_2 and CH_4 production were from ~1m deep pools from both the treed and open areas, while shallow and deep pools had similar production. There was however no difference in CO_2 (Kruskal-Wallis; P = 0.35) and in CH_4 (Kruskal-Wallis; P = 0.44) production between pools of the treed and open areas. Production rates of CO_2 were usually highest in the first week of incubation and decreased afterward (Figure 4.5C). For all pools, rates varied over time and between pools but were generally constant among replicates. For CH_4, total production and production rates were close to zero in the first days of incubation but generally increased from day 5 to day 35, possibly indicating the development of anaerobic conditions in the jars past the first week that would not be counterbalanced by the addition of ambient air after subsampling (Figure 4.5C-D). There was no correlation between CO_2 and CH_4 production rates (ρ = 0.04, P = 0.75).

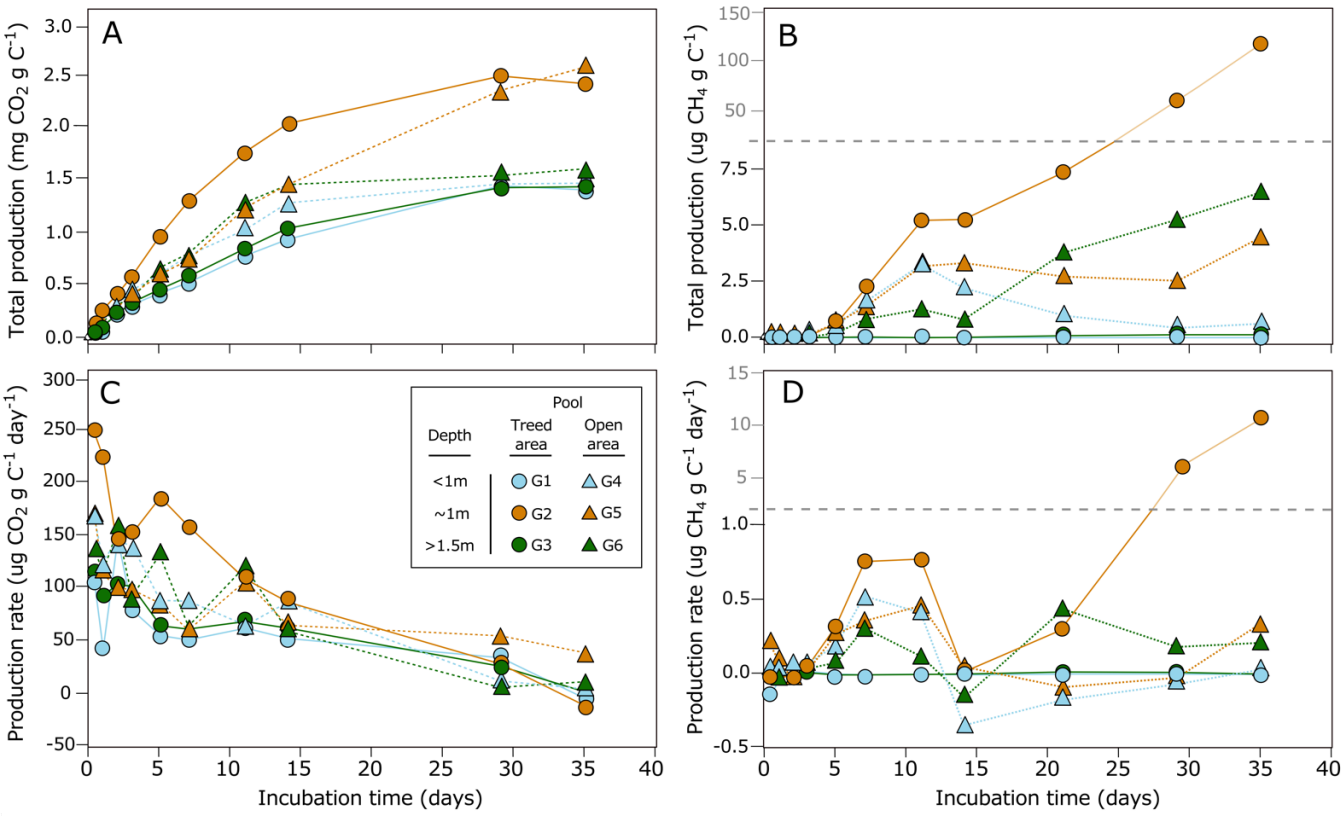

Figure 4.5. A) Total CO_2 and B) total CH_4 produced from the incubation of the first 30 cm of bottom material (including limnic material and the underlying peat) of the six studied pools (G1 to G5) over the 35-day period. C) Potential production rates for CO_2 (µg CO_2 g C^{-1} day^{-1}) and D) CH_4 (µg CH_4 g C^{-1} day^{-1}) for each pool sediment. Dots are average values of five replicates.

4.5.2.2 Effects of sediment chemistry on CO_2 and CH_4 production

Production of CO_2 and CH_4 varied between pools and replicates in relationship to different sediment chemical properties (Figure 4.6). Both CO_2 and CH_4 production tended to be higher for sediments with high P content (Table 4.3), suggesting P-limitation as a controlling factor for pool OM decomposition. Humification indices were also negatively correlated to CO_2 production (1420/1090 ratio, ρ = -0.37, P = 0.05; 1630/1090 ratio, ρ = -0.31, P = 0.09; 1720/1090 ratio, ρ = -0.36, P = 0.05) but had no effect on CH_4 (P > 0.1) (Table 4.4). For CH_4, sediment C content (ρ = 0.41, P = 0.02), $\delta^{13}C$ ratio (ρ = -0.34, P = 0.07) and N/P ratio (ρ = - 0.35, P = 0.06) had an influence on production (Table 4.4). Content in Na and K were also negatively correlated to CH_4 but not to CO_2 production (Table 4.4).

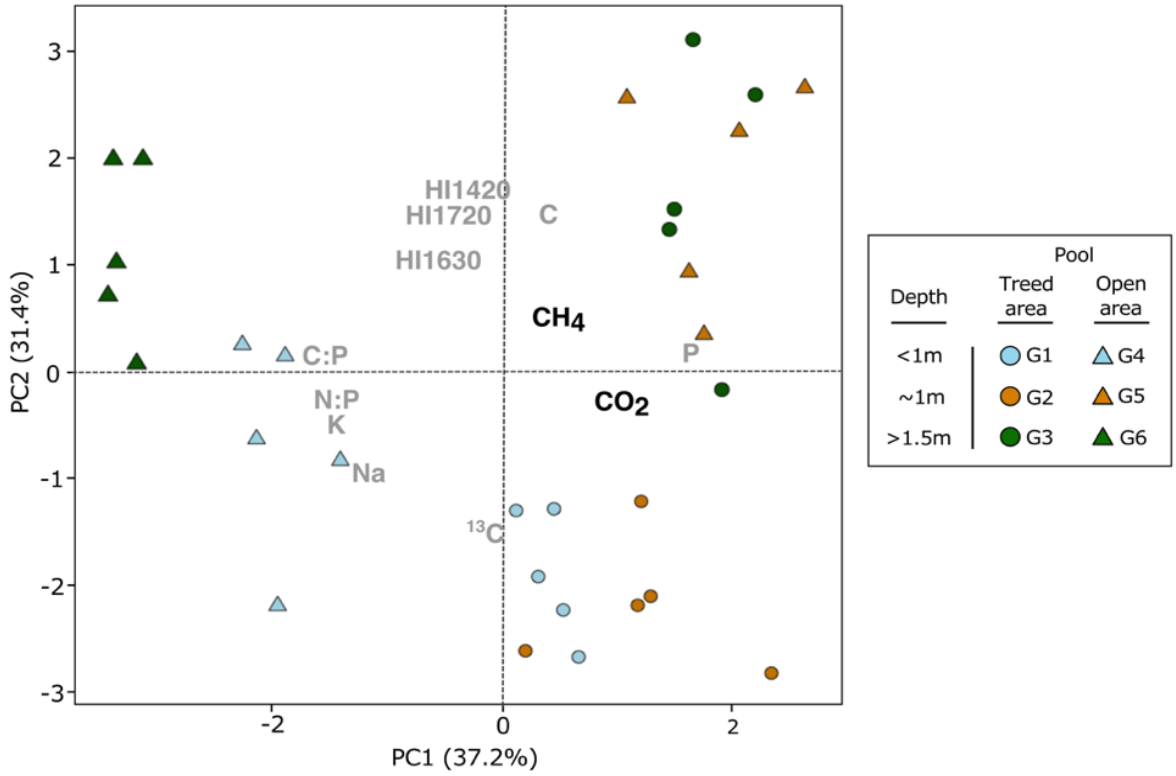

Figure 4.6. Principal component analysis of pool sediment chemistry and carbon dioxide (CO_2) and methane (CH_4) total production after 35 days of incubation. Only chemical variables that were correlated to CO_2 and CH_4 total production were included in the analysis (Table 4.4; P < 0.1).

Table 4.4. Spearman's rank correlation coefficient (ρ) of CO_2 and CH_4 total production and sediment chemical properties. Asterisks show correlations with p-values (P) < 0.05 (**) or < 0.1 (*).

	CO_2 production		CH_4 production	
	ρ	*P*	ρ	*P*
C content	0.01	0.98	** 0.41	0.02
N content	0.13	0.49	-0.11	0.55
P content	* 0.32	0.08	0.27	0.15
C/N ratio	-0.11	0.55	0.13	0.50
N/P ratio	-0.23	0.23	* -0.35	0.06
C/P ratio	*-0.33	0.07	-0.26	0.16
$\delta^{13}C$	-0.05	0.78	* -0.34	0.07
$\delta^{15}N$	-0.27	0.14	0.19	0.30
1420/1090 ratio	** -0.37	0.05	0.24	0.21
1510/1090 ratio	-0.16	0.39	0.14	0.45
1630/1090 ratio	* -0.32	0.09	0.14	0.45
1720/1090 ratio	** -0.36	0.05	0.18	0.33
Ca content	-0.14	0.43	-0.11	0.55
K content	-0.21	0.25	* -0.32	0.08
Mg content	-0.05	0.77	-0.27	0.15
Na content	-0.20	0.28	** -0.49	0.01

4.5.3 Comparing OM decomposition rates from fresh litter and pool sediments

Spatial patterns emerged when comparing fresh OM decomposition rates at the bottom of each pool and CO_2 and CH_4 production from pool sediments (Figure 4.7). For both the shallowest and deepest pools, CO_2 (P = 0.43) and CH_4 (P = 0.35) production were similar but decay k values of *S. capillifolium* and *T. latifolia* were different (P = 0.03). Opposingly, CO_2 (P = 0.01) production was higher in sediments from pools that were ~1m deep than in other pools, but decay k values from fresh litter were not different (P = 0.20). Therefore, there was no relationship between CO_2 and CH_4 production rates from pool sediments and litter decomposition rates.

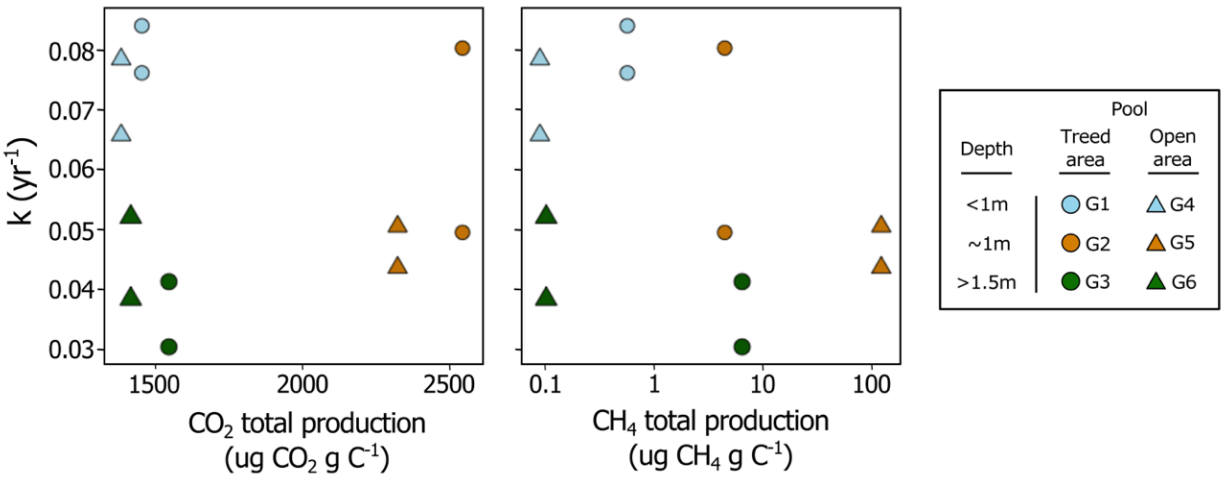

Figure 4.7. Relationship between fresh litter decomposition rates (decay *k* values) at the bottom of each pool and carbon dioxide (CO_2) and methane (CH_4) total production from pool sediments after 35 days of incubation. There are two symbols per pool, one for *Sphagnum capillifolium* and one for *Typha latifolia*.

4.6 Discussion

4.6.1 Decomposability of fresh OM in peatland pools

Studies on peatland pools are currently lacking to fully understand the drivers of the decomposition processes that occur within pools and, more generally, their biogeochemical patterns. This study is a step towards filling this gap in the literature. Our results show variations in decomposition rates of standardized litter among pools, among depths of incubation and also between the litter types, with decomposition rates for *T. latifolia* being much higher than for *S. capillifolium*. Differences in environmental conditions, biological activity and litter quality are major drivers of spatial variability in OM decomposition in terrestrial and aquatic systems (Bradford et al., 2016; Joly et al., 2023). For example, decomposition rates of *Sphagnum* species are normally low compared to that of vascular plants like *T. latifolia* because of their high content in recalcitrant organic compounds (e.g. phenolics) and low nutrient concentrations (Moore & Basiliko, 2006). In our study, the depth at which fresh OM decomposition occurred was the most important driver of spatial variations in decomposition rates. At the surface of the pools, decay *k* values for *S. capillifolium* and *T. latifolia* were higher than at any other depth and, at the bottom, decreased with increasing pool depth. We relate these patterns to within pool variations in dissolved O_2 concentrations, temperature and light intensity that could influence the structure of microbial communities

and the magnitude of decomposition processes. In aquatic ecosystems, litter decomposition rates are indeed positively correlated to O_2 availability and temperature (e.g. Hardwick et al., 2022; Lecerf et al., 2007) and are higher under high light intensity (Kuehn et al., 2014) because of increased microbial activity. At the study site, summer dissolved O_2 concentrations, water temperature and light intensity all decreased with increasing depth from the pool surface (Arsenault et al., 2018).

Dissolved O_2 concentration is a major driver of litter decay in freshwater systems because it constraints decomposition processes (Keiluweit et al. 2016). When O_2 concentrations decrease, other biogeochemical processes intensify (e.g. anaerobic respiration or fermentation) and this results in lower decomposition rates (Hedin et al., 1998). Dissolved O_2 in aquatic systems is positively correlated to litter decomposition rates because the proportion of microorganisms with the ability to decompose litter in microbial communities is higher under high O_2 availability (Liu et al., 2022). This relationship may then explain the decreasing patterns in decay *k* value for both *S. capillifolium* and *T. latifolia* with increasing depth from pool surface (Figure 4.4A), as peatland pool water is depleted in O_2 in depth.

Warmer temperature increases decomposition rates in both aquatic and terrestrial environments (e.g. Kim et al., 2015; Treat et al., 2014). A mesocosm experiment has shown that warmer water temperature accelerated the decomposition of plant material in aquatic systems and increased the activity and diversity of decomposition-related bacteria (Pan et al., 2021). In our study, water temperature at the pool surface was similar in all pools suggesting other environmental drivers were controlling the differences in litter decomposition among pools at this depth. However, during the growing season when most of the biological activity occurs, pool water temperature decreased with increasing depth from the surface (Arsenault et al., 2018), supporting the idea that spatial variations in litter decomposition within pools were partly related to water temperature.

Light has an indirect effect on litter decomposition as it affects microbial biomass and activity (Danger et al., 2013; Halvorson et al., 2019). In aquatic ecosystems, light may trigger the production of degradative enzymes from algae and stimulate litter decomposition (Danger et al., 2013; Francoeur et al., 2006). Higher light intensity at the surface than at depth could then enhance litter decomposition in the upper layer of the water column. Light penetration is however influenced by dissolved and suspended matter (Wetzel, 2001). In our pools, we estimated dissolved matter concentration and composition by measuring water color (A_{254}) and SUVA. Water color was negatively correlated to *T. latifolia* decay *k* values at the surface and to

both litter type in depth, meaning that light attenuation due to dissolved matter may influence litter decomposition rates in peatland pools. However, we did not measure suspended matter in our pools which could possibly have explained differences in litter decay *k* values among pools and areas (Table 4.1).

Decay *k* values for both *S. capillifolium* and *T. latifolia* in the pool sediments were similar to those measured at the bottom of the pools meaning that the environmental conditions 15 cm below the pools were not as suboptimal as we might have expected, even though we measured hypoxia below the water-sediment interface (Arsenault et al., 2018). In peatlands or in aquatic ecosystems, litter decomposition rates are lower in anoxic than in oxic conditions (e.g. Moore et al., 2007; Neckles & Neill, 1994). Liu et al (2022) however found that litter decomposition was still effective in anaerobic conditions because of distinct structures in microorganism communities. It is then possible that similar variations in microbial communities sustained fresh litter decomposition in the anoxic, low temperature and light-free conditions that normally prevail in peatland pool sediments. Another hypothesis explaining this discrepancy could be that litter in contact with the sediments may be more susceptible to colonization by decomposers than in pool water. This is supported by the positive relationship between *T. latifolia* decay *k* values and 1510/1090 and 1630/1090 ratios, which may be related to an increase in microbial proteins (Teickner & Knorr, 2022).

Overall, our results clearly show that changing environmental conditions with depth is a major driver of OM decomposition in peatland pools. Regardless of litter type, we measured the highest rates of decomposition in the warmest and more oxygenated locations of our pools. We have previously demonstrated that peatland pool biogeochemistry responds to changes in water temperature (Arsenault et al., 2023). This study supports these findings and further shows that biogeochemical processes of decomposition in peatland pools may be highly sensitive to changes in environmental conditions.

4.6.2 Decomposability of pool sediments

There were large variations in sediment decomposability under controlled conditions both among pools and between replicates. Production of CH_4 was especially variable, with the sediments of the two shallowest pools (G1 and G4) being overall sinks and the other pools being sources but having highly different production, ranging 0.2 to 123 μg CH_4 g C^{-1} on average after 35 days of incubation (Table 4.3, Figure 4.5). Both CO_2 and CH_4 production were generally higher in the sediments of the ~1 m deep pools than in shallower and deeper pools. Similar to

fresh litter decomposition, there was no difference in gas production among pools from the treed and open areas of the peatland. There were, however, differences in sediment chemistry among areas of the peatland, meaning that the controls OM chemistry and, more broadly, the structure of peatland vegetation exerts on decomposition processes in peatland pools may not be as critical as we might have expected.

The chemistry of peat and aquatic sediment OM is a key control of its degradability, with spatial variations in decomposability emerging in relation to the quality (aromatics vs carbohydrates) and chemical content of organic compounds (Broder et al., 2012; Praetzel et al., 2020). The results of our incubation experiment showed that OM chemistry could only partly explain spatial variations in pool sediment decomposition. For example, OM humification was a driver of production for CO_2, but not for CH_4 (Table 4.4). Similarly, CO_2 and CH_4 production were not related to the same sets of chemical properties (Table 4.4). Hence, while the incubations were conducted under the same conditions and samples were treated in the same way, our results do not point towards a specific control of inherent pool sediment properties of decomposition. The observed variations in CH_4 and CO_2 production from our pool sediments may thus be explained by other factors we did not measure, such as the structure of microbial communities found in the sediments (Oloo et al., 2016), or effect of inherent chemical properties were too small compared to the observed variations in the data.

4.6.3 Influence of OM chemistry on decomposition rates

Both litterbag and incubation experiments indicate controls of OM decomposition in peatland pools that are not only chemical, but also physical and biological. Spatial variations in fresh litter decay and pool sediment decomposition did not follow the same trends, and there was no relationship between both components of the study (Figure 4.7). While we may relate CO_2 and CH_4 production to OM chemistry, fresh litter decomposition in pool water primarily showed patterns of decreasing decay *k* values with increasing depth from the pool surface. This suggests that the chemistry of OM alone could not explain variations in OM decomposition in peatland pools.

Overall, CO_2 and CH_4 production were highest in the ~1 m deep pools (pools G2 and G5; Table 4.3, Figure 4.5A), in which OM chemistry may be ideal to support high rates of decomposition. For example, along with pool G6 which also had high CO_2 and CH_4 productions (Figure 4.5), pools G2 and G5 had the highest sediment P concentration (Table 4.3). Given that P is limiting in peatland pools (Arsenault et al., 2018), higher P concentrations in the substrate

may enhance its decomposition (Moore et al., 2008). The negative correlation between CO_2 production and humification indices (Table 4.4) is also indicative of chemical controls of sediment decomposability, with higher CO_2 production from sediments that contained higher proportion of easily degradable polysaccharides than aromatics (Broder et al., 2012). The relationships of CO_2 production to humification indices confirm the hypothesis of reduced decomposition rates with increasing OM aromaticity (Cocozza et al., 2003). Because we would expect the sediments of shallower pools to be composed of less degraded peat, higher CO_2 production from the ~1 m deep pool and the correlations between CO_2 and humification indices also show that the chemical composition of pool sediments and peat vary spatially but that other mechanisms we did not study are key drivers of OM decomposition in peatland pools. Then, we suggest that pool depth, by influencing the environmental, and possibly biological, conditions in which decomposition occurs, is a more important mechanism controlling decomposition processes in peatland pools than OM chemistry.

4.7 Conclusion

Our study showed that OM decomposition in peatland pools is highly variable and depends primarily on the environmental conditions in which it occurs, with spatial patterns emerging in both fresh litter and pool sediment decomposability as a function of pool depth (Figure 4.7). This means that, regardless of the type of litter that falls at the bottom of the pools, we may expect different decomposition rates in pools of different depths in response to distinct biogeochemical mechanisms and pathways. We have recently shown that peatland pools may act as climate sentinels because they strongly react to small climatic variations (Arsenault et al., 2023). With depth being the main driver of variations in OM decomposition, as it controls dissolved O_2 concentrations, light penetration and water temperature at the pool bottom, it is thus possible that changes in peatland hydrology and expected warmer summer temperature under climate change will modify both the structure and the biogeochemical function of peatland pools. Then, if pool depth was to decrease in drier conditions, or if water temperature was to increase, decomposition at the water-peat interface could rapidly intensify and affect the C balance of peatlands.

Chapitre 5. La géographie et la biogéochimie des mares de tourbières tempérées : patrons et processus à l'interface eau-tourbe

> "It is the business of wetlands scientists to identify and catalogue the ever-shifting ways in which water, land and plants combine." Annie Proulx, 2022.

Les mares de tourbières sont des écosystèmes hétérotrophes, où les taux de respiration surpassent largement les taux de production primaire (Wetzel, 2001), qui se forment à l'intérieur d'écosystèmes autotrophes qui accumulent de grandes quantités de C. Bien qu'elles soient communes dans les tourbières tempérées, les études qui se sont intéressées aux mares sont peu nombreuses. On ignore donc plusieurs pans de leur structure, de leurs fonctions ou simplement de leur distribution et de leurs modes de formation (voir chapitre 1). Les chapitres précédents ont tenté d'élucider certains de ces aspects, en mettant l'accent sur les mécanismes géographiques qui peuvent y contrôler la biogéochimie du C, du N et du P.

5.1 La géographie et la biogéochimie des mares de tourbières tempérées

Les mares de tourbières, en raison de leur géographie particulière, sont des écosystèmes aquatiques peu comparables avec la majorité des autres milieux limnologiques (voir chapitre 2). Leurs patrons biogéochimiques sont dictés par un ensemble de facteurs climatiques et du paysage (voir chapitre 3) et les processus de décomposition de la matière organique, essentiels à la structure et aux fonctions des mares, y sont spatialement hétérogènes (voir chapitre 4).

Le développement des mares tempérées et boréales se fait lentement, sur des échelles allant de la décennie au millénaire (Foster & Fritz, 1987; Koutaniemi, 1999; Seppala & Koutaniemi, 1985). L'étude longitudinale de la biogéochimie des mares de tourbières démontre que les caractéristiques biogéochimiques des mares varient quant à elles à une échelle de temps

beaucoup plus courte que celle qui gouverne leur développement (voir chapitre 3). Ce dynamisme intersaisonnier s'explique entre autres par leurs caractéristiques morphologiques. Bien que les mares de tourbières puissent atteindre plusieurs milliers de mètres carrés en superficie, elles demeurent des plans d'eau de faible profondeur (voir chapitre 2) car leur expansion dans le profil des sols organiques des tourbières est limitée (voir chapitre 1). Le relatif faible volume d'eau qu'elles contiennent en comparaison à d'autres écosystèmes aquatiques pourrait ainsi expliquer leur réponse rapide à des températures et précipitations changeantes, tel qu'observé dans des lacs de petite taille. En effet, les plus petits lacs sont ceux qui émettent la plus grande quantité de C par superficie (Kortelainen et al., 2006) entre autres en raison d'une capacité thermique plus faible (Wetzel, 2001) et d'une plus grande influence relative des apports en C provenant du bassin versant (Jones et al., 2018). Le métabolisme de ces lacs réagit alors plus fortement que d'autres aux variations de température et de précipitation car l'eau et les sédiments s'y réchauffent plus rapidement et parce que les intrants en C, et leur dilution et concentration, dépendent largement des épisodes de précipitations. Les mares de tourbières sont des systèmes où la température de l'eau varie beaucoup au cours d'une saison et où la température à la surface des sédiments est relativement élevée (Arsenault et al., 2018), facilitant probablement les processus de production et de décomposition de la MO. De même, parce qu'elles stockent l'eau en provenance du sol environnant et les éléments dissous qu'elle contient lors des épisodes de pluie ou à la fonte des neiges (Arsenault et al., 2019), des variations à court terme dans le volume de précipitations pourraient influencer leur métabolisme. Cette hypothèse doit par contre être vérifiée, par exemple en effectuant un suivi quotidien des variations hydrologiques et biogéochimiques des mares de tourbières non seulement au cours de la saison de croissance, mais tout au long de l'année.

Les mares de tourbières, en raison de leur volume beaucoup plus petit que celui des lacs, pourraient ainsi réagir plus fortement que ceux-ci à des variations de température et de niveau d'eau. Ces variations influenceraient alors rapidement les processus de production et de décomposition de la MO, d'importation et d'exportation des éléments chimiques, ou simplement la concentration et la dilution de solutés tels que le DOC. Si dans certaines régions du monde les projections climatiques font état d'une hausse des températures mais de régimes de précipitation relativement stables dans les décennies à venir (e.g. est du Canada; Prairie Climate Centre, 2019), d'autres régions où les mares de tourbières sont nombreuses (e.g. Patagonie du sud) subiront à la fois une hausse des températures et une baisse généralisée du nombre de jours de pluie et du volume total de précipitations annuelles (Pessacg et al., 2022).

Le futur de la structure et des fonctions de ces mares est donc incertain. Les mares de tourbières sont des systèmes morphologiquement stables à long terme (voir chapitre 1), mais leur potentiel de réactivité élevé face aux variations climatiques interannuelles (voir chapitre 3) accentue l'incertitude actuelle quant à leurs fonctions biogéochimiques dans le paysage et au devenir de ce rôle, particulièrement dans un contexte de changements climatiques.

La biogéochimie des mares est variable dans le temps et l'espace, et les patrons biogéochimiques locaux, régionaux et continentaux sont dictés par le climat, mais aussi par les conditions physiques du milieu dans lequel elles se développent (géomorphologie et végétation) (voir chapitres 1 et 3). Différentes études ont fait état d'une possible mutation de la structure des communautés végétales qui composent les tourbières sous l'influence des changements climatiques. Par exemple, dans une tourbière ombrotrophe comme celles étudiées dans cette thèse, un climat plus aride pourrait mener à une baisse du niveau de la nappe phréatique et à la transition d'une végétation composée majoritairement de sphaignes et de graminées vers des arbustes d'éricacées (Breeuwer et al., 2009). Sous cette impulsion, une rétroaction positive mènerait à un abaissement permanent du niveau de la nappe phréatique, à une croissance soutenue des plantes vasculaires et à un changement dans les communautés microbiennes du sol (e.g. Bragazza et al., 2013). Ceci réduirait *in fine* la capacité de séquestration du C de ces tourbières (e.g. Larmola et al., 2013) en augmentant les taux de décomposition et réduisant les taux d'accumulation de la MO (Dieleman et al., 2015). Les effets d'un changement dans la composition des communautés végétales des tourbières sur la biogéochimie des mares demeurent par contre méconnus.

Au regard des résultats présentés dans les chapitres précédents, les changements projetés dans la qualité de la litière qui atteint les mares pourraient modifier non seulement la magnitude des processus biogéochimiques de décomposition, en entraînant une transition dans la labilité de la MO (voir chapitre 4), mais aussi bouleverser leurs effets sur les cycles des nutriments dans les mares. En effet, la chimie de la litière varie selon son origine. Par exemple, une litière de graminées est plus riche en nutriments qu'une litière d'éricacées (Kaštovská et al., 2018). Une plus grande abondance d'éricacées dans les tourbières ombrotrophes pourrait alors potentiellement réduire la remise en circulation des nutriments dans les mares de tourbières ombrotrophes, des milieux déjà pauvres en N et P (Arsenault et al., 2018), mais ceci reste à déterminer. En somme, les résultats de cette thèse démontrent que la décomposition de la MO, qui permet en quelque sorte de les définir en tant qu'élément du paysage des tourbières (voir chapitres 1 et 2), et les autres processus biogéochimiques qui mènent aux patrons observés

(voir chapitre 3 et 4) sont entre autres dépendants de la structure des mares, de leur morphologie et de l'origine de la MO qui compose la tourbe et la litière (voir chapitre 4), mais aussi plus largement du climat, tous des paramètres foncièrement géographiques.

5.2 Patrons et processus biogéochimiques à l'interface eau-tourbe

Les émissions de C sont plus élevées dans les lacs de faible volume en raison d'un ratio élevé entre le volume d'eau et la surface couverte par les sédiments (Kelly et al., 2001; Kortelainen et al., 2006). Ceci suggère alors que la majorité des processus biogéochimiques des lacs ont lieu dans les sédiments, particulièrement dans les zones de faible profondeur où la décomposition de la MO est stimulée par la production primaire (Pace & Prairie, 2005). Le même phénomène semble s'appliquer aux mares de tourbières où l'interface eau-tourbe, qui les différencie des autres systèmes aquatiques (voir chapitre 2), contrôle localement leurs patrons et processus biogéochimiques (voir chapitres 3 et 4).

L'interface eau-tourbe qui caractérise le pourtour des mares de tourbières, à la jonction entre un milieu riche (l'eau) et un autre pauvre (la tourbe) en O_2, en fait un point chaud biogéochimique (Krause et al., 2017; McClain et al., 2003). Cette interface entre un milieu oxygéné et un milieu anoxique riche en MO stimule en effet les transformations biogéochimiques en raison du pouvoir oxydatif de l'O_2 lors de la dégradation des molécules organiques (Hedin et al., 1998). Les résultats de l'expérience de décomposition de la MO (voir chapitre 4) supportent cette affirmation et montrent que la dégradation de la litière végétale s'effectue de manière préférentielle dans l'eau des mares plutôt que dans les sols saturés en eau de la tourbière. Bien que les taux de décomposition soient plus élevés à la surface des mares qu'en profondeur, la production primaire qui s'effectue sur les sédiments par les cyanobactéries et autres périphytons (Hamilton et al., 1994) augmente les concentrations en O_2 à l'interface eau-tourbe. Les taux de décomposition de la MO en profondeur plus élevés dans les mares les moins profondes étudiées (voir chapitre 4) démontrent alors que l'interface eau-tourbe des mares de tourbières est le site de plusieurs réactions biogéochimiques dont la magnitude dépend des forts gradients chimiques (e.g. O_2) et physiques (e.g. température et luminosité) qui y stimulent la production primaire et la décomposition.

Les mares les moins profondes sont celles montrant les plus fortes concentrations en DOC, en TN et en CO_2 et CH_4 dissous (voir chapitre 3), proposant ainsi que la majeure partie des réactions biogéochimiques dans ces systèmes s'effectuent à l'interface eau-tourbe. Une

partie du matériel chimique qui est transformé dans les mares provient de la tourbe, via les intrants hydrologiques (Arsenault et al., 2019; Prijac et al., 2022). Une autre partie du matériel traité est produite *in situ*, par la production primaire et la fixation du N atmosphérique par les cyanobactéries et autres microorganismes (Hamilton et al., 1994). Cependant, ces intrants ne seraient pas suffisants pour soutenir la magnitude des processus biogéochimiques qui ont lieu dans les mares de tourbières. En effet, les processus de décomposition y dépassant ceux de production, la MO qui forme les sédiments des mares (composés d'une couche de matériel limnique et de tourbe) offre un substrat supplémentaire pour la décomposition dans les mares. Ce mécanisme explique d'ailleurs leur dynamique morphologique d'expansion spatiale au cours du temps (Foster & Glaser, 1986) et leur bilan C négatif (Pelletier et al., 2014). Ce même mécanisme, plus important dans les mares les moins profondes en raison de conditions environnementales optimales (voir chapitres 1 et 4), pourrait aussi permettre le relargage de nutriments dans les mares. Ceci apporterait alors une explication supplémentaire aux concentrations plus fortes en DOC et TN mesurées dans les mares peu profondes, et consoliderait l'idée de l'importance de l'interface eau-tourbe dans les patrons et processus biogéochimiques des mares de tourbières. Ainsi, si à l'échelle du paysage les mares semblent être des points chauds biogéochimiques dans les tourbières (voir chapitre 1), ce serait plus particulièrement l'interface eau-tourbe qui jouerait ce rôle à l'échelle métrique.

Les concentrations relativement élevées en DOC dans les mares de tourbières sont peu communes dans des systèmes aquatiques oligotrophes comme ceux-ci (voir chapitre 2) et se comparent plutôt à des systèmes mésotrophes, qui sont par définition plus riches en N et P (Wetzel, 2001). En milieu ombrotrophe, la tourbe est pauvre en N et P (Wang et al., 2015), limitant les possibles transferts de ces éléments vers les mares puisque leur recyclage, particulièrement pour le P, s'effectue rapidement à la surface de la tourbière (Wang et al., 2014). L'eau des tourbières est par contre riche en DOC (e.g. Fraser, Roulet & Moore, 2001). Dans les mares, une grande partie du DOC proviendrait du lessivage de la tourbe environnante plutôt qu'à de la production interne (Prijac et al., 2022). Les mares seraient donc des points chauds biogéochimiques à la fois parce que les contraintes à la production et à la décomposition de la MO y seraient moins élevées que dans la tourbe, mais aussi parce que la structure du paysage augmenterait de manière intrinsèque les quantités de substrat disponible à la décomposition.

Les chapitres précédents ont démontré le rôle essentiel que joue l'interface eau-tourbe des mares de tourbières tempérées dans leur biogéochimie. En effet, c'est tout d'abord cette

interface qui permet de différencier les mares et qui en définit la spécificité parmi les écosystèmes aquatiques (chapitre 2). Elle explique d'ailleurs une partie substantielle des patrons biogéochimiques observés dans les mares de différentes régions du monde (chapitre 3) et participe activement à la fois aux processus biogéochimiques de décomposition et à ceux de production primaire (chapitre 1 et 4). Ceci démontre que les mares de tourbière sont des écosystèmes aquatiques remarquables, influencés par une géographie particulière, et dont la structure et les fonctions sont indéniablement uniques.

5.3 Limites de la thèse

Les conclusions issues des travaux présentés dans cette thèse ne peuvent pas être simplement généralisées à l'ensemble des mares de tourbières de la planète. Les patrons biogéochimiques des mares de tourbières et la magnitude des processus sont en effet contrôlés par une multitude de paramètres (voir chapitres 3 et 4). Un hypothétique exercice d'extrapolation des résultats obtenus se heurterait alors à différentes limites d'ordres géographiques et, plus largement, méthodologiques.

On trouve des mares autant en tourbières tropicales (e.g. Dommain et al., 2015) que tempérées (e.g. Glaser & Janssens, 1986) ou en zone de pergélisol (e.g. Laurion et al., 2010), mais les mares étudiées ici provenaient toutes de milieux tempérés ou boréaux exempts de pergélisol. Les modes de formations des mares diffèrent en fonction de leur localisation (voir chapitre 1), ce qui influence aussi leur dynamique morphologique et biogéochimique (voir chapitre 2). Les mares tempérées et boréales se développent lentement, sur des échelles allant de la décennie au millénaire (Foster & Fritz, 1987; Koutaniemi, 1999; Seppala & Koutaniemi, 1985), et leur morphologie évolue sur des échelles temporelles allant du mois (Karofeld & Tõnisson, 2014) jusqu'au siècle (Arlen-Pouliot & Payette, 2015).

Dans les tourbières affectées par le pergélisol, les mares ont présenté une certaine stabilité spatiotemporelle au cours du dernier siècle, signe d'une résilience historique du pergélisol (Gamon et al., 2012). Les plus récents modèles font cependant état d'un actuel et futur développement accéléré de mares de tourbières en réponse aux changements climatiques. En effet, dans plusieurs régions subarctiques, le dégel du pergélisol pourrait s'exprimer par une augmentation dans le nombre et la superficie des mares (Dyke & Sladen, 2022). L'existence de ces écosystèmes pourrait par contre n'être que temporaire puisque les mares pourraient être rapidement drainées (Webb et al., 2022). La morphologie des mares de tourbières à pergélisol est donc aujourd'hui beaucoup plus dynamique que celles étudiées dans cette thèse. Ceci

pourrait possiblement différencier les patrons et la magnitude des processus biogéochimiques des mares entre ces régions. Par exemple, l'expansion du domaine aquatique dans les composantes terrestres des tourbières à pergélisol, entre autres par la formation de mares parfois connectées (Vonk et al., 2015), facilite la décomposition de la MO dissoute et la remise en circulation des nutriments séquestrés (Schuur et al., 2015). Ceci exposerait alors de grandes quantités de C ancien à l'activité microbienne, émettant de fait du C autrement stocké depuis plusieurs millénaires (Gandois et al., 2019). Le dynamisme des processus biogéochimiques de ces mares, en comparaison de celles des tourbières tempérées ou boréales, demeure par contre incertain en raison de conditions climatiques moins optimales et de C potentiellement moins labile (Gandois et al., 2019; Kane et al., 2014). L'application des conclusions des études qui composent cette thèse à des mares des régions froides devrait donc se faire de façon prudente.

En milieu tropical, les mares de tourbières qui se forment à la suite du déracinement d'arbres sont beaucoup plus dynamiques qu'en milieu tempéré ou froid. Ces mares, pouvant atteindre plusieurs mètres de diamètre, apparaissent dès l'arbre tombé et se referment relativement rapidement, par l'accumulation de MO fraîche sur leur fond à raison de 1 m par siècle (Dommain et al., 2015). Leur dynamique biogéochimique est aussi très différente de celle des autres milieux, car les processus de décomposition, qui caractérisent les mares tempérées et boréales, semblent peu importants. En effet, ces mares tropicales s'emplissent à grande vitesse par l'accumulation continue de litière végétale qui ne se décompose que très peu (Dommain et al., 2015). Les mécanismes responsables de ces taux d'accumulation, qui dépassent largement les taux de décomposition, sont actuellement indéfinis mais pourraient être liés à une forte récalcitrance à la décomposition de la MO qui compose les tourbières tropicales même en conditions optimales (Hodgkins et al., 2018). La forte productivité des forêts tropicales assure aussi un apport important et constant en nouvelle MO qui se dépose dans les mares (Hirano et al., 2009). Les conclusions issues des études présentées dans cette thèse peuvent donc difficilement s'appliquer aux mares de tourbières tropicales.

Un autre aspect de la géographie des mares qui pourrait influencer leur biogéochimie et qui n'a pas été considéré dans les chapitres précédents est le possible effet d'un contact entre l'eau des mares et un substrat minéral. Dans les tourbières où l'épaisseur de tourbe est faible, il est possible que les mares atteignent le substrat minéral sur lequel l'écosystème s'est développé (e.g. Quenta et al., 2016). Dans ces cas, les mares pourraient contenir de plus faibles quantités de DOC, de plus grandes quantités de nutriments et seraient plus alcalines que celles observées dans les mares de l'est du Canada, de la Patagonie et du Royaume-Uni (voir chapitre

3), comme le démontre le gradient biogéochimique des plans d'eau thermokarstiques présenté au chapitre 2. D'ailleurs, plusieurs éléments chimiques qui pourraient indiquer une possible influence lithologique sur la biogéochimie du C, du N et du P des mares de tourbières, comme les cations basiques (Whittle & Gallego-Sala, 2016) ou la silice (Reithmaier et al., 2017), n'ont pas été étudiés dans cette thèse. Ces éléments influencent la biogéochimie des tourbières, et possiblement celle des mares, en augmentant respectivement le pH des sols et de l'eau et les taux de décomposition de la MO.

Finalement, plusieurs autres paramètres influençant la biogéochimie des mares de tourbières n'ont pas été étudiés. La relative indépendance des variables climatiques et du paysage dans le contrôle de la biogéochimie des mares (voir chapitre 3) le démontre. La considération d'autres paramètres permettrait possiblement de combler ou d'expliquer cette dichotomie. Par exemple, l'hydrologie des tourbières est liée à la fois au climat, qui contrôle les intrants et extrants en eau des systèmes, et au paysage, qui contrôle la direction et la force de l'écoulement de l'eau. Considérant l'influence relative de l'hydrologie des mares dans leur biogéochimie et son hétérogénéité spatiale (Arsenault et al., 2019; Holden et al., 2018), l'étude de l'hydrologie des différentes tourbières où des mares ont été échantillonnées pourrait pointer vers des mécanismes de contrôle supplémentaires des patrons biogéochimiques des mares, tant à l'échelle locale qu'à l'échelle globale.

Chapitre 6. Conclusion

> « Nous voudrions terminer en insistant sur le caractère hypothétique de notre interprétation paléo-climatique [du développement] des tourbières [à mares] réticulées. Nous avons la certitude de n'être pas suffisamment informé pour avoir vidé la question. Nous espérons que celle-ci restera à l'étude, comme d'ailleurs beaucoup d'autres problèmes de géomorphologie. » Louis-Edmond Hamelin, 1957b.

Les écosystèmes aquatiques sont reconnus pour le rôle prépondérant qu'ils jouent dans les cycles biogéochimiques globaux (e.g. Tranvik et al., 2009). Les chapitres précédents ont démontré que les mares de tourbières tempérées sont des écosystèmes à la structure et aux fonctions particulières, et qui présentent un dynamisme peu commun parmi les milieux lentiques. Globalement, ces chapitres ont permis de remplir les trois objectifs spécifiques de la thèse qui étaient de i) définir la spécificité biogéochimique des mares de tourbières parmi les écosystèmes aquatiques; ii) déterminer les contrôles géographiques des patrons biogéochimiques des mares de tourbières tempérées; et iii) évaluer l'influence de l'interface eau-tourbe dans les processus biogéochimiques à l'œuvre dans les mares de tourbières. Au chapitre 1, nous avons posé les bases de notre argumentaire quant à l'importance de la géographie des mares en explorant les mécanismes structurels qui peuvent influencer leur biogéochimie. Au chapitre 2, nous avons prouvé la spécificité des mares de tourbières parmi les écosystèmes aquatiques et montré qu'elles occupent une position inédite dans les gradients biogéochimiques des milieux lentiques en raison de la structure de la matrice dans laquelle elles se développent. Au chapitre 3, nous avons établi que la réactivité des mares de tourbières varie dans le temps et l'espace en fonction de paramètres géographiques. La relative rapidité avec laquelle elles répondent aux variations environnementales illustre leur potentiel à agir comme sentinelles dans un climat changeant. Au chapitre 4, nous avons étudié des mécanismes environnementaux qui contrôlent la décomposition de la MO dans les mares de tourbières et à l'interface eau-tourbe et conclu que la profondeur des mares est le principal paramètre responsable de cette décomposition. Finalement, au chapitre 5, nous avons conjugué les conclusions des chapitres 1 à 4 pour remplir l'objectif principal de la thèse et démontrer que les

patrons et processus biogéochimiques observés dans les mares de tourbières tempérées sont effectivement dirigés par leur géographie particulière.

Par leur capacité à accumuler les éléments chimiques, les tourbières tendent à ralentir les cycles biogéochimiques locaux et globaux. Les résultats de cette thèse montrent que les mares contrastent avec cette fonction des tourbières et pourraient accélérer ces cycles en raison de leur grand pouvoir de décomposition de la matière organique et de transformation des éléments chimiques. Le poids des mares de tourbières dans les cycles biogéochimiques locaux et globaux pourrait ainsi être disproportionné. Un exercice d'estimation de leur contribution aux cycles biogéochimiques devrait alors être effectué pour réellement cerner leur importance environnementale, un exercice qui pourrait entre autres s'appuyer sur les conclusions de cette thèse. En effet, nous avons démontré que certains paramètres environnementaux influencent grandement la biogéochimie des mares. Par exemple, les variables climatiques, qui sont largement disponibles grâce à des données maillées, peuvent informer sur les patrons biogéochimiques à grande échelle des mares de tourbières. De même, la superficie et, possiblement, la profondeur des mares pourraient être estimées grâce des images satellitaires et des informations géographiques générales (e.g. type de tourbière ou localisation) ce qui permettrait d'évaluer les patrons biogéochimiques des mares de tourbières à une échelle plus fine. Malgré tout, bien que la thèse ait apporté de nouvelles connaissances quant aux mécanismes environnementaux qui dictent la biogéochimie des mares en milieux tempérés, un futur exercice d'extrapolation des résultats est présentement difficile à exécuter car le nombre de mares de tourbières sur la planète, la superficie qu'elles occupent ou simplement leur distribution géographique demeurent toujours inconnus. Il est donc primordial d'adresser cette question pour approfondir nos connaissances quant au fonctionnement de ces systèmes.

Les tourbières sont des écosystèmes relativement stables en raison de leur capacité à s'autoréguler (Morris et al., 2011). En milieu ombrotrophe tempéré, les mares pourraient d'ailleurs favoriser cette stabilité en raison de leur rôle de tampon hydrologique et, possiblement, biogéochimique (Arsenault et al., 2019). Par leur capacité à recevoir, accumuler et redistribuer l'eau et les éléments chimiques, les mares pourraient en effet favoriser le maintien de la structure (e.g. la composition de la végétation) et des fonctions de séquestration de C et d'autres éléments des tourbières malgré les changements d'ordre climatique annoncés. Les résultats présentés dans cette thèse laissent cependant penser que la hausse attendue des températures moyennes annuelles et des températures maximales estivales au cours du prochain siècle pourrait faire contrepoids aux avantages hydrologiques que procurent les mares

en accentuant les taux de décomposition des tourbières à mares et l'émission de C. De même, une hausse des taux d'évapotranspiration sous l'effet d'un climat plus chaud pourrait diminuer la profondeur des mares de tourbières et aussi augmenter les taux de décomposition et l'émission de C. Les recherches portant sur la structure et les fonctions des mares de tourbières étant toujours parcellaires, il demeure toutefois difficile de déterminer le devenir des mares et la résilience des tourbières où on les retrouve face aux changements climatiques. Ce vide devra être comblé dans les prochaines années pour assurer une réelle compréhension des mares de tourbières et de l'influence qu'elles ont ou peuvent avoir dans le paysage.

Comme Louis-Edmond Hamelin, grand géographe québécois, j'ai aussi la certitude de ne pas avoir vidé la question de la géographie et de la biogéochimie des mares de tourbières. À l'image de toutes les études scientifiques, mes travaux se sont appuyés sur d'autres qui m'ont permis d'élaborer ma pensée et sur lesquels j'ai basé mes hypothèses. La roue continuera de tourner et j'espère que les travaux qui composent cette thèse permettront à leur tour d'alimenter la réflexion sur la distribution, la structure et le fonctionnement des mares de tourbières, sur leur rôle dans la circulation biogéochimique locale, et sur leur importance dans les cycles globaux.

Échantillonnage d'une mare de tourbière à Puerto Williams (île de Navarino, Chili). Photo par Julie Talbot, mettant en vedette Panda (à gauche), Sofi (à droite) et moi-même (au centre).

Bibliographie

Abell, J. M., Özkundakci, D., Hamilton, D. P., & Jones, J. R. (2012). Latitudinal variation in nutrient stoichiometry and chlorophyll-nutrient relationships in lakes : A global study. *Fundamental and Applied Limnology*, *181*, 1-14.

Aerts, R. (1997). Climate, leaf litter chemistry and leaf litter decomposition in terrestrial ecosystems : A triangular relationship. *Oikos*, *79*, 439-449.

Arlen-Pouliot, Y., & Payette, S. (2015). The influence of climate on pool inception in boreal fens. *Botany*, *93*, 637-649.

Arsenault, J., Talbot, J., Brown, L. E., Helbig, M., Holden, J., Hoyos-Santillan, J., Jolin, E., Mackenzie, R., Martinez-Cruz, K., Sepulveda-Jauregui, A. & Lapierre, J.-F. (2023). Climate-driven spatial and temporal patterns in peatland pool biogeochemistry. *Global Change Biology, 29*, 4056-4068.

Arsenault, J., Talbot, J., Brown, L., Holden, J., Martinez-Cruz, K., Sepulveda-Jauregui, A., Swindles, G. T., Wauthy, M., & Lapierre, J. F. (2022). Biogeochemical distinctiveness of peatland ponds, thermokarst waterbodies, and lakes. *Geophysical Research Letters*, *49*, e2021GL097492.

Arsenault, J., Talbot, J., & Moore, T. R. (2018). Environmental controls of C, N and P biogeochemistry in peatland pools. *Science of the Total Environment*, *631-632*, 714-722.

Arsenault, J., Talbot, J., Moore, T. R., Beauvais, M.-P., Franssen, J., & Roulet, N. T. (2019). The spatial heterogeneity of vegetation, hydrology and water chemistry in a peatland with open-water pools. *Ecosystems*, *22*, 1352-1367.

Bastviken, D., Tranvik, L. J., Downing, J. A., Crill, P. M., & Enrich-Prast, A. (2011). Freshwater methane emissions offset the continental carbon sink. *Science*, *331*, 50.

Beleites, C., & Sergo, V. (2021). *hyperSpec : A package to handle hyperspectral data sets in R*. https://CRAN.R-project.org/package=hyperSpec

Belyea, L. R. (2007). Climatic and topographic limits to the abundance of bog pools. *Hydrological Processes*, *21*, 675-687.

Belyea, L. R., & Lancaster, J. (2002). Inferring landscape dynamics of bog pools from scaling relationships and spatial patterns. *Journal of Ecology*, *90*, 223-234.

Bernhardt, E. S., Blaszczak, J. R., Ficken, C. D., Fork, M. L., Kaiser, K. E., & Seybold, E. C. (2017). Control points in ecosystems : Moving beyond the hot spot hot moment concept. *Ecosystems*, *20*, 665-682.

Bouchard, F., Fortier, D., Paquette, M., Boucher, V., Pienitz, R., & Laurion, I. (2020). Thermokarst lake development in syngenetic ice-wedge polygon terrain in the Eastern Canadian Arctic (Bylot Island, Nunavut). *The Cryosphere*, *14*, 2607-2627.

Bradford, M. A., Berg, B., Maynard, D. S., Wieder, W. R., & Wood, S. A. (2016). Understanding the dominant controls on litter decomposition. *Journal of Ecology*, *104*, 229-238.

Bragazza, L., Parisod, J., Buttler, A., & Bardgett, R. D. (2013). Biogeochemical plant–soil microbe feedback in response to climate warming in peatlands. *Nature Climate Change*, *3*, 273-277.

Breeuwer, A., Robroek, B. J. M., Limpens, J., Heijmans, M. M. P. D., Schouten, M. G. C., & Berendse, F. (2009). Decreased summer water table depth affects peatland vegetation. *Basic and Applied Ecology*, *10*, 330-339.

Bridgham, S. D., Pastor, J., Dewey, B., Weltzin, J. F., & Updegraff, K. (2008). Rapid carbon response of peatlands to climate change. *Ecology*, *89*, 3041-3048.

Broder, T., Blodau, C., Biester, H., & Knorr, K. H. (2012). Peat decomposition records in three pristine ombrotrophic bogs in southern Patagonia. *Biogeosciences*, *9*, 1479-1491.

Brown, L. E., Ramchunder, S. J., Beadle, J. M., & Holden, J. (2016). Macroinvertebrate community assembly in pools created during peatland restoration. *Science of the Total Environment*, *569-570*, 361-372.

Cael, B. B., Heathcote, A. J., & Seekell, D. A. (2017). The volume and mean depth of Earth's lakes. *Geophysical Research Letters*, *44*, 209-218.

Calmels, F., Allard, M., & Delisle, G. (2008). Development and decay of a lithalsa in Northern Québec : A geomorphological history. *Geomorphology*, *97*, 287-299.

Cao, Q., Liu, Y., Georgescu, M., & Wu, J. (2020). Impacts of landscape changes on local and regional climate : A systematic review. *Landscape Ecology*, *35*, 1269-1290.

Carignan, R., Planas, D., & Vis, C. (2000). Planktonic production and respiration in oligotrophic shield lakes. *Limnology and Oceanography*, *45*, 189-199.

Chapman, P. J., Moody, C. S., Turner, T. E., McKenzie, R., Dinsmore, K. J., Baird, A. J., Billett, M. F., Andersen, R., Leith, F., & Holden, J. (2022). Carbon concentrations in natural and restoration pools in blanket peatlands. *Hydrological Processes*, *36*, 14520.

Cliche Trudeau, N., Garneau, M., & Pelletier, L. (2014). Interannual variability in the CO_2 balance of a boreal patterned fen, James Bay, Canada. *Biogeochemistry*, *118*, 371-387.

Cocozza, C., D'Orazio, V., Miano, T. M., & Shotyk, W. (2003). Characterization of solid and aqueous phases of a peat bog profile using molecular fluorescence spectroscopy, ESR and FT-IR, and comparison with physical properties. *Organic Geochemistry*, *34*, 49-60.

Collins, S. M., Yuan, S., Tan, P. N., Oliver, S. K., Lapierre, J. F., Cheruvelil, K. S., Fergus, C. E., Skaff, N. K., Stachelek, J., Wagner, T., & Soranno, P. A. (2019). Winter precipitation and summer temperature predict lake water quality at macroscales. *Water Resources Research*, *55*, 2708-2721.

Comas, X., Slater, L., & Reeve, A. (2005). Stratigraphic controls on pool formation in a domed bog inferred from ground penetrating radar (GPR). *Journal of Hydrology*, *315*, 40-51.

Conant, R. T., Ryan, M. G., Ågren, G. I., Birge, H. E., Davidson, E. A., Eliasson, P. E., Evans, S. E., Frey, S. D., Giardina, C. P., Hopkins, F. M., Hyvönen, R., Kirschbaum, M. U. F., Lavallee, J. M., Leifeld, J., Parton, W. J., Megan Steinweg, J., Wallenstein, M. D., Martin Wetterstedt, J. Å., & Bradford, M. A. (2011). Temperature and soil organic matter decomposition rates—Synthesis of current knowledge and a way forward. *Global Change Biology*, *17*, 3392-3404.

Cory, R. M., & Kling, G. W. (2018). Interactions between sunlight and microorganisms influence dissolved organic matter degradation along the aquatic continuum. *Limnology and Oceanography Letters*, *3*, 102-116.

Covino, T. (2017). Hydrologic connectivity as a framework for understanding biogeochemical flux through watersheds and along fluvial networks. *Geomorphology*, *277*, 133-144.

Damman, A. W. H. (1986). Hydrology, development, and biogeochemistry of ombrogenous peat bogs with special reference to nutrient relocation in a western Newfoundland bog. *Canadian Journal of Botany*, *64*, 384-394.

Danger, M., Cornut, J., Chauvet, E., Chavez, P., Elger, A., & Lecerf, A. (2013). Benthic algae stimulate leaf litter decomposition in detritus-based headwater streams : A case of aquatic priming effect? *Ecology*, *94*, 1604-1613.

DeGasparro, S. L., Beresford, D. V., Prater, C., & Frost, P. C. (2020). Leaf litter decomposition in boreal lakes : Variable mass loss and nutrient release ratios across a geographic gradient. *Hydrobiologia*, *847*, 819-830.

del Giorgio, P. A., & Peters, R. H. (1994). Patterns in planktonic *P:R* ratios in lakes : Influence of lake trophy and dissolved organic carbon. *Limnology and Oceanography*, *39*, 772-787.

DelSontro, T., Beaulieu, J. J., & Downing, J. A. (2018). Greenhouse gas emissions from lakes and impoundments : Upscaling in the face of global change. *Limnology and Oceanography Letters*, *3*, 64-75.

Dieleman, C. M., Branfireun, B. A., Mclaughlin, J. W., & Lindo, Z. (2015). Climate change drives a shift in peatland ecosystem plant community : Implications for ecosystem function and stability. *Global Change Biology*, *21*, 388-395.

Dieleman, C. M., Lindo, Z., McLaughlin, J. W., Craig, A. E., & Branfireun, B. A. (2016). Climate change effects on peatland decomposition and porewater dissolved organic carbon biogeochemistry. *Biogeochemistry*, *128*, 385-396.

Dodds, W. K., Bruckerhoff, L., Batzer, D., Schechner, A., Pennock, C., Renner, E., Tromboni, F., Bigham, K., & Grieger, S. (2019). The freshwater biome gradient framework : Predicting macroscale properties based on latitude, altitude, and precipitation. *Ecosphere*, *10*, e02786.

Dommain, R., Cobb, A. R., Joosten, H., Glaser, P. H., Chua, A. F. L., Gandois, L., Kai, F. M., Noren, A., Salim, K. A., Su'ut, N. S. H., & Harvey, C. F. (2015). Forest dynamics and tip-up pools

drive pulses of high carbon accumulation rates in a tropical peat dome in Borneo (Southeast Asia). *Journal of Geophysical Research: Biogeosciences*, *120*, 617-640.

Downing, J. A. (2010). Emerging global role of small lakes and ponds : Little things mean a lot. *Limnetica*, *29*, 9-24.

Downing, J. A. (2012). Global abundance and size distribution of streams and rivers. *Inland Waters*, *2*, 229-236.

Dyke, L. D., & Sladen, W. E. (2022). Modelling tundra ponds as initiators of peat plateau thaw, northern Hudson Bay Lowland, Manitoba. *Arctic*, *75*, 364-377.

Elder, C. D., Xu, X., Walker, J., Schnell, J. L., Hinkel, K. M., Townsend-Small, A., Arp, C. D., Pohlman, J. W., Gaglioti, B. V., & Czimczik, C. I. (2018). Greenhouse gas emissions from diverse Arctic Alaskan lakes are dominated by young carbon. *Nature Climate Change*, *8*, 166-171.

Environment Canada. (2022). *Canadian Climate Data—Saint-Michel Station*. https://climate.weather.gc.ca/climate_normals/index_e.html

Evans, C. D., Chapman, P. J., Clark, J. M., Monteith, D. T., & Cresser, M. S. (2006). Alternative explanations for rising dissolved organic carbon export from organic soils. *Global Change Biology*, *12*, 2044-2053.

Farrés, M., Platikanov, S., Tsakovski, S., & Tauler, R. (2015). Comparison of the variable importance in projection (VIP) and of the selectivity ratio (SR) methods for variable selection and interpretation. *Journal of Chemometrics*, *29*, 528-536.

Fontaine, N., Poulin, M., & Rochefort, L. (2007). Plant diversity associated with pools in natural and restored peatlands. *Mires and Peat*, *2*, 1-17.

Foster, D. R., & Fritz, S. C. (1987). Mire development, pool formation and landscape processes on patterned fens in Dalarna, Central Sweden. *Journal of Ecology*, *75*, 409-437.

Foster, D. R., & Glaser, P. H. (1986). The raised bogs of South-Eastern Labrador, Canada : Classification, distribution, vegetation and recent dynamics. *Journal of Ecology*, *74*, 47-71.

Foster, D. R., King, G. A., Glaser, P. H., & Wright Jr, H. E. (1983). Origin of string patterns in boreal peatlands. *Nature*, *306*, 256-258.

Foster, D. R., King, G. A., & Santelmann, M. V. (1988). Patterned fens of western Labrador and adjacent Quebec : Phytosociology, water chemistry, landform features, and dynamics of surface patterns. *Canadian Journal of Botany*, *66*, 2402-2418.

Foster, D. R., & Wright Jr, H. E. (1990). Role of ecosystem development and climate change in bog formation in Central Sweden. *Ecology*, *71*, 450-463.

Foster, D. R., Wright Jr, H. E., Thelaus, M., & King, G. A. (1988). Bog development and landform dynamics in Central Sweden and South-Eastern Labrador, Canada. *Journal of Ecology*, *76*, 1164-1185.

Francoeur, S. N., Schaecher, M., Neely, R. K., & Kuehn, K. A. (2006). Periphytic photosynthetic stimulation of extracellular enzyme activity in aquatic microbial communities associated with decaying *Typha* litter. *Microbial Ecology*, *52*, 662-669.

Fraser, C. J. D., Roulet, N. T., & Lafleur, M. (2001). Groundwater flow patterns in a large peatland. *Journal of Hydrology*, *246*, 142-154.

Fraser, C. J. D., Roulet, N. T., & Moore, T. R. (2001). Hydrology and dissolved organic carbon biogeochemistry in an ombrotrophic bog. *Hydrological Processes*, *15*, 3151-3166.

Freeman, C., Evans, C. D., Monteith, D. T., Reynolds, B., & Fenner, N. (2001). Export of organic carbon from peat soils. *Nature*, *412*, 785.

Gamon, J. A., Kershaw, G. P., Williamson, S., & Hik, D. S. (2012). Microtopographic patterns in an arctic baydjarakh field : Do fine-grain patterns enforce landscape stability? *Environmental Research Letters*, *7*, 015502.

Gandois, L., Hoyt, A. M., Hatté, C., Jeanneau, L., Teisserenc, R., Liotaud, M., & Tananaev, N. (2019). Contribution of peatland permafrost to dissolved organic matter along a thaw gradient in north Siberia. *Environmental Science and Technology*, *53*, 14165-14174.

Glaser, P. H., & Janssens, J. A. (1986). Raised bogs in eastern North America : Transitions in landforms and gross stratigraphy. *Canadian Journal of Botany*, *64*, 395-415.

Halvorson, H. M., Barry, J. R., Lodato, M. B., Findlay, R. H., Francoeur, S. N., & Kuehn, K. A. (2019). Periphytic algae decouple fungal activity from leaf litter decomposition via negative priming. *Functional Ecology*, *33*, 188-201.

Hamelin, L.-E. (1957a). Les tourbières réticulées du Québec-Labrador subarctique. *Bulletin de l'Association de géographes français*, *34*, 47-48.

Hamelin, L.-E. (1957b). Les tourbières réticulées du Québec-Labrador subarctique : Interprétation morphoclimatique. *Cahiers de géographie du Québec*, *2*, 87-106.

Hamilton, J. D., Kelly, C. A., Rudd, J. W. M., Hesslein, H., & Roulet, N. T. (1994). Flux to the atmosphere of CH_4 and CO_2 from wetland ponds on the Hudson Bay lowlands (HBLs). *Journal of Geophysical Research: Atmospheres*, *99*, 1495-1510.

Hardwick, L. J., Fryirs, K. A., & Hose, G. C. (2022). Spatial and temporal variation in macrophyte litter decomposition in a rare chain-of-ponds, an intermittent stream and wetland system. *Wetlands*, *42*, 33.

Harris, I., Osborn, T. J., Jones, P., & Lister, D. (2020). Version 4 of the CRU TS monthly high-resolution gridded multivariate climate dataset. *Scientific Data*, *7*, 109.

Hassan, M., Talbot, J., Arsenault, J., Martinez-Cruz, K., Sepulveda-Jauregui, A., Hoyos-Santillan, J., & Lapierre, J.-F. (2023). Linking dissolved organic matter to CO_2 and CH_4 concentrations in canadian and chilean peatlandpools. *Global Biogeochemical Cycles*, *37*, e2023GB007715.

Hedin, L. O., von Fischer, J. C., Ostrom, N. E., Kennedy, B. P., Brown, M. G., & Robertson, G. P. (1998). Thermodynamic constraints on nitrogen transformations and other biogeochemical processes at soil-stream interfaces. *Ecology*, *79*, 684-703.

Heslop, J. K., Walter Anthony, K. M., Sepulveda-Jauregui, A., Martinez-Cruz, K., Bondurant, A., Grosse, G., & Jones, M. C. (2015). Thermokarst lake methanogenesis along a complete talik profile. *Biogeosciences*, *12*, 4317-4331.

Hirano, T., Jauhiainen, J., Inoue, T., & Takahashi, H. (2009). Controls on the carbon balance of tropical peatlands. *Ecosystems*, *12*, 873-887.

Hodgkins, S. B., Richardson, C. J., Dommain, R., Wang, H., Glaser, P. H., Verbeke, B., Winkler, B. R., Cobb, A. R., Rich, V. I., Missilmani, M., Flanagan, N., Ho, M., Hoyt, A. M., Harvey, C. F., Vining, S. R., Hough, M. A., Moore, T. R., Richard, P. J. H., De La Cruz, F. B., … Chanton, J. P. (2018). Tropical peatland carbon storage linked to global latitudinal trends in peat recalcitrance. *Nature Communications*, *9*, 3640.

Holden, J., & Burt, T. P. (2003). Runoff production in blanket peat covered catchments. *Water Resources Research*, *39*, 1191.

Holden, J., Moody, C. S., Edward Turner, T., McKenzie, R., Baird, A. J., Billett, M. F., Chapman, P. J., Dinsmore, K. J., Grayson, R. P., Andersen, R., Gee, C., & Dooling, G. (2018). Water-level dynamics in natural and artificial pools in blanket peatlands. *Hydrological Processes*, *32*, 550-561.

Holgerson, M. A., & Raymond, P. A. (2016). Large contribution to inland water CO2 and CH4 emissions from very small ponds. *Nature Geoscience*, *9*, 222-226.

Huang, Y., Ciais, P., Luo, Y., Zhu, D., Wang, Y., Qiu, C., Goll, D. S., Guenet, B., Makowski, D., De Graaf, I., Leifeld, J., Kwon, M. J., Hu, J., & Qu, L. (2021). Tradeoff of CO_2 and CH_4 emissions from global peatlands under water-table drawdown. *Nature Climate Change*, *11*, 618-622.

Humboldt's legacy. (2019). *Nature Ecology & Evolution*, *3*, 1265-1266.

IPCC. (2022). *Climate Change 2022 : Impacts, Adaptation and Vulnerability* (Contribution of Working Group II to the IPCC Sixth Assessment Report).

Joly, F.-X., Scherer-Lorenzen, M., & Hättenschwiler, S. (2023). Resolving the intricate role of climate in litter decomposition. *Nature Ecology & Evolution*, *7*, 214-223.

Jones, S. E., Zwart, J. A., Kelly, P. T., & Solomon, C. T. (2018). Hydrologic setting constrains lake heterotrophy and terrestrial carbon fate. *Limnology And Oceanography Letters*, *3*, 256-264.

Juutinen, S., Moore, T. R., Bubier, J. L., Arnkil, S., Humphreys, E., Marincak, B., Roy, C., & Larmola, T. (2018). Long-term nutrient addition increased CH_4 emission from a bog through direct and indirect effects. *Scientific Reports*, *8*, 3838.

Kane, E. S., Mazzoleni, L. R., Kratz, C. J., Hribljan, J. A., Johnson, C. P., Pypker, T. G., & Chimner, R. (2014). Peat porewater dissolved organic carbon concentration and lability increase with warming : A field temperature manipulation experiment in a poor-fen. *Biogeochemistry*, *119*, 161-178.

Karberg, N. J., Scott, N. A., & Giardina, C. P. (2008). Methods for estimating litter decomposition. Dans C. M. Hoover (Éd.), *Field Measurements for Forest Carbon Monitoring* (p. 103-111). Springer.

Karofeld, E., & Tõnisson, H. (2014). Spatio-temporal changes in bog pool bottom topography—Temperature effect and its influence on pool development : An example from a raised bog in Estonia. *Hydrological Processes*, *28*, 958-968.

Kaštovská, E., Straková, P., Edwards, K., Urbanová, Z., Bárta, J., Mastný, J., Šantrůčková, H., & Picek, T. (2018). Cotton-grass and blueberry have opposite effect on peat characteristics and nutrient transformation in peatland. *Ecosystems*, *21*, 443-458.

Keiluweit, M., Nico, P. S., Kleber, M., & Fendorf, S. (2016). Are oxygen limitations under recognized regulators of organic carbon turnover in upland soils?. *Biogeochemistry*, *127*, 157-171.

Kelly, C. A., Fee, E., Ramlal, P. S., Rudd, J. W. M., Hesslein, R. H., Anema, C., & Schindler, E. U. (2001). Natural variability of carbon dioxide and net epilimnetic production in the surface waters of boreal lakes of different sizes. *Limnology and Oceanography*, *46*, 1054-1064.

Kim, J., Rochefort, L., Hogue-Hugron, S., Alqulaiti, Z., Dunn, C., Pouliot, R., Jones, T. G., Freeman, C., & Kang, H. (2021). Water table fluctuation in peatlands facilitates fungal proliferation, impedes *Sphagnum* growth and accelerates decomposition. *Frontiers in Earth Science*, *8*, 579329.

Kim, Y., Ullah, S., Roulet, N. T., & Moore, T. R. (2015). Effect of inundation, oxygen and temperature on carbon mineralization in boreal ecosystems. *Science of the Total Environment*, *511*, 381-392.

Kleinebecker, T., Hölzel, N., & Vogel, A. (2008). South Patagonian ombrotrophic bog vegetation reflects biogeochemical gradients at the landscape level. *Journal of Vegetation Science*, *19*, 151-160.

Kokelj, S. V., & Jorgenson, M. T. (2013). Advances in thermokarst research. *Permafrost and Periglacial Processes*, *24*, 108-119.

Kortelainen, P., Rantakari, M., Huttunen, J. T., Mattsson, T., Alm, J., Juutinen, S., Larmola, T., Silvola, J., & Martikainen, P. J. (2006). Sediment respiration and lake trophic state are important predictors of large CO_2 evasion from small boreal lakes. *Global Change Biology*, *12*, 1554-1567.

Koutaniemi, L. (1999). Twenty-one years of string movements on the Liippasuo aapa mire, Finland. *Boreas*, *28*, 521-530.

Krause, S., Lewandowski, J., Grimm, N. B., Hannah, D. M., Pinay, G., McDonald, K., Martí, E., Argerich, A., Pfister, L., Klaus, J., Battin, T., Larned, S. T., Schelker, J., Fleckenstein, J., Schmidt, C., Rivett, M. O., Watts, G., Sabater, F., Sorolla, A., & Turk, V. (2017). Ecohydrological interfaces as hot spots of ecosystem processes. *Water Resources Research*, *53*, 6359-6376.

Kuehn, K. A., Francoeur, S. N., Findlay, R. H., & Neely, R. K. (2014). Priming in the microbial landscape : Periphytic algal stimulation of litter-associated microbial decomposers. *Ecology*, *95*, 749-762.

Kuhn, M. A., Thompson, L. M., Winder, J. C., Braga, L. P. P., Tanentzap, A. J., Bastviken, D., & Olefeldt, D. (2021). Opposing effects of climate and permafrost thaw on CH_4 and CO_2 emissions from northern lakes. *AGU Advances*, *2*, 1-16.

Kuhn, M. A., Varner, R. K., Bastviken, D., Crill, P., Macintyre, S., Turetsky, M., Walter Anthony, K., McGuire, A. D., & Olefeldt, D. (2021). BAWLD-CH4 : A comprehensive dataset of methane fluxes from boreal and arctic ecosystems. *Earth System Science Data*, *13*, 5151-5189.

Lapierre, J. F., Seekell, D. A., & del Giorgio, P. A. (2015). Climate and landscape influence on indicators of lake carbon cycling through spatial patterns in dissolved organic carbon. *Global Change Biology*, *21*, 4425-4435.

Larmola, T., Bubier, J. L., Kobyljanec, C., Basiliko, N., Juutinen, S., Humphreys, E., Preston, M., & Moore, T. R. (2013). Vegetation feedbacks of nutrient addition lead to a weaker carbon sink in an ombrotrophic bog. *Global Change Biology*, *19*, 3729-3739.

Laurion, I., Vincent, W. F., MacIntyre, S., Retamal, L., Dupont, C., Francus, P., & Pienitz, R. (2010). Variability in greenhouse gas emissions from permafrost thaw ponds. *Limnology and Oceanography*, *55*, 115-133.

Lavoie, M., Colpron-Tremblay, J., & Robert, É. C. (2012). Développement d'une vaste tourbière ombrotrophe non perturbée en contexte périurbain au Québec méridional. *Ecoscience*, *19*, 285-297.

Lecerf, A., Risnoveanu, G., Popescu, C., Gessner, M. O., & Chauvet, E. (2007). Decomposition of diverse litter mixtures in streams. *Ecology*, *88*, 219-227.

Legendre, P., & Legendre, L. (2012). *Numerical Ecology* (3rd éd.). Elsevier.

Lindgren, F., Geladi, P., & Wold, S. (1993). The kernel algorithm for PLS. *Journal of Chemometrics*, *7*, 45-59.

Liu, S., He, G., Fang, H., Xu, S., & Bai, S. (2022). Effects of dissolved oxygen on the decomposers and decomposition of plant litter in lake ecosystem. *Journal of Cleaner Production*, *372*, 133837.

Loisel, J., Gallego-Sala, A. V., Amesbury, M. J., Magnan, G., Anshari, G., Beilman, D. W., Benavides, J. C., Blewett, J., Camill, P., Charman, D. J., Chawchai, S., Hedgpeth, A., Kleinen, T., Korhola, A., Large, D., Mansilla, C. A., Müller, J., van Bellen, S., West, J. B., … Wu, J. (2021). Expert assessment of future vulnerability of the global peatland carbon sink. *Nature Climate Change*, *11*, 70-77.

Loisel, J., van Bellen, S., Pelletier, L., Talbot, J., Hugelius, G., Karran, D., Yu, Z., Nichols, J., & Holmquist, J. (2017). Insights and issues with estimating northern peatland carbon stocks and fluxes since the Last Glacial Maximum. *Earth-Science Reviews*, *165*, 59-80.

Maranger, R., Jones, S. E., & Cotner, J. B. (2018). Stoichiometry of carbon, nitrogen, and phosphorus through the freshwater pipe. *Limnology and Oceanography Letters*, *3*, 89-101.

Mataloni, G., González Garraza, G., & Vinocur, A. (2015). Landscape-driven environmental variability largely determines abiotic characteristics and phytoplankton patterns in peat bog pools (Tierra del Fuego, Argentina). *Hydrobiologia*, *751*, 105-125.

Mathijssen, P. J. H., Galka, M., Borken, W., & Knorr, K. H. (2019). Plant communities control long term carbon accumulation and biogeochemical gradients in a Patagonian bog. *Science of the Total Environment*, *684*, 670-681.

Matthews, E., Johnson, M. S., Genovese, V., Du, J., & Bastviken, D. (2020). Methane emission from high latitude lakes : Methane-centric lake classification and satellite-driven annual cycle of emissions. *Scientific Reports*, *10*, 12465.

McClain, M. E., Boyer, E. W., Dent, C. L., Gergel, S. E., Grimm, N. B., Groffman, P. M., Hart, S. C., Harvey, J. W., Johnston, C. A., Mayorga, E., McDowell, W. H., & Pinay, G. (2003). Biogeochemical hot spots and hot moments at the interface of terrestrial and aquatic ecosystems. *Ecosystems*, *6*, 301-312.

McEnroe, N. A., Roulet, N. T., Moore, T. R., & Garneau, M. (2009). Do pool surface area and depth control CO_2 and CH_4 fluxes from an ombrotrophic raised bog, James Bay, Canada? *Journal of Geophysical Research: Biogeosciences*, *114*, G01001.

Modenutti, B. E., Balseiro, E. G., Elser, J. J., Navarro, M. B., Cuassolo, F., Laspoumaderes, C., & Souza, M. S. (2013). Effect of volcanic eruption on nutrients, light, and phytoplankton in oligotrophic lakes. *Limnology and Oceanography*, *58*, 1165-1175.

Monteith, D. T., Stoddard, J. L., Evans, C. D., de Wit, H. A., Forsius, M., Høga, T., Kopacek, J., & Vesely, J. (2007). Dissolved organic carbon trends resulting from changes in atmospheric deposition chemistry. *Nature*, *450*, 537-540.

Moore, T. R., & Basiliko, N. (2006). Decomposition in boreal peatlands. Dans R. K. Wieder & D. H. Vitt (Éds.), *Boreal Peatland Ecosystems* (p. 125-143). Springer.

Moore, T. R., Bubier, J. L., & Bledzki, L. (2007). Litter decomposition in temperate peatland ecosystems : The effect of substrate and site. *Ecosystems*, *10*, 949-963.

Moore, T. R., Trofymow, J. A., Siltanen, M., & Kozak, L. M. (2008). Litter decomposition and nitrogen and phosphorus dynamics in peatlands and uplands over 12 years in central Canada. *Oecologia*, *157*, 317-325.

Morris, P. J., Baird, A. J., Young, D. M., & Swindles, G. T. (2015). Untangling climate signals from autogenic changes in long-term peatland development. *Geophysical Research Letters*, *42*, 10788-10797.

Morris, P. J., Belyea, L. R., & Baird, A. J. (2011). Ecohydrological feedbacks in peatland development : A theoretical modelling study. *Journal of Ecology*, *99*, 1190-1201.

Neckles, H. A., & Neill, C. (1994). Hydrologic control of litter decomposition in seasonally flooded prairie marshes. *Hydrobiologia*, *286*, 155-165.

Olefeldt, D., Goswami, S., Grosse, G., Hayes, D., Hugelius, G., Kuhry, P., Mcguire, A. D., Romanovsky, V. E., Sannel, A. B. K., Schuur, E. A. G., & Turetsky, M. R. (2016). Circumpolar distribution and carbon storage of thermokarst landscapes. *Nature Communications*, *7*, 13043.

Oleksy, I. A., Jones, S. E., & Solomon, C. T. (2022). Hydrologic setting dictates the sensitivity of ecosystem metabolism to climate variability in lakes. *Ecosystems*, *25*, 1328-1345.

Oloo, F., Valverde, A., Quiroga, M. V., Vikram, S., Cowan, D., & Mataloni, G. (2016). Habitat heterogeneity and connectivity shape microbial communities in South American peatlands. *Scientific Reports*, *6*, 25712.

Pace, M. L., & Prairie, Y. T. (2005). Respiration in lakes. Dans P. A. Del Giorgio & P. Williams (Éds.), *Respiration in Aquatic Ecosystems* (p. 103-121). Oxford University Press.

Pan, M., Wang, T., Hu, B., Shi, P., Xu, J., & Zhang, M. (2021). Mesocosm experiments reveal global warming accelerates macrophytes litter decomposition and alters decomposition-related bacteria community structure. *Water*, *13*, 1940.

Pan, Y., Birdsey, R. A., Fang, J., Houghton, R., Kauppi, P. E., Kurz, W. A., Phillips, O. L., Shvidenko, A., Lewis, S. L., Canadell, J. G., Ciais, P., Jackson, R. B., Pacala, S. W., McGuire, A. D., Piao, S., Rautiainen, A., Sitch, S., & Hayes, D. (2011). A large and persistent carbon sink in the world's forests. *Science*, *333*, 988-993.

Parikh, S., Goyne, K. W., Margenot, A. J., Mukome, F. N. D., & Calderon, F. J. (2014). Soil chemical insights provided through vibrational spectroscopy. Dans D. L. Sparks (Éd.), *Advances in Agronomy, volume 126* (p. 1-64). Academic Press.

Payette, S., Delwaide, A., Caccianiga, M., & Beauchemin, M. (2004). Accelerated thawing of subarctic peatland permafrost over the last 50 years. *Geophysical Research Letters*, *31*, L18208.

Péaud, L. (2018). Épistémologie(s) de la géographie. Dans A. Ciattoni & Y. Veyret (Éds.), *Les fondamentaux de la géographie* (p. 16-42). Armand Colin.

Pelletier, L., Strachan, I. B., Garneau, M., & Roulet, N. T. (2014). Carbon release from boreal peatland open water pools : Implication for the contemporary C exchange. *Journal of Geophysical Research: Biogeosciences*, *119*, 207-222.

Pelletier, L., Strachan, I. B., Roulet, N. T., & Garneau, M. (2015). Can boreal peatlands with pools be net sinks for CO_2? *Environmental Research Letters*, *10*, 035002.

Pessacg, N., Blázquez, J., Lancelotti, J., & Solman, S. (2022). Climate changes in coastal areas of Patagonia : Observed trends and future projections. Dans E. W. Helbling, M. A. Narvarte, R. A. González, & V. E. Villafañe (Éds.), *Global Change in Atlantic Coastal Patagonian Ecosystems* (p. 13-42). Springer.

Peura, S., Wauthy, M., Simone, D., Eiler, A., Einarsdóttir, K., Rautio, M., & Bertilsson, S. (2020). Ontogenic succession of thermokarst thaw ponds is linked to dissolved organic matter quality and microbial degradation potential. *Limnology and Oceanography*, *65*, S248-S263.

Pilla, R. M., Griffiths, N. A., Gu, L., Kao, S., McManamay, R., Ricciuto, D. M., & Shi, X. (2022). Anthropogenically driven climate and landscape change effects on inland water carbon dynamics : What have we learned and where are we going? *Global Change Biology*, *28*, 5601-5629.

Pokrovsky, O. S., Shirokova, L. S., Kirpotin, S. N., Kulizhsky, S. P., & Vorobiev, S. N. (2013). Impact of western Siberia heat wave 2012 on greenhouse gases and trace metal concentration in thaw lakes of discontinuous permafrost zone. *Biogeosciences*, *10*, 5349-5365.

Pokrovsky, O. S., Shirokova, L. S., Manasypov, R. M., Kirpotin, S. N., Kulizhsky, S. P., Kolesnichenko, L. G., Loiko, S. V., & Vorobyev, S. N. (2014). Thermokarst lakes of Western Siberia : A complex biogeochemical multidisciplinary approach. *International Journal of Environmental Studies*, *71*, 733-748.

Polishchuk, Y. M., Bogdanov, A. N., Muratov, I. N., Polishchuk, V. Y., Lim, A., Manasypov, R. M., Shirokova, L. S., & Pokrovsky, O. S. (2018). Minor contribution of small thaw ponds to the pools of carbon and methane in the inland waters of the permafrost-affected part of the Western Siberian Lowland. *Environmental Research Letters*, *13*, 045002.

Praetzel, L. S. E., Plenter, N., Schilling, S., Schmiedeskamp, M., Broll, G., & Knorr, K. H. (2020). Organic matter and sediment properties determine in-lake variability of sediment CO_2 and CH_4 production and emissions of a small and shallow lake. *Biogeosciences*, *17*, 5057-5078.

Prairie Climate Centre. (2019). *Climate Atlas of Canada*. https://climateatlas.ca/

Prairie, Y. T., Bird, D. F., & Cole, J. J. (2002). The summer metabolic balance in the epilimnion of southeastern Quebec lakes. *Limnology and Oceanography*, *47*, 316-321.

Prijac, A., Gandois, L., Jeanneau, L., Taillardat, P., & Garneau, M. (2022). Discontinuity of the concentration and composition of dissolved organic matter at the peat-pool interface in a boreal peatland. *Biogeosciences*, *19*, 4571-4588.

Proulx, A. (2022). *Fen, bog and swamp : A short history of peatland destruction and Its role in the climate crisis*. Scribner.

Quenta, E., Molina-Rodriguez, J., Gonzales, K., Rebaudo, F., Casas, J., Jacobsen, D., & Dangles, O. (2016). Direct and indirect effects of glaciers on aquatic biodiversity in high Andean peatlands. *Global Change Biology*, *22*, 3196-3205.

Quiroga, M. V., Unrein, F., González Garraza, G., Küppers, G., Lombardo, R., Marinone, M. C., Menu Marque, S., Vinocur, A., & Mataloni, G. (2013). The plankton communities from peat bog pools : Structure, temporal variation and environmental factors. *Journal of Plankton Research*, *35*, 1234-1253.

R Core Team. (2022). *R: A language and environment for statistical computing*. R Foundation for Statistical Computing. https://www.r-project.org/

Rautio, M., Dufresne, F., Laurion, I., Bonilla, S., Vincent, W. F., & Christoffersen, K. S. (2011). Shallow freshwater ecosystems of the circumpolar Arctic. *Écoscience*, *18*, 204-222.

Raymond, P. A., Hartmann, J., Lauerwald, R., Sobek, S., McDonald, C., Hoover, M., Butman, D., Striegl, R., Mayorga, E., Humborg, C., Kortelainen, P., Dürr, H., Meybeck, M., Ciais, P., & Guth, P. (2013). Global carbon dioxide emissions from inland waters. *Nature*, *503*, 355-359.

Reithmaier, G.-M. S., Knorr, K.-H., Arnhold, S., Planer-Friedrich, B., & Schaller, J. (2017). Enhanced silicon availability leads to increased methane production, nutrient and toxicant mobility in peatlands. *Scientific Reports*, *7*, 8728.

Rietkerk, M., Dekker, S. C., Wassen, M. J., Verkroost, A. W. M., & Bierkens, M. F. P. (2004). A putative mechanism for bog patterning. *The American Naturalist*, *163*, 699-708.

Riordan, B., Verbyla, D., & McGuire, A. D. (2006). Shrinking ponds in subarctic Alaska based on 1950-2002 remotely sensed images. *Journal of Geophysical Research: Biogeosciences*, *111*, G04002.

Rosentreter, J. A., Borges, A. V., Deemer, B. R., Holgerson, M. A., Liu, S., Song, C., Melack, J., Raymond, P. A., Duarte, C. M., Allen, G. H., Olefeldt, D., Poulter, B., Battin, T. I., & Eyre, B. D. (2021). Half of global methane emissions come from highly variable aquatic ecosystem sources. *Nature Geoscience*, *14*, 225-230.

Rosset, T., Binet, S., Rigal, F., & Gandois, L. (2022). Peatland dissolved organic carbon export to surface waters : Global significance and effects of anthropogenic disturbance. *Geophysical Research Letters*, *49*, e2021GL096616.

Rydin, H., & Jeglum, J. K. (2013). *The Biology of Peatlands* (2nd éd.). Oxford University Press.

Schädel, C., Beem-Miller, J., Aziz Rad, M., E. Crow, S., E. Hicks Pries, C., Ernakovich, J., M. Hoyt, A., Plante, A., Stoner, S., C. Treat, C., & A. Sierra, C. (2020). Decomposability of soil organic matter over time : The Soil Incubation Database (SIDb, version 1.0) and guidance for incubation procedures. *Earth System Science Data*, *12*, 1511-1524.

Schmidt, M. W. I., Torn, M. S., Abiven, S., Dittmar, T., Guggenberger, G., Janssens, I. A., Kleber, M., Kögel-Knabner, I., Lehmann, J., Manning, D. A. C., Nannipieri, P., Rasse, D. P., Weiner, S.,

& Trumbore, S. E. (2011). Persistence of soil organic matter as an ecosystem property. *Nature*, *478*, 49-56.

Schuur, E. A. G., McGuire, A. D., Schädel, C., Grosse, G., Harden, J. W., Hayes, D. J., Hugelius, G., Koven, C. D., Kuhry, P., Lawrence, D. M., Natali, S. M., Olefeldt, D., Romanovsky, V. E., Schaefer, K., Turetsky, M. R., Treat, C. C., & Vonk, J. E. (2015). Climate change and the permafrost carbon feedback. *Nature*, *520*, 171-179.

Seekell, D. A., Lapierre, J.-F., & Cheruvelil, K. S. (2018). A geography of lake carbon cycling. *Limnology and Oceanography Letters*, *3*, 49-56.

Seppala, M., & Koutaniemi, L. (1985). Formation of a string and pool topography as expressed by morphology, stratigraphy and current processes on a mire in Kuusamo, Finland. *Boreas*, *14*, 287-309.

Sepulveda-Jauregui, A., Walter Anthony, K. M., Martinez-Cruz, K., Greene, S., & Thalasso, F. (2015). Methane and carbon dioxide emissions from 40 lakes along a north-south latitudinal transect in Alaska. *Biogeosciences*, *12*, 3197-3223.

Serikova, S., Pokrovsky, O. S., Laudon, H., Krickov, I. V., Lim, A. G., Manasypov, R. M., & Karlsson, J. (2019). High carbon emissions from thermokarst lakes of Western Siberia. *Nature Communications*, *10*, 1552.

Sjörs, H. (1961). Surface patterns in boreal peatlands. *Endeavour*, *20*, 217-224.

Sobek, S., Tranvik, L. J., Prairie, Y. T., Kortelainen, P., & Cole, J. J. (2010). Patterns and regulation of dissolved organic carbon : An analysis of 7,500 widely distributed lakes. *Limnology and Oceanography*, *52*, 1208-1219.

Soranno, P. A., Wagner, T., Collins, S. M., Lapierre, J., Lottig, N. R., & Oliver, S. K. (2019). Spatial and temporal variation of ecosystem properties at macroscales. *Ecology Letters*, *22*, 1587-1598.

Soranno, P. A., Webster, K. E., Cheruvelil, K. S., & Bremigan, M. T. (2009). The lake landscape-context framework : Linking aquatic connections, terrestrial features and human effects at multiple spatial scales. *Verhan International Verein Limnology*, *30*, 695-700.

Stanley, E. H., Collins, S. M., Lottig, N. R., Oliver, S. K., Webster, K. E., Cheruvelil, K. S., & Soranno, P. A. (2019). Biases in lake water quality sampling and implications for macroscale research. *Limnology and Oceanography*, *64*, 1572-1585.

Stolpmann, L., Coch, C., Morgenstern, A., Boike, J., Fritz, M., Herzschuh, U., Stoof-Leichsenring, K., Dvornikov, Y., Heim, B., Lenz, J., Larsen, A., Walter Anthony, K., Jones, B., Frey, K., & Grosse, G. (2021). First pan-Arctic assessment of dissolved organic carbon in lakes of the permafrost region. *Biogeosciences*, *18*, 3917-3936.

Strack, M., Kellner, E., & Waddington, J. M. (2005). Dynamics of biogenic gas bubbles in peat and their effects on peatland biogeochemistry. *Global Biogeochemical Cycles*, *19*, GB1003.

Strack, M., Waddington, J. M., Bourbonniere, R. A., Buckton, E. L., Shaw, K., Whittington, P., & Price, J. S. (2008). Effect of water table drawdown on peatland dissolved organic carbon export and dynamics. *Hydrological Processes*, *22*, 3373-3385.

Stuart, B. H. (2004). *Infrared Spectroscopy : Fundamentals and Applications* (1re éd.). Wiley.

Swanson, D. K., & Grigal, D. F. (1988). A simulation model of mire patterning. *Oikos*, *53*, 309-314.

Tallis, J. H. (1994). Pool-and-hummock patterning in a southern Pennine blanket mire II. The formation and erosion of the pool system. *The Journal of Ecology*, *82*, 789.

Teickner, H. (2023). *ir : Functions to handle and preprocess infrared spectra*. https://doi.org/10.5281/ZENODO.6644806

Teickner, H., & Hodgkins, S. B. (2022). *irpeat 0.2.0 : Functions to analyze mid-infrared spectra of peat samples*. https://doi.org/10.5281/ZENODO.7262744

Teickner, H., & Knorr, K.-H. (2022). Improving models to predict holocellulose and Klason lignin contents for peat soil organic matter with mid-infrared spectra. *SOIL*, *8*, 699-715.

Tonin, A. M., Ubiratan Hepp, L., & Gonçalves, J. F. (2018). Spatial variability of plant litter decomposition in stream networks : From litter bags to watersheds. *Ecosystems*, *21*, 567-581.

Tranvik, L. J., Downing, J. A., Cotner, J. B., Loiselle, S. A., Striegl, R. G., Ballatore, T. J., Dillon, P., Finlay, K., Fortino, K., Knoll, L. B., Kortelainen, P. L., Kutser, T., Larsen, S., Laurion, I., Leech, D. M., Leigh McCallister, S., McKnight, D. M., Melack, J. M., Overholt, E., … Weyhenmeyer, G. A. (2009). Lakes and reservoirs as regulators of carbon cycling and climate. *Limnology and Oceanography*, *54*, 2298-2314.

Treat, C. C., Wollheim, W. M., Varner, R. K., Grandy, A. S., Talbot, J., & Frolking, S. (2014). Temperature and peat type control CO_2 and CH_4 production in Alaskan permafrost peats. *Global Change Biology*, *20*, 2674-2686.

Trofymow, J. A., Moore, T. R., Titus, B., Prescott, C., Morrison, I., Siltanen, M., Smith, S., Fyles, J., Wein, R., Camiré, C., Duschene, L., Kozak, L., Kranabetter, M., & Visser, S. (2002). Rates of litter decomposition over 6 years in Canadian forests : Influence of litter quality and climate. *Canadian Journal of Forest Research*, *32*, 789-804.

Turner, T. E., Billett, M. F., Baird, A. J., Chapman, P. J., Dinsmore, K. J., & Holden, J. (2016). Regional variation in the biogeochemical and physical characteristics of natural peatland pools. *Science of the Total Environment*, *545-546*, 84-94.

UNEP. (2022). *Global Peatlands Assessment—The State of the World's Peatlands : Evidence for action toward the conservation, restoration, and sustainable management of peatlands*. Global Peatland Initiative, United Nation Environment Programme.

Verpoorter, C., Kutser, T., Seekell, D. A., & Tranvik, L. J. (2014). A global inventory of lakes based on high-resolution satellite imagery. *Geophysical Research Letters*, *41*, 6396-6402.

Vidal de la Blache, P. (1913). Des caractères distinctifs de la géographie. *Annales de Géographie*, *22*, 289-299.

Vincent, W. F. (2014). *François-Alphonse Forel (1841-1912)*. https://limnology.org/notable-limnologists/f-a_forel/

Vizza, C., Zwart, J. A., Jones, S. E., Tiegs, S. D., & Lamberti, G. A. (2017). Landscape patterns shape wetland pond ecosystem function from glacial headwaters to ocean. *Limnology and Oceanography*, *62*, S207-S221.

von Humboldt, A. (1849). *Views of Nature*. University of Chicago Press.

Vonk, J. E., Tank, S. E., Bowden, W. B., Laurion, I., Vincent, W. F., Alekseychik, P., Amyot, M., Billet, M. F., Canário, J., Cory, R. M., Deshpande, B. N., Helbig, M., Jammet, M., Karlsson, J., Larouche, J., Macmillan, G., Rautio, M., Walter Anthony, K. M., & Wickland, K. P. (2015). Reviews and syntheses : Effects of permafrost thaw on Arctic aquatic ecosystems. *Biogeosciences*, *12*, 7129-7167.

Vonk, J. E., Tank, S. E., & Walvoord, M. A. (2019). Integrating hydrology and biogeochemistry across frozen landscapes. *Nature Communications*, *10*, 3-6.

Walter Anthony, K., Schneider von Deimling, T., Nitze, I., Frolking, S., Emond, A., Daanen, R., Anthony, P., Lindgren, P., Jones, B., & Grosse, G. (2018). 21st-century modeled permafrost carbon emissions accelerated by abrupt thaw beneath lakes. *Nature Communications*, *9*, 3262.

Walter, J. A., Fleck, R., Pace, M. L., & Wilkinson, G. M. (2020). Scaling relationships between lake surface area and catchment area. *Aquatic Sciences*, *82*, 47.

Wang, M., Moore, T. R., Talbot, J., & Richard, P. J. H. (2014). The cascade of C:N:P stoichiometry in an ombrotrophic peatland : From plants to peat. *Environmental Research Letters*, *9*, 024003.

Wang, M., Moore, T. R., Talbot, J., & Riley, J. L. (2015). The stoichiometry of carbon and nutrients in peat formation. *Global Biogeochemical Cycles*, *29*, 113-121.

Wauthy, M., Rautio, M., Christoffersen, K. S., Forsström, L., Laurion, I., Mariash, H. L., Peura, S., & Vincent, W. F. (2018). Increasing dominance of terrigenous organic matter in circumpolar freshwaters due to permafrost thaw. *Limnology and Oceanography Letters*, *3*, 186-198.

Webb, E. E., Liljedahl, A. K., Cordeiro, J. A., Loranty, M. M., Witharana, C., & Lichstein, J. W. (2022). Permafrost thaw drives surface water decline across lake-rich regions of the Arctic. *Nature Climate Change*, *12*, 841-846.

Weedon, J. T., A. Kowalchuk, G., Aerts, R., van Hal, J., van Logtestijn, R., Taş, N., F. M. Röling, W., & M. van Bodegom, P. (2012). Summer warming accelerates sub-arctic peatland nitrogen cycling without changing enzyme pools or microbial community structure. *Global Change Biology*, *18*, 138-150.

Weishaar, J. L., Aiken, G., Bergamaschi, B., Fram, M., Fujii, R., & Mopper, K. (2003). Evaluation of specific ultra-violet absorbance as an indicator of the chemical content of dissolved organic carbon. *Environmental Science and Technology*, *37*, 4702-4708.

Wetzel, R. G. (2001). *Limnology : Lake and river ecosystems* (3rd éd.). Academic Press.

Whittle, A., & Gallego-Sala, A. V. (2016). Vulnerability of the peatland carbon sink to sea-level rise. *Scientific Reports*, *6*, 28758.

Wik, M., Varner, R. K., Anthony, K. W., MacIntyre, S., & Bastviken, D. (2016). Climate-sensitive northern lakes and ponds are critical components of methane release. *Nature Geoscience*, *9*, 99-105.

Williamson, C. E., Saros, J. E., & Schindler, D. W. (2009). Sentinels of change. *Science*, *323*, 887-888.

Wulf, A. (2016). *The Invention of Nature : Alexander von Humboldt's New World*. Vintage Books.

Xu, J., Morris, P. J., Liu, J., & Holden, J. (2018). PEATMAP: Refining estimates of global peatland distribution based on a meta-analysis. *Catena*, *160*, 134-140.

Yin, T., Feng, M., Qiu, C., & Peng, S. (2022). Biological nitrogen fixation and nitrogen accumulation in peatlands. *Frontiers in Earth Science*, *10*, 1-13.

Yu, Z., Loisel, J., Brosseau, D. P., Beilman, D. W., & Hunt, S. J. (2010). Global peatland dynamics since the Last Glacial Maximum. *Geophysical Research Letters*, *37*, L13402.

Yvon-Durocher, G., Allen, A. P., Bastviken, D., Conrad, R., Gudasz, C., St-Pierre, A., Thanh-Duc, N., & del Giorgio, P. A. (2014). Methane fluxes show consistent temperature dependence across microbial to ecosystem scales. *Nature*, *507*, 488-491.

Živković, T., Helbig, M., & Moore, T. R. (2022). Seasonal and spatial variability of biological N_2 fixation in a cool temperate bog. *Journal of Geophysical Research: Biogeosciences*, *127*(2).

Zwart, J. A., Hanson, Z. J., Vanderwall, J., Bolster, D., Hamlet, A., & Jones, S. E. (2018). Spatially explicit, regional-scale simulation of lake carbon fluxes. *Global Biogeochemical Cycles*, *32*, 1276-1293.

Annexe I. Matériel supplémentaire au chapitre 2

Text S2.1. Supplementary methodology

Data gathering

Ecosystems in our datasets include lakes, thermokarst waterbodies and peatland ponds. The goal of our study being to distinguish these three types of ecosystems, all freshwater ecosystems that were clearly identified as another type of ecosystem (e.g. reservoir, retention basin, vernal ponds) were excluded.

The articles from which published data were taken were found with the search engine 'Web of Science' using broad keywords: 'lake biogeochemistry database', 'waterbody database', 'lake biogeochemistry', 'peatland pond biogeochemistry', 'peatland open-water pool biogeochemistry', 'thermokarst biogeochemistry', 'thermokarst lake biogeochemistry', 'permafrost lake waterbodies', 'lake nutrient biogeochemistry', 'thermokarst lake nutrient biogeochemistry', 'peatland waterbody'. Articles were retrieved between April and July 2019, and new data were added in February 2022.

The data used in this study and the list of articles from which we built the dataset are available online at http:// www.doi.org/10.5281/zenodo.5619484.

Statistical analyses

General linear models (GLMs) were used to test if and how individual variables (area, depth, pH, and DOC, TN and TP concentrations) differed among freshwater systems, as classified according to the source material. GLMs allow the comparison of data that are not normally distributed by letting the modeler determine the family of the data distribution (Dunn & Smyth, 2018). Here, we used *gamma* (for depth, and DOC, TN and TP concentrations) and *Gaussian* (for pH and area, the latter having primarily been $\log_{10}$-transformed to account for the very large range of data) distribution families. For each variable, we ran the model twice, once with lakes as the reference system and a second time with peatland ponds as the reference to determine how the other systems compared to the reference. We also used GLMs to investigate the interaction of the system type and their morphometry (area or depth) on pH and DOC concentrations as they were the most widely available measurements.

We conducted unsupervised k-means clustering analyses followed by principal component analyses (PCA) on two subsets of data to 1) provide a data-driven classification of all ecosystems included in our analyses and 2) compare these results with the a priori classification provided by the authors of previous studies. The k-means analysis allows partitioning of freshwater ecosystems in groups of similar biogeochemical characteristics and to isolate the factor primarily driving the difference to the other groups without any prior assumption of similarity among the observations, while the ordination of the k-means clustering in a reduced space (PCA) highlights general gradients between the observations and categories that can then be interpreted (Legendre & Legendre, 2012). A first subset was composed of only the waterbodies for which DOC, TN, TP and pH data were available to illustrate differences in water chemistry between ecosystem types. Following the elbow method to determine the optimal number of clusters, freshwater ecosystems were split into five clusters. The second subset was composed of freshwater ecosystems of <0.1 km^2 for which data for morphometric properties and DOC and pH were available to determine the effect of size on biogeochemistry. The optimal number of clusters for this analysis was three. Data, with the exception of pH, were log_{10}-transformed before the analyses.

To further segregate lakes, peatland ponds and thermokarst waterbodies and distinguish the systems from one another, we performed a discriminant analysis based on the same subset of waterbodies used for the first k-means/PCA (n = 837) and for which we had DOC, TN, TP and pH data. The discriminant analysis allows the prediction of the type of a given freshwater using its biogeochemical characteristics. Given the large dataset and because of the uneven number of freshwater ecosystems among the three groups, we used a quadratic model (Wahl & Kronmal, 1977). We performed the discriminant analysis twice, first using a model based on a random sample of 80% of the 837 waterbodies and second on a random sample of 30% of the data. The two models showed only a 1.4% difference in predictions accuracy (r^2 = 0.881 vs 0.867) and we retained the second model. Then, to determine the variables driving the system distinctiveness we also created a classification tree (n = 1690, including 1347 lakes, 166 peatland ponds and 177 thermokarst waterbodies) based on the morphometric and DOC and pH data for freshwaters of all sizes. All analyses were undertaken using R, version 4.0.3 (R Core Team, 2020).

References

Dunn, P. K., & Smyth, G. K. (2018). *Generalized Linear Models with Examples in R* (3rd ed.). Springer

Legendre, P. & Legendre, L. (2012). *Numerical Ecology* (3rd ed.). Elsevier

R Core Team. (2020). R: A language and environment for statistical computing. Vienna, Austria: R Foundation for Statistical Computing. Retrieved from https://www.r-project.org/

Wahl, P. & Kronmal, R. A. (1977). Discriminant functions when covariances are unequal and sample sizes are moderate. *Biometrics, 33*, 479-484.

Table S2.1. Results of the generalized linear models (GLMs) performed to compared peatland ponds, thermokarst waterbodies and lakes morphometric and chemical data. *Gamma* (for depth, and DOC, TN and TP concentrations) and *Gaussian* (for area, after log-transformation, and pH) distribution families were used. Reference system for each model is in parentheses. Systems with different level letters are statistically different at a significance level of 5% ($P < 0.05$).

Response	n	System	t	*P*	System	t	*P*	Level
Area (log)	7 015	(Lakes)	-69.55	-	Lakes	46.43	<0.001	A
	211	Peatland ponds	-46.43	<0.001	(Peatland ponds)	-59.18	-	B
	452	Thermokarst waterbodies	-43.49	<0.001	Thermokarst waterbodies	13.65	<0.001	C
Depth	2 029	(Lakes)	24.86	-	Lakes	-8.90	<0.001	A
	286	Peatland ponds	8.90	<0.001	(Peatland ponds)	9.34	-	B
	248	Thermokarst waterbodies	8.08	<0.001	Thermokarst waterbodies	-2.57	0.010	B
DOC	8 286	(Lakes)	83.82	-	Lakes	22.48	<0.001	A
	278	Peatland ponds	-22.48	<0.001	(Peatland ponds)	15.35	-	B
	656	Thermokarst waterbodies	-34.21	<0.001	Thermokarst waterbodies	-1.10	0.273	B
pH	9 576	(Lakes)	594.82	-	Lakes	34.63	<0.001	A
	233	Peatland ponds	-34.63	<0.001	(Peatland ponds)	57.75	-	B
	600	Thermokarst waterbodies	-26.14	<0.001	Thermokarst waterbodies	15.63	<0.001	C
TN	2 185	(Lakes)	23.32	-	Lakes	-0.88	0.381	A
	237	Peatland ponds	0.88	0.381	(Peatland ponds)	7.71	-	A
	163	Thermokarst waterbodies	-1.26	0.206	Thermokarst waterbodies	-1.57	0.118	A
TP	3 022	(Lakes)	5.49	-	Lakes	-1.49	0.135	A
	237	Peatland ponds	1.49	0.135	(Peatland ponds)	1.54	-	A
	243	Thermokarst waterbodies	1.46	0.145	Thermokarst waterbodies	-0.81	0.418	A

Table S2.2. Composition of the 5 k-means clusters based on the analysis of the pH and the dissolved organic carbon (DOC), total nitrogen (TN) and total phosphorus (TP) concentrations for 837 freshwater ecosystems.

	Peatland ponds	Thermokarst waterbodies	Lakes
K1 (n = 234)	82.0 % (n = 192)	1.3 % (n = 3)	16.7 % (n = 39)
K2 (n = 50)	34.0 % (n = 17)	60.0 % (n = 30)	6.0 % (n = 3)
K3 (n = 85)	0.0 % (n = 0)	1.2 % (n = 1)	98.8 % (n = 84)
K4 (n = 236)	0.9 % (n = 2)	22.0 % (n = 52)	77.1 % (n = 182)
K5 (n = 232)	0.9 % (n = 2)	9.5 % (n =22)	89.6 % (n = 208)

Table S2.3. Composition of the 3 k-means clusters based on the analysis of the area, depth, dissolved organic carbon (DOC) concentrations and pH for 1235 freshwater ecosystems < 0.1 km².

	Peatland ponds	Thermokarst waterbodies	Lakes
K1 (n = 290)	56.5 % (n = 164)	41.4 % (n = 120)	2.1 % (n = 6)
K2 (n = 654)	0.0 % (n = 0)	0.5 % (n = 3)	99.5 % (n = 651)
K3 (n = 291)	2.4 % (n = 7)	21.6 % (n = 63)	76.0 % (n = 221)

Table S2.4. Absolute number of predicted systems and proportion of rightfully predicted systems as determined by the discriminant analysis of 837 freshwater ecosystems based on pH and dissolved organic carbon (DOC), total nitrogen (TN) and total phosphorus (TP) concentrations. The model is based on a random subsample of 30% of the initial sample.

		Predicted system		
		Peatland ponds	Thermokarst waterbodies	Lakes
A priori classification	Peatland ponds (n = 149)	**142 (95.3%)**	3	4
	Thermokarst waterbodies (n = 75)	1	**25 (33.3%)**	49
	Lakes (n = 361)	12	9	**340 (94.2%)**

Table S2.5. Results of the generalized linear models (GLMs) of interacting effects of freshwater system type and their morphometry (area and depth) on DOC concentrations and pH. Reference systems in the models are peatland ponds (in parentheses).

Response	Interaction	t	*P*
DOC vs Area	(Peatland ponds)	12.57	<0.001
	Area	1.47	0.141
	Thermokarst waterbodies	-1.70	0.090
	Lakes	18.03	<0.001
	Area:Thermokarst waterbodies	-1.47	0.141
	Area:Lakes	-1.47	0.141
DOC vs Depth	(Peatland ponds)	4.93	<0.001
	Depth	0.45	0.655
	Thermokarst waterbodies	-2.87	0.004
	Lakes	5.12	<0.001
	Depth: Thermokarst waterbodies	1.59	0.111
	Depth:Lakes	0.17	0.868
pH vs Area	(Peatland ponds)	55.82	<0.001
	Area	2.18	0.029
	Thermokarst waterbodies	8.99	<0.001
	Lakes	34.10	<0.001
	Area: Thermokarst waterbodies	-2.18	0.029
	Area:Lakes	-2.18	0.029
pH vs Depth	(Peatland ponds)	44.35	<0.001
	Area	-0.52	0.602
	Thermokarst waterbodies	5.84	<0.001
	Lakes	30.21	<0.001
	Depth: Thermokarst waterbodies	3.44	<0.001
	Depth:Lakes	0.51	0.609

Annexe II. Matériel supplémentaire au chapitre 3

Table S3.1. Coefficients of variation (%) of each constituent for each site.

Site	pH	DOC	TN	TP	A_{254}	SUVA	CH_4	CO_2
Grande plée Bleue	3.4	21.7	19.8	80.6	36.2	20.5	100.0	53.6
Riviere-au-Tonnerre	4.9	32.9	38.9	61.9	38.2	12.5	57.0	38.9
Kegaska	2.8	25.6	20.2	28.1	24.5	3.9	24.6	37.8
Havre-Saint-Pierre	4.3	47.6	73.3	84.7	45.8	19.9	148.2	83.7
La Romaine	2.7	46.6	50.0	16.2	28.7	42.6	83.1	37.9
Saint-Alexandre-de-Kamouraska	1.2	10.1	8.6	20.7	12.3	3.5	20.5	18.1
Miscou	3.5	44.9	27.1	15.5	59.3	21.6	63.7	31.3
Cross Lochs	0.7	29.0	21.8	16.2		18.8	97.0	28.9
Loch Lier	2.3	30.6	10.4	47.2		14.2	72.9	28.0
Munsary	2.4	9.9	18.9	15.6		7.1	63.7	29.3
Silver Flowe	4.0	30.0	54.8	57.7		50.2	115.4	71.8
Slieveanorra	2.7	17.9	23.7	27.6		21.4	44.8	53.5
Garron Plateau	3.4	23.5	22.7	34.1		37.8	83.4	55.2
Upper Midhope	1.7	20.2						
Moor House	2.2	3.5						
Cold Fell	2.6	8.9						
Navarino	5.1	44.4	66.2	161.5	51.4	13.7	111.1	61.3
Punta Arenas	8.2	48.5	50.9	138.3	50.4	11.2	166.6	126.3
Karukinka	5.9	24.9	44.7	65.7	30.8	10.1	60.9	52.2
Cape Horn	9.6	32.9	41.8	55.3	33.4	7.5		

Table S3.2. Coefficients of the partial least square regressions performed on biogeochemical, climate and terrain data from 150 pools of eastern Canada, southern Patagonia and the United Kingdom.

	pH	**DOC**	**TN**	**TP**	**SUVA**	**CH_4**	**CO_2**
Area	0.24	-0.38	-0.14	-0.08	-0.02	-0.54	-0.71
Depth	0.14	-0.08	-0.16	-0.04	-0.26	0.12	0.19
Elevation	0.19	-0.08	0.43	0.71	-0.20	-0.33	-0.19
MAAT	0.19	-0.15	-0.06	-0.12	0.03	-0.22	-0.04
MAP	-0.26	-0.14	0.04	0.09	0.13	-0.09	0.07
PET	-0.09	0.13	0.23	0.20	0.21	-0.16	0.10
P:PET	-0.10	-0.21	0.04	0.16	-0.02	-0.17	-0.11
Frost days	-0.27	0.16	0.11	0.14	0.08	0.16	0.06
Wet days	0.04	-0.14	-0.31	-0.45	0.02	0.08	0.08

Table S3.3. Summary of generalized linear mixed effects models of DOC and TN variations, using gamma distribution families. In both models, regions and peatland types were used as random effects. Asterisks (*) indicate relationships with p-values < 0.05.

Linear mixed models	Response variable	Explanatory variable	Estimate	Std error	n	t-value	p-value
Model 1	**DOC**	(intercept)	21.669	11.307	150	1.916	0.055
		MAAT	10.711	2.392	150	4.477	< 0.001*
		MAP	-2.801	0.521	150	-5.380	< 0.001*
		PET	-2.028	1.671	150	-1.214	0.225
		Elevation	2.088	0.819	150	2.550	0.011*
		Area	-1.230	0.359	150	-3.428	< 0.001*
		Depth	-3.213	0.659	150	-4.873	< 0.001*
			Variance of random effects				
		Region	54.055				
		Peatland type	1.844				
		Residuals	0.129				
Model 2	**TN**	(intercept)	0.863	0.350	150	2.463	0.014*
		MAAT	0.265	0.112	150	2.366	0.018*
		MAP	0.035	0.035	150	0.993	0.321
		PET	-0.081	0.073	150	-1.091	0.275
		Elevation	0.174	0.033	150	5.251	< 0.001*
		Area	-0.028	0.013	150	-2.241	0.025*
		Depth	-0.077	0.022	150	-3.445	< 0.001*
			Variance of random effects				
		Region	0.069				
		Peatland type	0.003				
		Residuals	0.175				

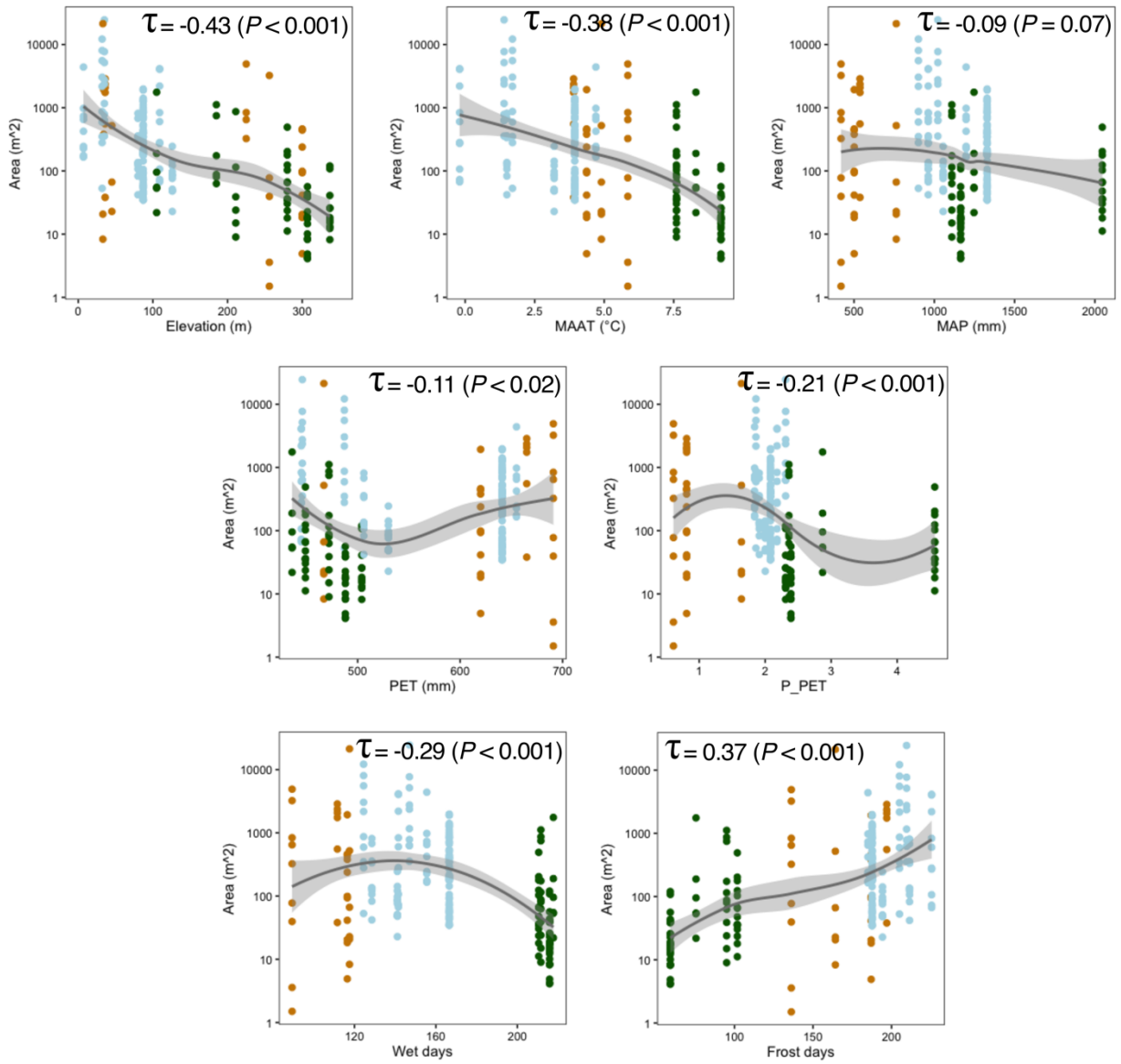

Figure S3.1. Peatland pool area patterns across different geographic settings. Panels show locally-weighted scatterplot smoothing (LOWESS) with 95% confidence interval, and Kendall rank correlations' tau (τ) and p-value.

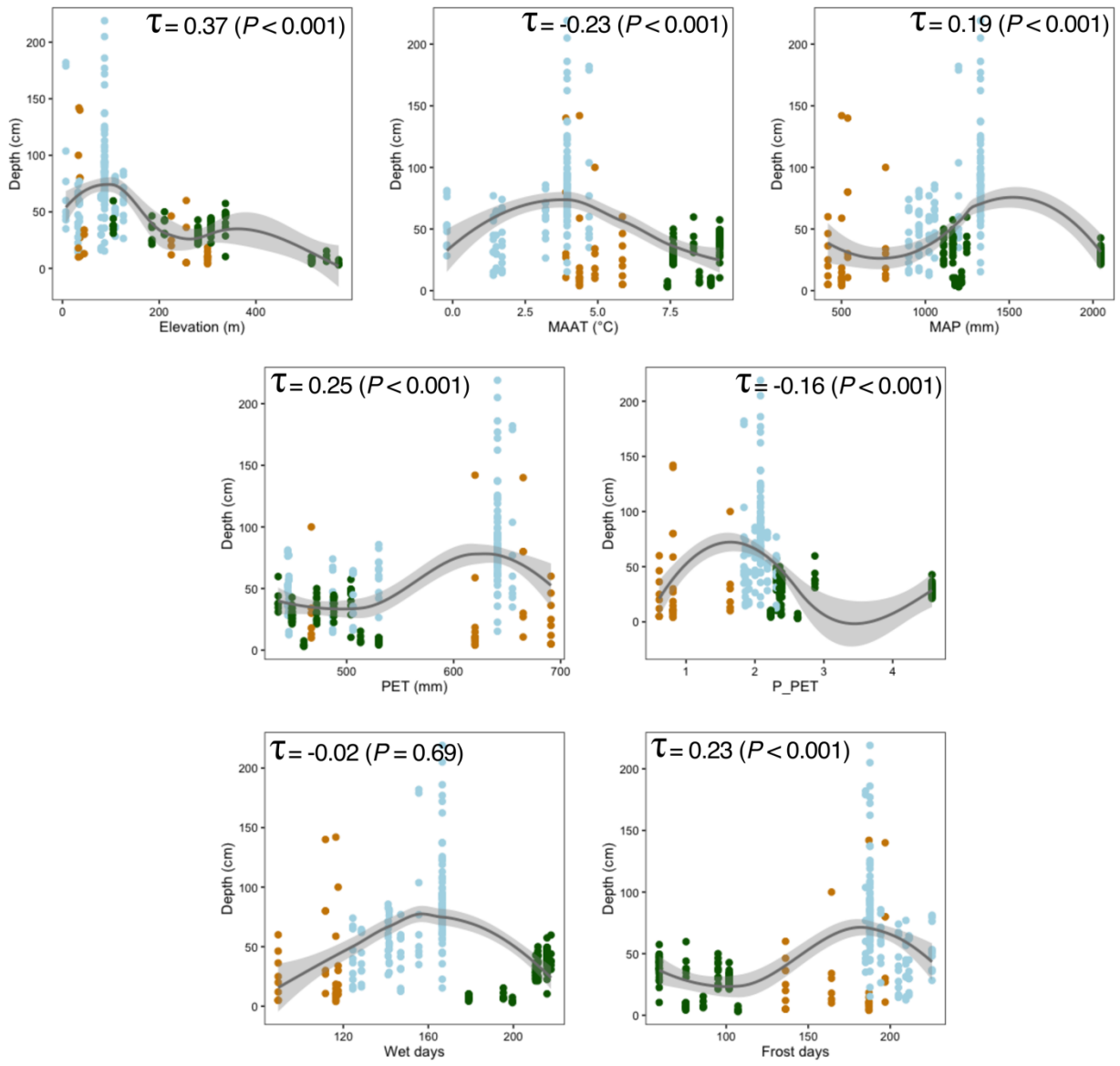

Figure S3.2. Peatland pool depth patterns across different geographic settings. Panels show locally-weighted scatterplot smoothing (LOWESS) with 95% confidence interval, and Kendall correlations' tau (τ) and p-value.

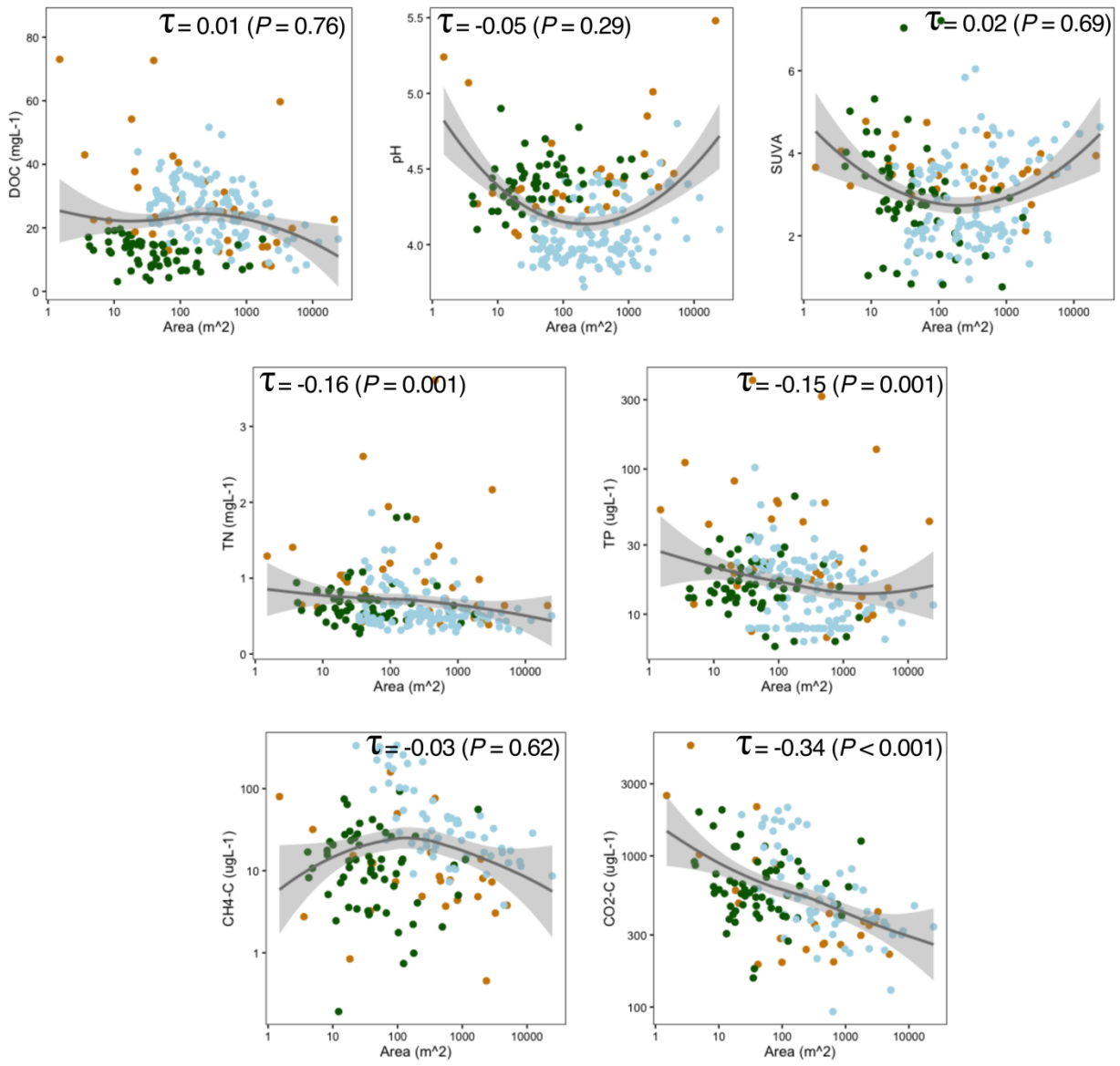

Figure S3.3. Peatland pool biogeochemistry and area relationships. Panels show locally-weighted scatterplot smoothing (LOWESS) with 95% confidence interval, and Kendall correlations' tau (τ) and p-value.

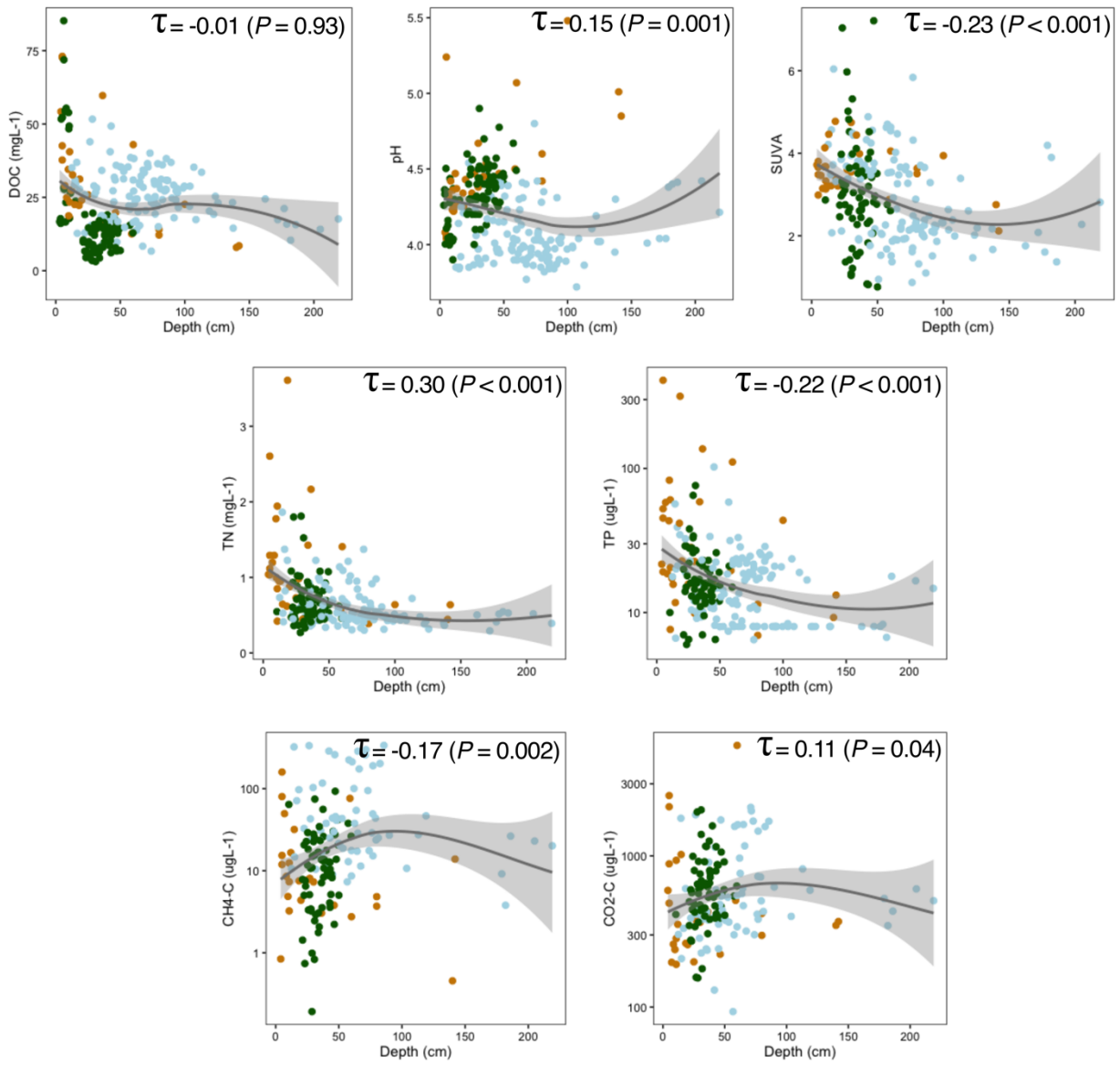

Figure S3.4. Peatland pool biogeochemistry and depth relationships. Panels show locally-weighted scatterplot smoothing (LOWESS) with 95% confidence interval, and Kendall correlations' tau (τ) and p-value.

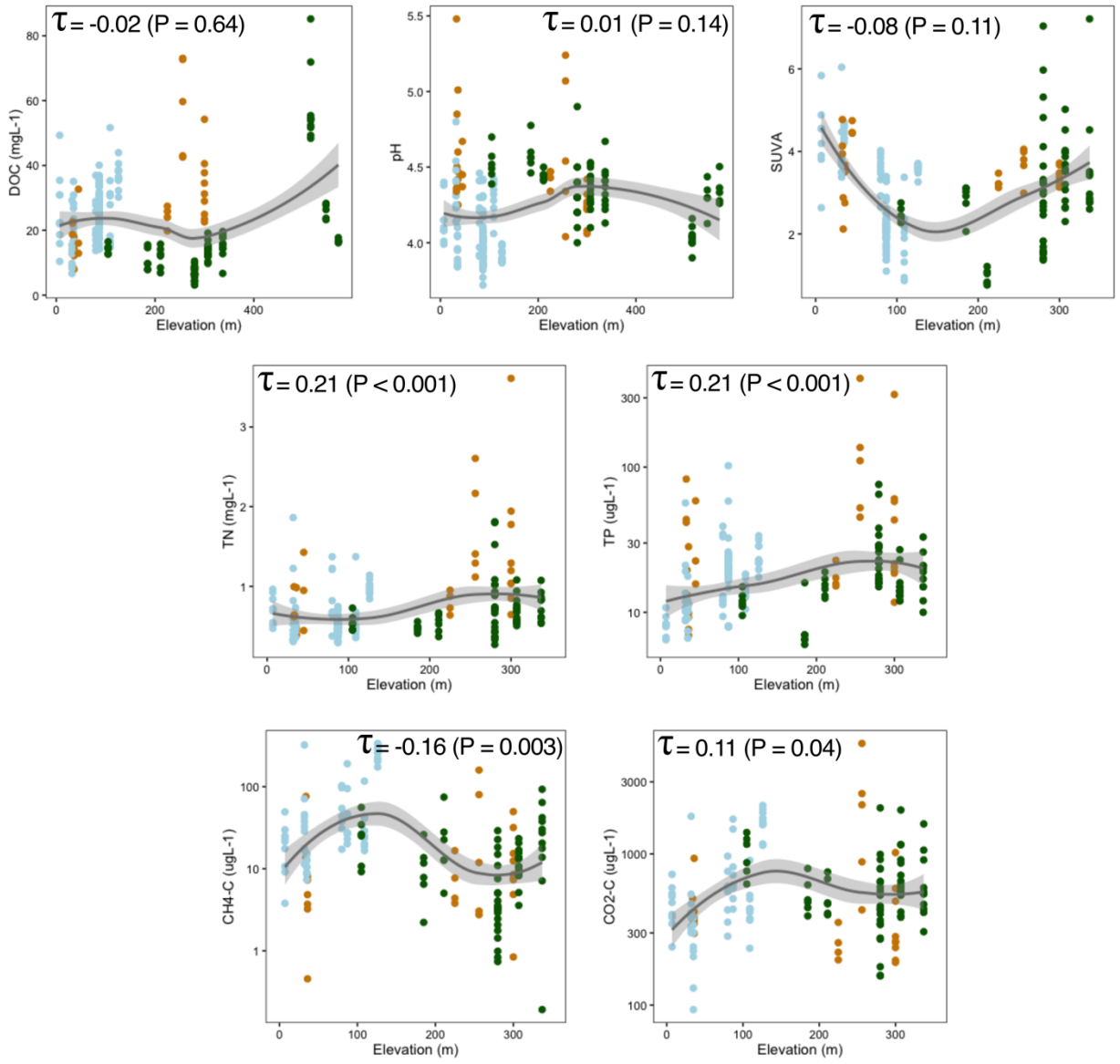

Figure S3.5. Peatland pool biogeochemistry and peatland elevation relationships. Panels show locally-weighted scatterplot smoothing (LOWESS) with 95% confidence interval, and Kendall correlations' tau (τ) and p-value.

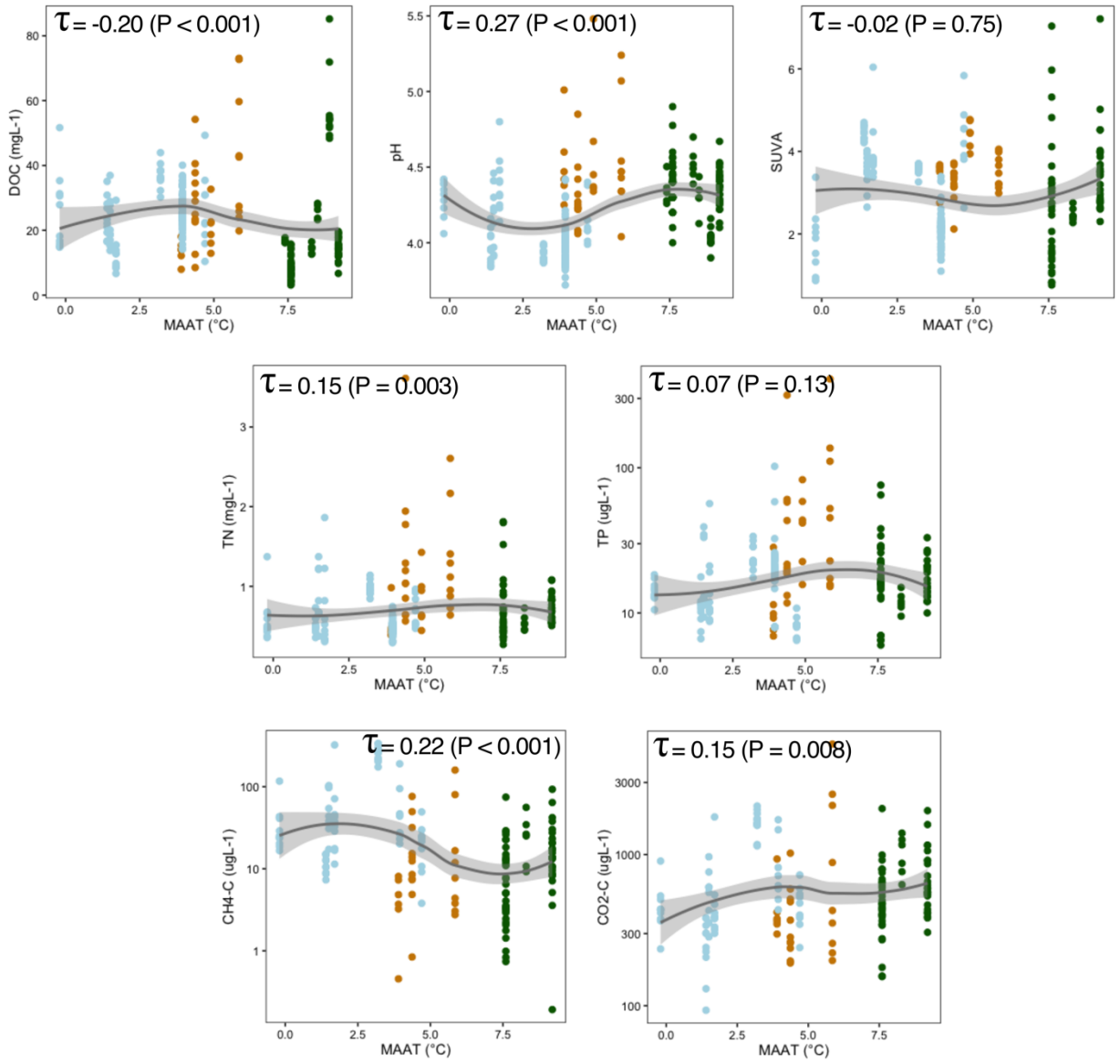

Figure S3.6. Peatland pool biogeochemistry and mean annual air temperature (MAAT) relationships. Panels show locally-weighted scatterplot smoothing (LOWESS) with 95% confidence interval, and Kendall correlations' tau (τ) and p-value.

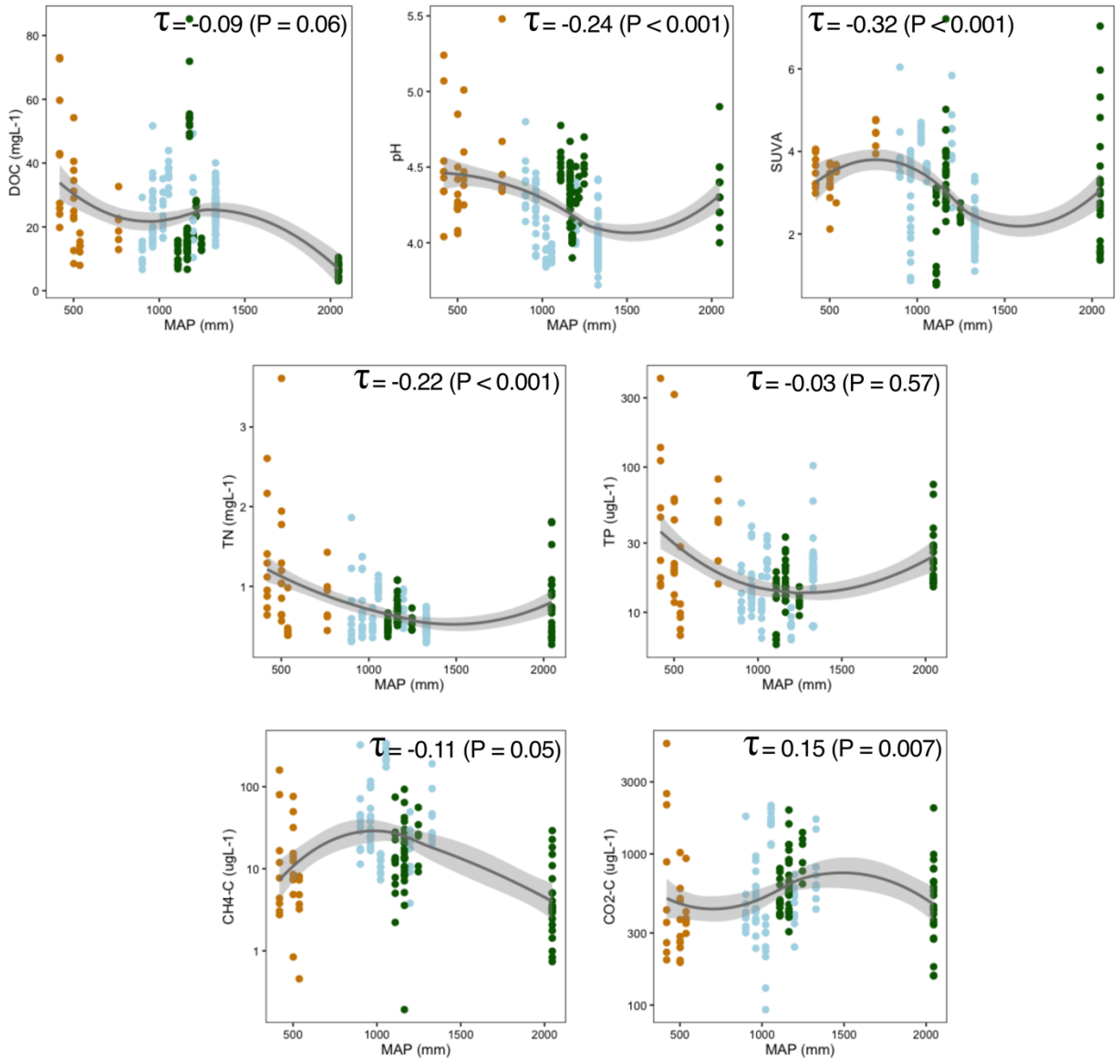

Figure S3.7. Peatland pool biogeochemistry and mean annual precipitation (MAP) relationships. Panels show locally-weighted scatterplot smoothing (LOWESS) with 95% confidence interval, and Kendall correlations' tau (τ) and p-value.

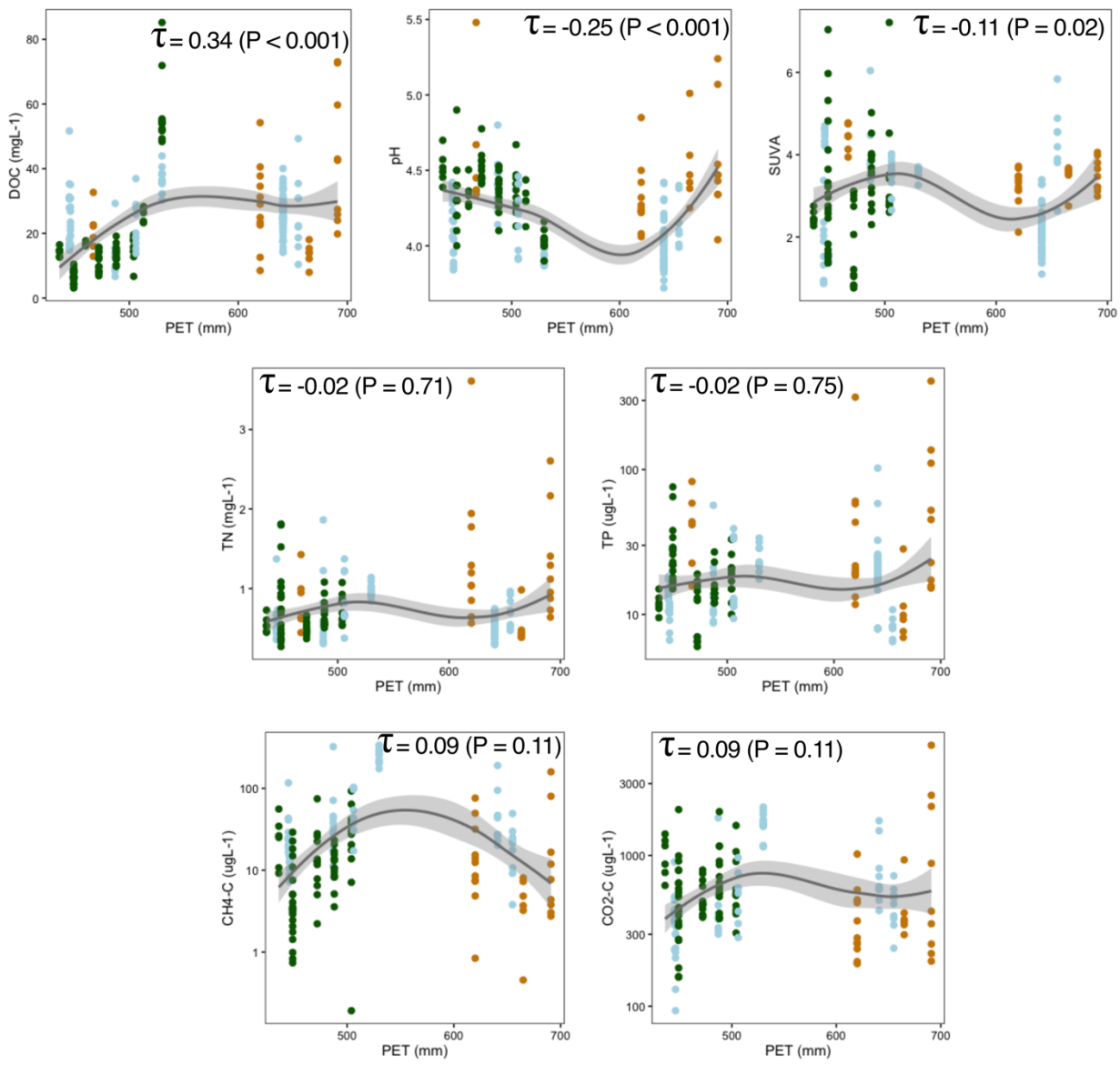

Figure S3.8. Peatland pool biogeochemistry and potential evapotranspiration (PET) relationships. Panels show locally-weighted scatterplot smoothing (LOWESS) with 95% confidence interval, and Kendall correlations' tau (τ) and p-value.

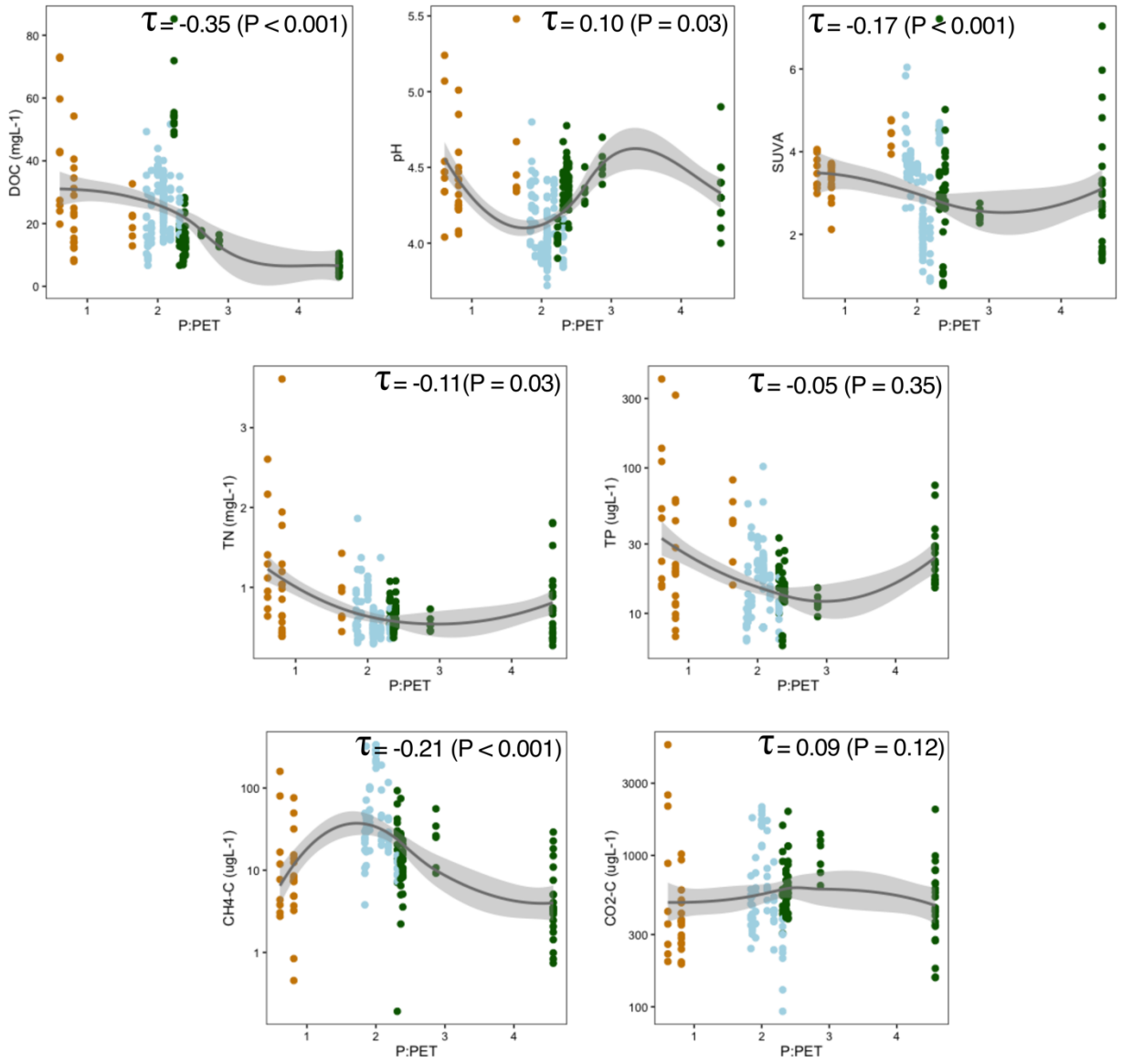

Figure S3.9. Peatland pool biogeochemistry and precipitation-to-potential evapotranspiration ratio (P:PET) relationships. Panels show locally-weighted scatterplot smoothing (LOWESS) with 95% confidence interval, and Kendall correlations' tau (τ) and p-value.

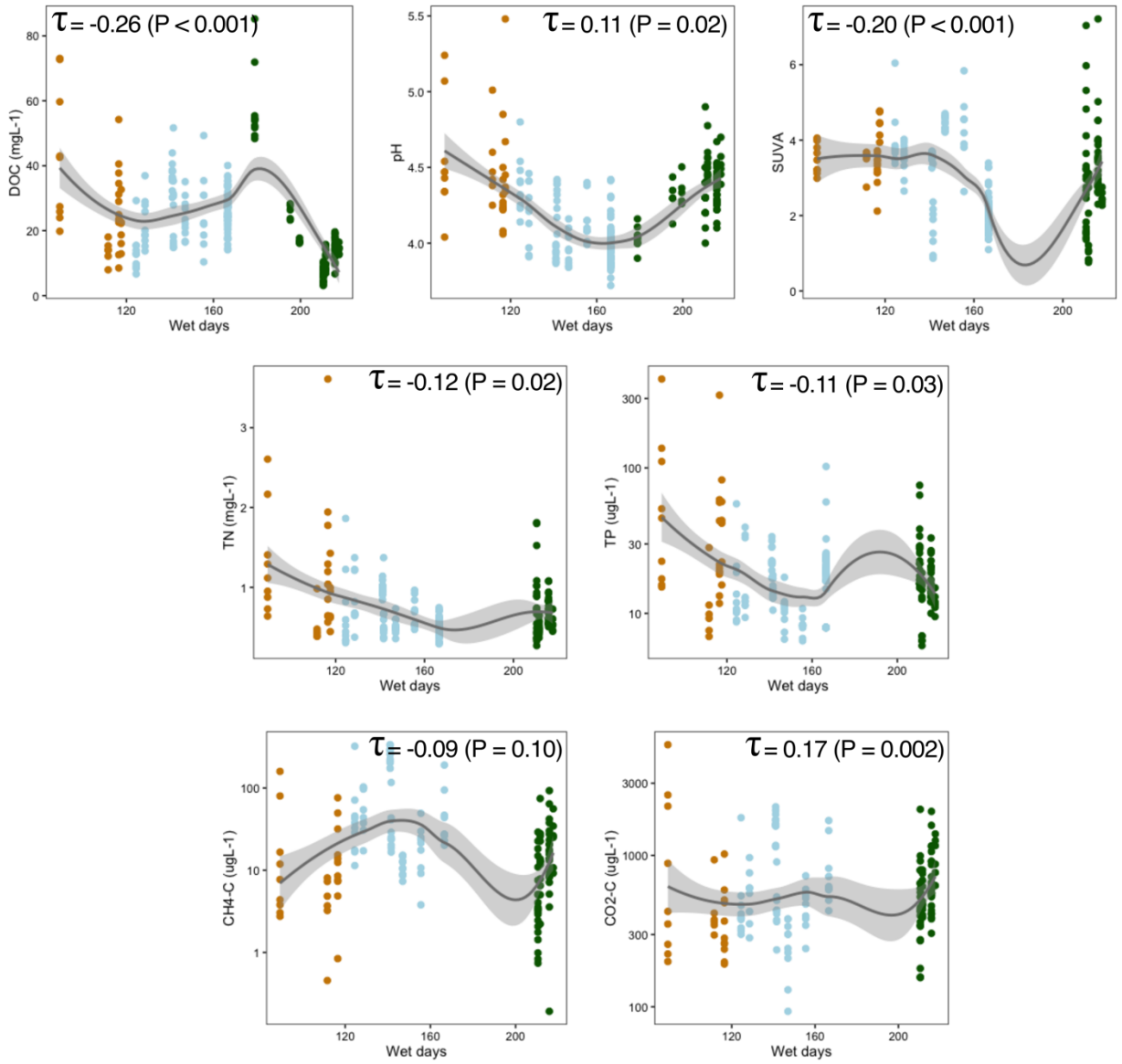

Figure S3.10. Peatland pool biogeochemistry and annual number of wet days relationships. Panels show locally-weighted scatterplot smoothing (LOWESS) with 95% confidence interval, and Kendall correlations' tau (τ) and p-value.

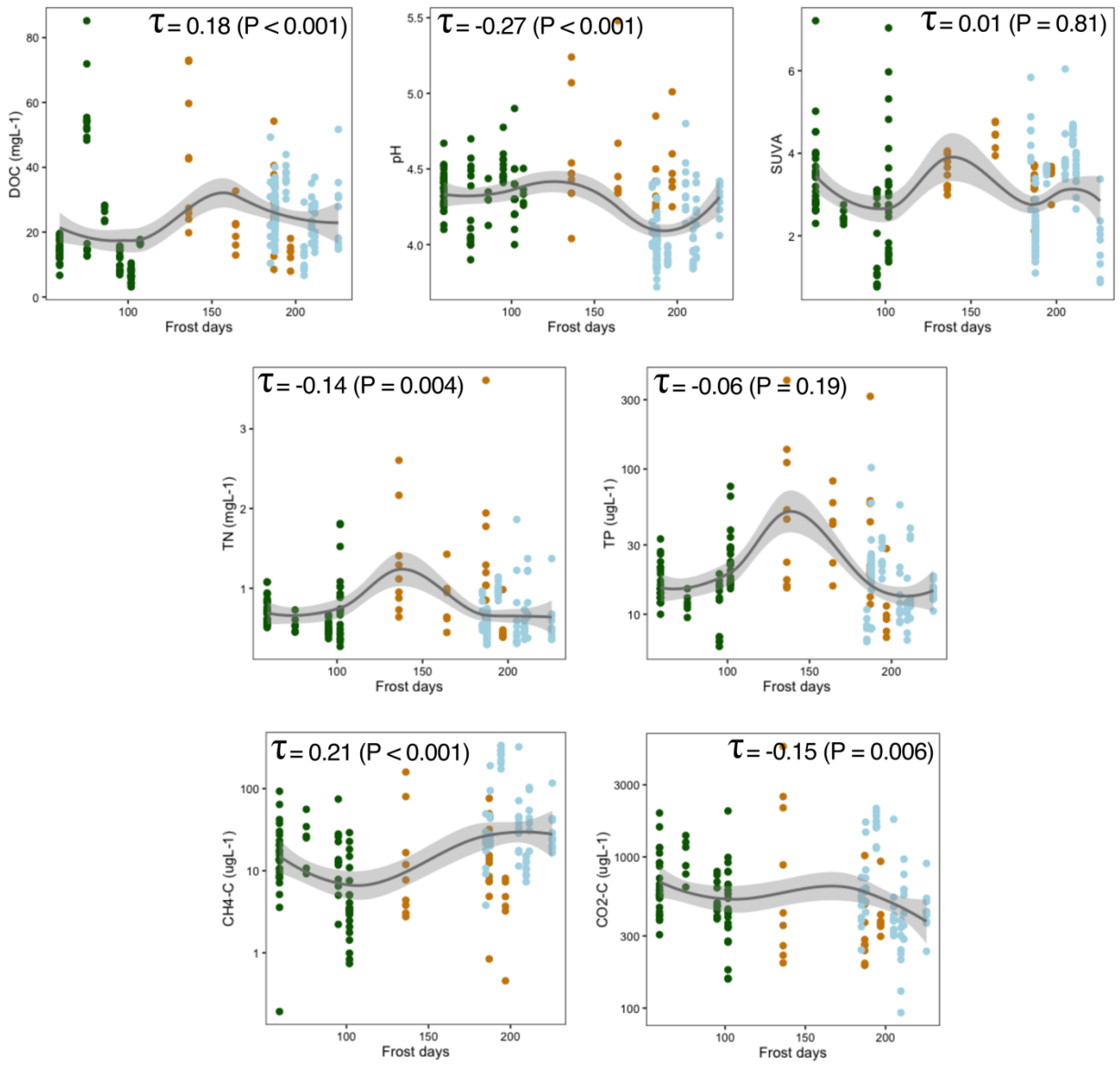

Figure S3.11. Peatland pool biogeochemistry and annual number of frost days relationships. Panels show locally-weighted scatterplot smoothing (LOWESS) with 95% confidence interval, and Kendall correlations' tau (τ) and p-value.

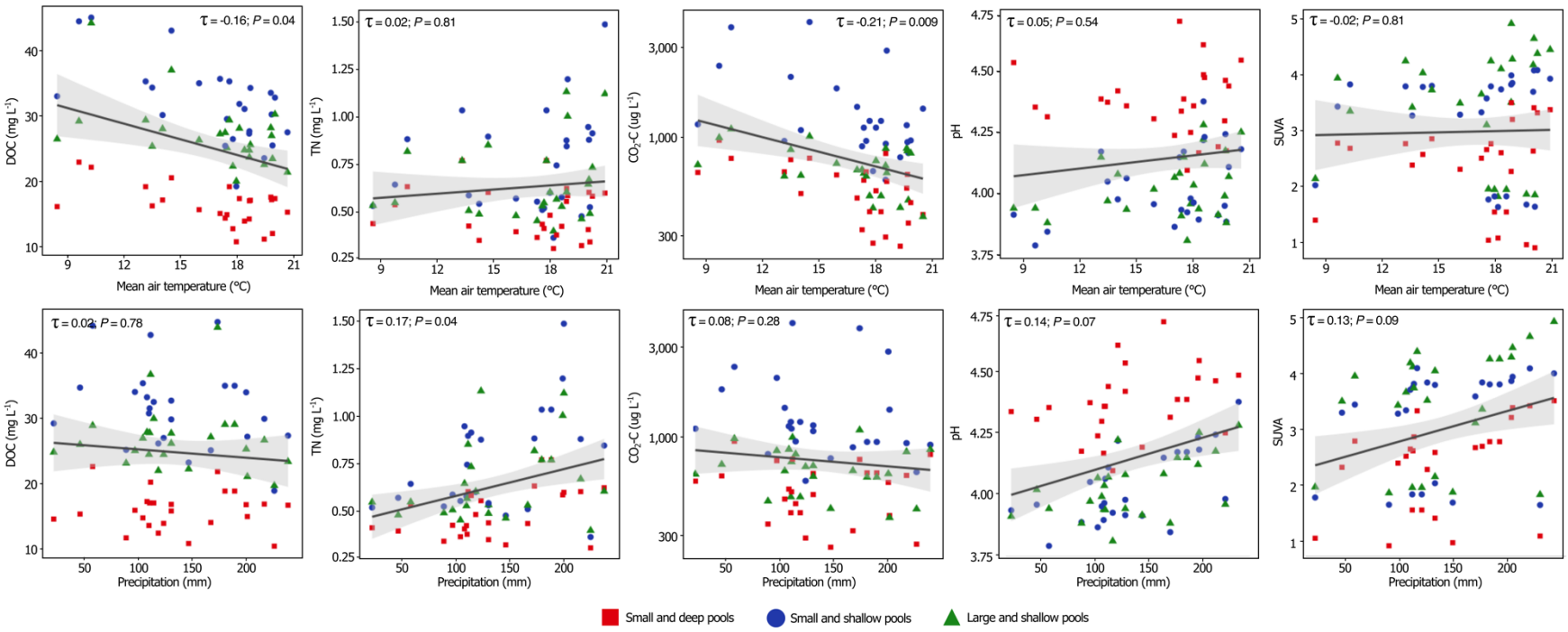

Figure S3.12. Relationships between pool dissolved organic carbon (DOC), total nitrogen (TN) and carbon dioxide (CO_2) concentrations, pH and specific UV absorbance (SUVA), and mean air temperature (upper boxes) and precipitations (lower boxes), measured at the GPB site (eastern Canada). Colors and shapes symbolize the three groups of pools. Each dot represents the group mean for a given day of the year (DOY), between 2016 and 2021. Gray shades show linear smoothing with 95% confidence interval. Kendall rank correlation's tau (τ) and p-values (*P*) are shown.

Table S3.4. Coefficients of variation of each constituent sampled at the Grande plée Bleue site for each year.

Site	pH	DOC	TN	TP	A_{254}	SUVA	CH_4	CO_2
2016	1.7	23.5	20.4	40.5	33.4	13.0	101.3	50.3
2017	2.1	19.8	8.1	13.4	16.5	0.7		
2019	3.0	13.0	16.2	12.3	16.0	5.4	55.3	40.1
2020	4.1	19.1	16.5	37.6	20.6	13.0	86.4	60.0
2021	2.0	16.7	20.9	30.8	9.6	9.5	154.5	16.0

Table S3.5. Summary of linear mixed effects models of temporal (Year or DOY) variations in pool biogeochemistry at the Grande plée Bleue site, with pool morphology used as random intercept, and subsequent analyses of variance to test for fixed effects structure. Asterisks (*) indicate relationships with p-values < 0.05.

Response variable	Explanatory variable		Estimate	Std error	DF	t-value	p-value	numDF	denDF	t-value	p-value
DOC	Year	(2016)	20.826	4.760	68	4.376	-	4	68	5.725	<0.001*
		2017	3.280	1.615	68	2.032	0.046*				
		2019	5.535	1.615	68	3.428	<0.001*				
		2020	7.128	1.615	68	4.415	<0.001*				
		2021	5.205	1.615	68	3.224	0.002*				
	DOY	(175)	20.829	4.739	68	4.396	-	4	68	11.072	<0.001*
		200	2.114	1.453	68	1.455	0.15				
		225	4.048	1.453	68	2.787	0.007*				
		250	6.239	1.453	68	4.295	<0.001*				
		275	8.735	1.453	68	6.013	<0.001*				
pH	Year	(2016)	4.042	0.117	68	34.474	-	4	68	12.443	<.0001*
		2017	-0.003	0.041	68	-0.080	0.936				
		2019	0.092	0.041	68	2.268	0.027*				
		2020	0.170	0.041	68	4.188	<0.001*				
		2021	0.225	0.041	68	5.525	<0.001*				
	DOY	(175)	4.205	0.119	68	35.339	-	4	68	1.143	0.344
		200	-0.069	0.052	68	-1.338	0.185				
		225	-0.083	0.052	68	-1.600	0.114				
		250	-0.077	0.052	68	-1.483	0.143				
		275	-0.103	0.052	68	-1.987	0.051				

Response variable	Explanatory variable		Estimate	Std error	DF	t-value	p-value	numDF	denDF	t-value	p-value
TN	Year	(2016)	-0.342	0.051	68	-6.725	-	4	68	52.206	<0.001*
		2017	0.054	0.023	68	2.299	0.025*				
		2019	0.083	0.023	68	3.576	0.001*				
		2020	0.277	0.023	68	11.868	<0.001*				
		2021	0.232	0.023	68	9.935	<0.001*				
	DOY	(175)	-0.240	0.057	68	-4.211	-	4	68	0.341	0.849
		200	0.045	0.047	68	0.973	0.334				
		225	0.022	0.047	68	0.474	0.637				
		250	0.020	0.047	68	0.429	0.669				
		275	0.046	0.047	68	0.978	0.332				
TP	Year	(2016)	1.188	0.037	68	32.530	-	4	68	6.461	<0.001*
		2017	0.153	0.04	68	3.770	<0.001*				
		2019	-0.041	0.04	68	-1.004	0.319				
		2020	0.041	0.04	68	1.015	0.314				
		2021	0.016	0.04	68	0.394	0.695				
	DOY	(175)	1.186	0.039	68	30.101	-	4	68	0.600	0.663
		200	0.072	0.047	68	1.547	0.127				
		225	0.034	0.047	68	0.724	0.472				
		250	0.036	0.047	68	0.771	0.443				
		275	0.038	0.047	68	0.806	0.423				

Response variable	Explanatory variable		Estimate	Std error	DF	t-value	p-value	numDF	denDF	t-value	p-value
CO_2	Year	(2016)	2.749	0.123	68	22.326	-	4	68	3.447	0.012*
		2017	0.145	0.059	68	2.451	0.017*				
		2019	0.151	0.059	68	2.544	0.013*				
		2020	0.212	0.059	68	3.572	0.001*				
		2021	0.130	0.059	68	2.197	0.032*				
	DOY	(175)	2.759	0.122	68	22.582	-	4	68	7.595	<0.001*
		200	0.041	0.054	68	0.768	0.445				
		225	0.105	0.054	68	1.938	0.057*				
		250	0.183	0.054	68	3.381	0.001*				
		275	0.260	0.054	68	4.815	<0.001*				
CH_4	Year	(2016)	1.477	0.27	68	5.481	-	4	68	2.298	0.068
		2017	0.056	0.127	68	0.440	0.661				
		2019	-0.002	0.127	68	-0.014	0.989				
		2020	-0.055	0.127	68	-0.430	0.669				
		2021	0.293	0.127	68	2.295	0.025				
	DOY	(175)	1.449	0.271	68	5.352	-	4	68	0.394	0.813
		200	0.139	0.134	68	1.039	0.303				
		225	0.049	0.134	68	0.365	0.716				
		250	0.127	0.134	68	0.947	0.347				
		275	0.116	0.134	68	0.861	0.392				

Response variable	Explanatory variable		Estimate	Std error	DF	t-value	p-value	numDF	denDF	t-value	p-value
A_{254}	Year	(2016)	0.366	0.213	68	1.717	-	4	68	32.696	<0.001*
		2017	0.325	0.072	68	4.533	<0.001*				
		2019	0.557	0.072	68	7.764	<0.001*				
		2020	0.672	0.072	68	9.372	<0.001*				
		2021	0.69	0.072	68	9.618	<0.001*				
	DOY	(175)	0.657	0.221	68	2.980	-	4	68	2.463	0.053
		200	0.059	0.115	68	0.511	0.611				
		225	0.185	0.115	68	1.610	0.112				
		250	0.234	0.115	68	2.041	0.045*				
		275	0.311	0.115	68	2.713	0.008*				
SUVA	Year	(2016)	1.587	0.333	68	4.771	-	4	68	77.803	<0.001*
		2017	0.975	0.148	68	6.571	<0.001*				
		2019	1.818	0.148	68	12.251	<0.001*				
		2020	1.958	0.148	68	13.198	<0.001*				
		2021	2.294	0.148	68	15.461	<0.001*				
	DOY	(175)	2.757	0.387	68	7.124	-	4	68	0.397	0.810
		200	0.202	0.346	68	0.584	0.561				
		225	0.419	0.346	68	1.211	0.230				
		250	0.284	0.346	68	0.821	0.415				
		275	0.285	0.346	68	0.823	0.413				

Table S3.6. Coefficients of the partial least square regressions performed on meteorological vs. biogeochemical data from nine pools of eastern Canada (GPB site) sampled over the 2016, 2017, 2019, 2020 and 2021 growing seasons.

	pH	**DOC**	**TN**	**TP**	**A_{254}**	**SUVA**	**CO_2**	**CH_4**
Day of the year	-0.24	0.69	0.04	0.04	0.39	0.11	0.62	0.22
Days >30°C	0.33	0.14	0.39	-0.09	0.26	0.29	0.08	0.05
Mean previous fall temperature	0.16	0.25	0.31	0.18	0.34	0.33	0.26	0.07
Mean previous winter temperature	-0.12	-0.17	-0.23	-0.21	-0.27	-0.27	-0.21	-0.04
Total summer precipitation	0.35	0.13	0.40	-0.13	0.25	0.28	0.05	0.05

Table S3.7. Meteorological information for the GPB site for the studied years. Data are from the nearest weather station, located 13 km from the study site.

Year	Total amount of snow received the previous winter (cm)	Total previous fall precipitation (% as snow) (mm)	Total spring rain (mm)	Total summer rain (mm)	Number of summer rain days	Average rain amount per rainy day (total summer rain / number rainy day) (mm)	Mean previous fall air temperature (°C)	Mean previous winter air temperature (°C)	Mean summer air temperature (°C)	Mean maximum summer air temperature (°C)	Number of summer frost days	Number of extreme heat days (>30°C)	Mean July air temperature (°C)	Mean August air temperature (°C)
2016	163	164 (0.2%)	104.5	382.2	106	3.61	3.9	-5.5	18.4	23.9	0	10	19.6	20.3
2017	181	282 (8.1%)	261.5	317.4	117	2.71	5.2	-7.8	17.4	23.1	0	6	19.0	17.3
2019	268	224 (18.6%)	219.7	377.7	102	3.70	4.7	-6.7	17.1	23.0	0	8	21.3	18.4
2020	170	221 (13.2%)	119.6	412.1	98	4.21	5.3	-7.3	17.6	23.3	5	14	21.1	18.5
2021	118	239 (3.3%)	87.7	472.3	109	4.33	4.8	-7.0	18.4	24.0	0	13	18.6	21.3

Table S3.8. Pool biogeochemistry (means of nine pools) at the GPB site at day of the year 175, 200, 225, 250 and 275 for years 2016, 2017, 2019, 2020 and 2021.

Year	DOY	pH	DOC (mg L^{-1})	TN (mg L^{-1})	TP (ug L^{-1})	A_{254}	SUVA	CH_4 (ug L^{-1})	CO_2 (ug L^{-1})
2016	150-200	4.06	16.57	0.37	18.1	0.276	1.51	15.42	445.96
	175-225	4.00	19.01	0.44	17.3	0.323	1.50	27.02	483.73
	200-250	3.97	20.25	0.47	14.1	0.335	1.47	31.44	539.53
	225-275	4.05	23.14	0.51	12.2	0.402	1.59	87.37	778.69
	250-300	4.12	25.17	0.52	16.4	0.495	1.86	83.63	836.99
2017	150-200	3.94	20.44	0.58	22.1	0.378	1.78	38.78	632.17
	175-225	3.99	23.21	0.53	22.7	0.378	1.78	38.78	632.17
	200-250	4.05	25.98	0.47	23.2	0.842	3.18	50.25	858.06
	225-275	4.09	25.63	0.50	21.8	0.891	3.04	66.37	1050.51
	250-300	4.13	25.28	0.52	20.3	0.967	3.04	63.77	1229.25
2019	150-200	4.31	22.36	0.51	11.7	0.751	3.13	21.07	623.25
	175-225	4.07	26.41	0.68	15.8	0.979	3.52	89.88	848.07
	200-250	4.11	25.74	0.58	15.2	0.941	3.50	66.15	790.34
	225-275	4.15	25.07	0.48	14.6	0.902	3.48	42.43	732.61
	250-300	4.02	32.23	0.59	14.0	1.108	3.47	55.38	1443.34
2020	150-200	4.35	22.04	0.87	12.9	0.862	3.21	13.14	525.36
	175-225	4.32	21.33	1.08	26.3	0.853	3.94	22.66	721.82
	200-250	4.27	25.63	0.94	22.4	0.990	3.80	74.48	1365.09
	225-275	4.11	33.57	0.80	15.8	1.205	3.48	106.73	1954.30
	250-300	4.01	37.20	0.79	13.1	1.282	3.30	87.16	1900.24
2021	150-200	4.38	22.74	0.71	15.3	0.983	4.17	333.83	863.32
	175-225	4.29	24.76	0.73	13.5	1.047	4.06	181.38	800.30
	200-250	4.20	26.79	0.76	11.7	1.102	3.95	28.93	737.28
	225-275	4.23	27.93	0.87	22.8	1.056	3.62	28.93	736.43
	250-300	4.23	27.93	0.87	22.8	1.056	3.62	28.93	736.43

Annexe III. Matériel supplémentaire au chapitre 4.

Table S4.1. Results of the two-way analysis of variance of decay *k* values, regardless of the litter type, with interacting effects between pool and depth of incubation, and of the Tukey HSD posthoc test performed to differentiate depths of incubation. Asterisks show relationships with p-values (*P*) < 0.05. Depths with different level letters are statistically different at a significance level of 5% (*P* < 0.05).

Factor	**df**	**Sum of squares**	**Mean square**	**F**	***P***	**Depths**	***P***
Depth	2	0.020	0.010	8.936	0.002*	**Surface-Bottom**	0.002*
Pool	5	0.005	0.001	0.864	0.524	**Surface-Sediments**	0.020*
Depth:Pool	10	0.004	0.000	0.320	0.965	**Bottom-Sediments**	0.544
Residuals	18	0.020	0.001				

		Depth	**Level**
		Surface	A
		Bottom	B
		Sediments	B

Table S4.2. Results of the analysis of variance and of the Tukey HSD posthoc test of *Typha latifolia* decay *k* values in relation to depth of incubation. Asterisks show relationships with p-values (*P*) < 0.05. Depths with different level letters are statistically different at a significance level of 5% (*P* < 0.05).

Factor	df	Sum of squares	Mean square	F	*P*	Depths	*P*
Depth	2	0.317	0.106	78.28	<0.001*	**Surface-Bottom**	0.011*
Residuals	16	0.022	0.001			**Surface-Sediments**	0.005*
						Bottom-Sediments	0.979
						Depth	**Level**
						Surface	A
						Bottom	B
						Sediments	B

Table S4.3. Results of the analysis of variance and of the Tukey HSD posthoc test of *Sphagnum capillifolium* decay *k* values in relation to depth of incubation. Asterisks show relationships with p-values (*P*) < 0.05. Depths with different level letters are statistically different at a significance level of 5% (*P* < 0.05).

Factor	df	Sum of squares	Mean square	F	*P*	Depths	*P*
Depth	2	0.003	0.001	2.471	0.1	**Surface-Bottom**	-
Residuals	16	0.006	0.001			**Surface-Sediments**	-
						Bottom-Sediments	-
						Depth	**Level**
						Surface	A
						Bottom	A
						Sediments	A

Table S4.4. Results of the two-way analysis of variance of decay *k* values with interacting effects between litter species and depth of incubation, and of the Tukey HSD posthoc test performed to differentiate depths of incubation. Asterisks show relationships with p-values (*P*) < 0.05. Systems with different level letters are statistically different at a significance level of 5% (*P* < 0.05).

Factor	df	Sum of squares	Mean square	F	*P*	Depths	*P*
Species	1	0.006	0.005	11.779	0.002*	**Surface-Bottom**	<0.001*
Depth	2	0.020	0.010	20.804	<0.001*	**Surface-Sediments**	<0.001*
Species:Depth	2	0.009	0.004	8.8114	0.001*	**Bottom-Sediments**	0.248
Residuals	30	0.015	0.000				
						Depth	**Level**
						Surface	A
						Bottom	B
						Sediments	B

Table S4.5. Results of the generalized linear models (GLMs) with gamma distribution of the decay *k* values in relation to depth of incubation and final litter chemistry for both *Typha latifolia* and *Sphagnum capillifolium* after 27 months of incubation in the pools of the Grande plée Bleue peatland. Asterisks show relationships with p-values (*P*) < 0.05.

	Typha latifolia				***Sphagnum capillifolium***			
Coefficients	**Estimate**	**Std. error**	**t**	***P***	**Estimate**	**Std. error**	**t**	***P***
(Intercept)	0.127	0.125	10.169	<0.001*	0.079	0.008	9.522	<0.001*
Depth	-0.001	0.001	-4.722	<0.001*	-0.001	0.001	-1.987	0.064
(Intercept)	0.216	0.026	8.251	<0.001*	0.110	0.030	3.683	0.002*
C/N	-0.002	0.001	-5.623	<0.001*	-0.001	0.001	-1.480	0.158
(Intercept)	0.174	0.041	4.231	<0.001*	-0.107	-0.030	3.557	0.003*
C/P	-0.001	-0.001	-2.218	0.041*	-0.001	0.001	-1.354	0.195
(Intercept)	-0.016	0.034	-0.474	0.642	0.064	0.043	1.494	0.155
N/P	0.003	0.001	2.928	0.001*	0.001	0.001	0.080	0.938
(Intercept)	-2.396	1.071	-2.237	0.040*	0.414	0.629	0.659	0.519
$\delta^{13}C$	-0.093	0.040	-2.316	0.034*	0.012	0.023	0.552	0.589
(Intercept)	0.107	0.013	8.422	<0.001*	0.107	0.034	3.176	0.006*
$\delta^{15}N$	0.013	0.006	2.239	0.040*	0.005	0.004	1.196	0.249
(Intercept)	-0.225	0.224	-1.006	0.329	0.155	0.130	1.188	0.252
1420/1090	0.589	0.419	1.407	0.179	-0.203	0.303	-0.670	0.513
(Intercept)	-0.217	0.095	-2.290	0.036*	0.026	0.087	0.304	0.765
1510/1090	0.725	0.231	3.141	0.006*	0.168	0.352	0.476	0.640
(Intercept)	-0.232	0.092	-2.518	0.023*	0.063	0.093	0.681	0.506
1630/1090	0.529	0.156	3.389	0.003*	0.009	0.178	0.049	0.962
(Intercept)	-0.202	0.206	-0.979	0.342	0.191	0.126	1.524	0.147
1720/1090	0.525	0.372	1.413	0.177	-0.262	0.264	-0.990	0.337

Table S4.6. Results of the generalized linear models (GLMs) with gamma distribution of the percentage of litter mass remaining at the surface (upper table) and the bottom (bottom table) of the pools with water chemistry measured at each retrieving time. Asterisks show relationships with p-values (P) < 0.05

Pool surface	***Typha latifolia***				***Sphagnum capillifolium***			
Coefficients	Estimate	Std. error	t	*P*	Estimate	Std. error	t	*P*
(Intercept)	0.931	0.784	1.188	0.249	0.945	0.550	1.719	0.101
pH	-0.078	0.150	-0.520	0.609	-0.067	0.107	-0.626	0.539
DOC	0.015	0.020	0.763	0.454	0.013	0.014	0.922	0.367
TN	0.035	0.124	0.284	0.780	0.103	0.091	1.132	0.271
TP	0.001	0.001	0.337	0.740	0.001	0.001	0.509	0.616
NO_3	0.001	0.005	0.670	0.511	-0.001	0.004	-0.082	0.936
NH_4	-0.001	0.001	-0.474	0.641	-0.001	0.001	-1.607	0.124
PO_4	-0.013	0.005	-2.345	0.030*	-0.008	0.004	-2.131	0.045*
A_{254}	-0.421	0.490	-0.858	0.401	-0.380	0.352	-1.079	0.293
SUVA	-0.061	0.120	0.516	0.612	0.061	0.087	0.708	0.487

Pool bottom	***Typha latifolia***				***Sphagnum capillifolium***			
Coefficients	Estimate	Std. error	t	*P*	Estimate	Std. error	t	*P*
(Intercept)	0.921	0.389	2.371	0.028*	0.701	0.405	1.733	0.098
pH	-0.071	0.075	-0.945	0.356	0.032	0.079	0.406	0.698
DOC	0.015	0.010	1.530	0.142	0.006	0.010	0.614	0.546
TN	0.007	0.063	0.104	0.918	-0.090	0.067	-1.346	0.193
TP	0.001	0.001	0.732	0.472	0.001	0.001	0.600	0.555
NO_3	0.002	0.003	0.630	0.536	0.003	0.003	1.274	0.217
NH_4	-0.001	0.001	-0.590	0.562	0.001	0.001	0.620	0.542
PO_4	-0.004	0.003	-1.547	0.138	-0.002	0.003	-0.496	0.626
A_{254}	-0.440	0.239	-1.842	0.080	-0.158	0.255	-0.620	0.542
SUVA	-0.089	0.059	1.503	0.149	0.034	0.063	0.546	0.591

Annexe IV. Photographies

Mares de la tourbières Grande plée Bleue (Lévis, Québec, Canada). Crédits photos : Julien Arsenault

Mares d’une tourbière du parc de Karukinka (Patagonie, Chili). Crédits photo : Julien Arsenault

Échantillonnages en équipe des mares de la Patagonie, janvier 2019. Photo du haut : Jorge Hoyos-Santillan, Marie-Pierre Beauvais & Nicola Raggi-Ramirez, parc national de Karukinka (crédit : Julien Arsenault). Photo du bas : Julie Talbot, Thora Herrmann, Gaëlle Crête, Roy Mackenzie, Marie-Pierre Beauvais & moi-même, île de Navarino (crédit : Julie Talbot).

Une directrice heureuse du travail accompli en Patagonie. Crédit photo : Julien Arsenault